EAST ENGR. LIBRARY

TRANSACTIONS

of the American Society for Steel Treating

CONTENTS

The Surface Energy of Iron Carbide
—YAP, CHU-PHAY 289

Study of Low Carbon Wires by X-ray Diffraction Methods
—NORMAN P. GOSS 314

Brittleness in Low Carbon Steel
—H. H. BLEAKNEY 321

The Chemistry of Liquid Hardening Baths
—GEORGE BARSKY 347

The Iron-Vanadium-Oxygen System
—C. H. MATHEWSON, E. SPIRE AND C. H. SAMANS 357

Vol. XX No. 4
October, 1932

The TRANSACTIONS *of the* AMERICAN SOCIETY *for* STEEL TREATING

Published monthly and Copyrighted, 1932, by the AMERICAN SOCIETY FOR STEEL TREATING, *1016 Euclid Avenue, Cleveland, Ohio*

SUBSCRIPTIONS: (members) $2.50 per year
(non-members) $5.00 per year, $1.00 per copy
Foreign (non-members) $6.50 per year, $1.25 per copy

Entered as second class matter, November 9, 1931, at the Post Office at Cleveland, Ohio, under the Act of March 3, 1879.

RAY T. BAYLESS, *Editor*

Vol. XX October, 1932 No. 4

The object of the Society shall be to promote the arts and sciences connected with either the manufacture or treatment of metals, or both.—Constitution A. S. S. T., Art. II.

Officers and Board of Directors

A. H. d'ARCAMBAL, President
Pratt & Whitney Co., Hartford, Conn.

W. B. COLEMAN, Vice-Pres.
W. B. Coleman and Co., Philadelphia

A. T. CLARAGE, Treasurer
Columbia Tool Steel Co., Chicago Hts. Ill.

W. H. EISENMAN, Secretary
7016 Euclid Avenue, Cleveland

DIRECTORS

J. M. WATSON, Past President
Hupp Motor Car Corporation, Detroit

F. B. DRAKE
Johnson Gear Co., Berkeley, California

C. F. PASCOE,
Canadian Steel Fdrys. Co., Ltd.
Montreal, Canada

B. F. SHEPHERD
Ingersoll-Rand Co., Phillipsburg
New Jersey

H. D. McKINNEY
Driver-Harris Co., Harrison
New Jersey

Publication Committee

V. O. HOMERBERG, Chairman Boston
RAY T. BAYLESS, Secretary 7016 Euclid Ave., Cleveland

Members:

Clair Upthegrove, Detroit '32
G. M. Enos, Cincinnati '32
W. C. Hamilton, Chicago '32
O. W. Ellis, Ontario '32
S. L. Hoyt, Milwaukee '32
W. B. Coleman, Philadelphia
H. S. Rawdon, Washington '33
Alexander Feild, Baltimore, '33
E. H. Dix, Jr., Pittsburgh '33
G. R. Brophy, Schenectady '34
T. Holland Nelson, Philadelphia '34
Robert Sergeson, Massillon, Ohio '34
A. B. Kinzel, New York '34

THE SURFACE ENERGY OF IRON CARBIDE

(A Critique of the Theories of Precipitation Hardening)

By Yap, Chu-Phay

Abstract

The theoretical relationship between particle-size and solubility has been developed, together with certain equations governing the change of the equilibrium particle-size with respect to temperature. The theory of supersaturation is discussed with particular reference to the A_{cm} line in steel.

The surface energy of Fe_3C has been calculated to be about 4900 and 3800 ergs per square centimeter at 20 degrees and 1136 degrees Cent. respectively. These values are not excessive, taking into consideration the extreme hardness of Fe_3C.

The hardening of steel is discussed theoretically from the standpoint of the surface energy of the dispersed Fe_3C. Quantitative calculations show that the surface energy of Fe_3C can adequately account for the hardness of martensite. The particle-size of the Fe_3C dispersed in ferrite in martensite is of the order of $3–4 \times 10^{-7}$ centimeter in radius—beyond the present microscopic range.

The view that all precipitation hardening can be accounted for by the surface energy of the dispersed phase, has been advanced. A physico-chemical picture of the rôle of surface energy on the hardening of alloys has been presented.

Introduction

IT IS the main purpose of this paper[1] to direct attention to the various influences of the particle-size and surface energy of Fe_3C on the equilibria of iron-carbon alloys, and to present certain views

[1]This is the third of a series of theoretical papers by the author on the iron-carbon system. The first two papers are: "A Thermodynamic Study of the Phasial Equilibria in the System: Iron-carbon"; and "Influence of Dissolved Carbide on the Equilibria of the System: Iron-carbon"; A.I.M.E. Tech. Pub. No. 381 and 382, 1931.

A paper presented before the Thirteenth Annual Convention of the society held in Boston, September 21 to 25, 1931. The author, Yap, Chu-Phay, is a member of the society. He is consulting metallurgist and chemist, New York City. Manuscript received April 1, 1931.

regarding the hardening of steels. Although considerable work has been done by physical chemists on the influence of particle-size on the solubility of inorganic salts in aqueous solutions,[2] the writer is unaware that anyone has ever applied this concept to metallic systems in discussing the nature and extent of equilibria obtained. Thus metallurgists have repeatedly determined the A_{cm} line as if it were constant, irrespective of the particle-size of the Fe_3C present in the steel.

We shall discuss in some detail the theoretical basis of the equations developed in this paper, so that we shall have a clearer understanding of the way the equations can be used to determine the magnitude of the influence due to the particle-size and surface energy of Fe_3C on the properties of steel. It will be shown below that the hardness of martensite can be adequately accounted for by the high surface energy of the finely dispersed Fe_3C in quenched steels.

Theoretical Discussions

Inasmuch as most text books on physical chemistry treat in some detail the historical development of the equations relating to solubility and particle-size, we shall not repeat them here. Instead, we shall directly present the well-known Kelvin-Freundlich equation

$$\frac{RT}{M} \ln \frac{s_2}{s_1} = \frac{2\sigma}{\rho} \left(\frac{1}{r_2} - \frac{1}{r_1} \right) \qquad (1)$$

in which RT has the usual significance, M is the molecular weight of the solute (Fe_3C in the case of steel) s_1 and s_2 are the molar concentrations of the solutions in equilibrium with particles of radii r_1 and r_2 respectively, σ the surface energy, and ρ the density of the solid. If s_1 is the normal solubility, (s_∞), when the particle-size is large, then r_1 will be so large compared to r_2 that r_1 can be safely neglected.[3] Equation (1) then reduces simply to

$$\ln \frac{s_2}{s_\infty} = \frac{2M\sigma}{RT\rho r_2} \qquad (2)$$

[2]For an excellent resumé of the work on solubility and particle-size consult Jerome Alexander's Colloid Chemistry, Vol. I, p. 637. The Chemical Catalog Co., New York. 1926.

[3]Moreover, under normal conditions the surfaces of the solid particles co-existing with the liquid, will be planes; hence r_1 will be infinity and the term $1/r_\infty$ will become zero.

which upon transposing gives

$$\ln s_2 = \ln s_\infty + \frac{2M\sigma}{RT\rho r_2} = \ln s_\infty + \frac{!}{r_2} \qquad (3)$$

Equation (3) shows that with particles of very small size, the degree of supersolubility will be large. Equation (2) clearly implies that in a supersaturated solution of a given concentration at temperature T, there is a definite radius r which will be in equilibrium with the solution—that is, there is an equilibrium particle-size. Towards larger particles, the solution behaves as a supersaturated one, but towards smaller particles, it behaves as an unsaturated solution.[4] It is, therefore, important to know the relation of the change in the equilibrium particle-size with respect to temperature.

The van't Hoff isochore as applied to the change of solubility with respect to temperature is

$$\frac{d \ln s}{dT} = \frac{-Q}{RT^2} \qquad (4)$$

in which s is the concentration at temperature T and —Q is the molal heat of solution. Substituting the value of s for s_∞ (the normal solubility) in equation (2), we obtain

$$\ln s_{(T)} = \frac{2M\sigma}{RT\rho r} + \frac{Q}{RT} + k \qquad (5)$$

Suppose we now study the equilibrium conditions at some other temperature, $T + \Delta T$, then we shall have a new equilibrium radius $r + \Delta r$, and correspondingly new values of $\rho + \Delta\rho$ and $s + \Delta s$. The new equilibrium will now be represented as

$$\ln s_{(T+\Delta T)} = \frac{2M(\sigma + \Delta\sigma)}{R(T + \Delta T)(\rho + \Delta\rho)(r + \Delta r)} + \frac{Q}{RT} + k \qquad (6)$$

Imposing the condition that no precipitation (or dissolution) has

[4] This is the reason why, when we add to an undercooled solution minute particles of the crystal which will be precipitated from solution, crystallization (that is, precipitation) is often immediately induced. The particles which we add as nuclei of crystallization are probably always larger than the equilibrium particle-size for that particular temperature and concentration.

taken place on account of the minute change in temperature, the right-hand side of equation (5) is then equal to the right-hand side of equation (6). Since from the experiments of Laplace and others we know that as a close approximation $\sigma/\rho = K$ (constant), we can, therefore, substitute ϕ for σ/ρ, as

$$\frac{\sigma + \Delta\sigma}{\rho + \Delta\rho} = \frac{\sigma}{\rho} = K \tag{7}$$

Equations (5) and (6) upon combining, give

$$\frac{2M\phi}{RTr} + \frac{Q}{RT} = \frac{2M\phi}{R(T + \Delta T)(r + \Delta r)} + \frac{Q}{RT} \tag{8}$$

which reduces to

$$\frac{2M\phi}{Q} \underset{\substack{\Delta T \doteq O \\ \Delta r \doteq O}}{\mathscr{L}} \Delta\left(\frac{1}{Tr}\right) = \underset{\Delta T \doteq O}{\mathscr{L}} \Delta\left(\frac{1}{T}\right) \tag{9}$$

$$\frac{2M\phi}{Q} d\left(\frac{1}{Tr}\right) = d\left(\frac{1}{T}\right) \tag{10}$$

Integrating between (T, ∞) and (T', r'), we obtain

$$\frac{2M\phi}{Q} \int_{T_1 \infty}^{T', r'} d\left(\frac{1}{Tr}\right) = \int_{T}^{T'} d\left(\frac{1}{T}\right)$$

$$T' = T\left(1 - \frac{2M\phi}{Qr}\right) = T\left(1 - \frac{2M\sigma}{Q\rho r}\right) \tag{11}$$

in which T' is the temperature to which the solution can be undercooled without precipitation. As the particle-size increases, $\left[\frac{2M\sigma}{Q\rho r}\right]$ approaches zero and T' then approaches T, the equilibrium temperature.

An even simpler method of obtaining equation (11) is by the direct integration of the van't Hoff reaction isochore[5] (equation 4) between the limits (T,s_∞) and (T',s_2') representing respectively as before the normal solubility at temperature T and the supersolubility at T'. We then have

$$\int_{s_\infty}^{s_2} d \ln s = \frac{Q}{R} \int_{T}^{T'} - \frac{dT}{T^2}$$

$$\therefore \quad \ln \frac{s_2}{s_\infty} = \frac{Q}{RT'} - \frac{Q}{RT} \qquad (12)$$

Substituting the value of $\left[\ln \frac{s_2}{s_\infty} \right]$ from equation (2) we obtain

$$\frac{2M\sigma}{RT'\rho r} = \frac{Q}{RT'} - \frac{Q}{RT} \qquad (13)$$

which, upon equating, reduces again to equation (11).

There is, of course, the objection that the heats of solution in the two cases are not equal due to the work-equivalent of the surface energy, w, thus:

$$W = RT \ln K = RT \ln K' - w \qquad (14)$$

so that actually at constant temperature we can calculate from the change in the heat of solution the amount of surface energy per unit area. We can, however, justify our direct integration if we can prove that

$$T \, dQ = Q \, dT$$

If we let $Q' = (Q - \triangle Q)$ and $T' = (T - \triangle T)$, then from equations (12) and (14)

$$\frac{Q' - Q}{RT} = \frac{Q}{RT'} - \frac{Q}{RT}$$

[5]The writer wishes to thank Mr. H. DeWet Erasmus for calling attention to this method of obtaining equation (11). The mathematical proof of the validity of direct integration in this instance, is solely the present writer's responsibility, however.

or

$$-\frac{\Delta Q}{RT} = \frac{Q}{R(T-\Delta T)} - \frac{Q}{RT}$$

so that

$$\int_{\Delta Q \doteq 0} -\frac{\Delta Q}{T} = Q \int_{\Delta T \doteq 0} -\Delta\left(\frac{1}{T}\right)$$

$$\frac{dQ}{T} = Q\, d\left(\frac{1}{T}\right)$$

Therefore,

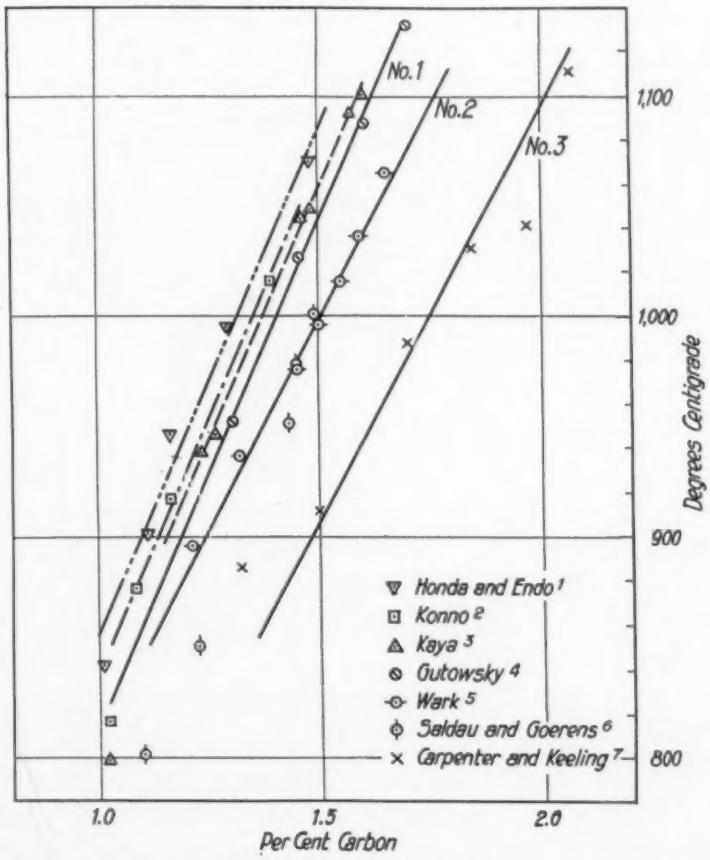
$$T\, dQ = Q\, dT$$

Equation (11) was first derived by Jones and Partington[6] in a somewhat different way, much less simple, even, than that shown in the first method above. We clearly note again that when the heat of solution is negative, that is, when the solute dissolves with an absorption of heat, the value inside the parentheses in equation (11) will be less than 1, so that undercooling can take place. If the radius of the nuclei is less than the equilibrium radius r, the temperature T′ decreases without precipitation and the solution consequently becomes supersaturated. In such solutions, the tendency towards crystallization is, however, extremely small at a low degree of supersaturation. The smaller nuclei (that is, $<r$) which could form comparatively easily due to molecular collisions, are unstable, however, and dissolve again immediately; the larger particles (that is, $>r$) which are stable are not readily formed on account of their size, even in spite of the probably high velocity of crystal growth. According to equation (11) as T′ decreases, the equilibrium particle-size r decreases similarly and the conditions thus become more favorable for the formation of a larger number of nuclei, so that when crystallization finally takes place, the crystallization velocity will be large, as was demonstrated by the work of Miers and Isaacs in their study of labile solutions.

The A_{cm} Line Under Normal and Labile Conditions

Before we proceed to calculate the free surface energy of Fe_3C, let us first examine critically the nature of the A_{cm} lines obtained by

[6]W. J. Jones and J. R. Partington, "A Theory of Supersaturation," *Philosophical Magazine*, Vol. 29, 1915, p. 35.



[1]Honda and Endo, *Science Reports*, Tohoku Imperial University (1927), 16, 627. Magnetic method.
[2]Konno, Ibid. (1923), 12, 127. Dilatometric.
[3]Kaya, Ibid. (1925), 14, 529. Resistance.
[4]Gutowsky, Metallurgie (1909), 6, 737. Heycock and Neville method.
[5]Wark, Ibid. (1911), 8, 704. Annealing and quenching.
[6]Saldau and Georens. Original paper inaccessible.
[7]Carpenter and Keeling, *Journal*, Iron and Steel Institute (1904), 65, 224. Thermal analysis from the melt.

Fig. 1—The A_{cm} Line as Determined by Various Methods of Investigation.

various investigators and determine if we cannot account for their disagreement on the basis of the influence of particle-size and surface energy of Fe_3C.

In connection with the writer's theoretical studies in the equilibria of the iron-carbon system, he has noticed the disagreement in the results of various careful investigations on the A_{cm} line, as shown in Fig. 1. The A_{cm} line No. 1 is one obtained by the writer from Sato's data and the method of obtaining it will be published in these transactions. It is noteworthy that the points obtained by Gutowsky all fall on curve No. 1, which the writer has good reasons to believe is the most nearly correct one. It should be noted that all the points

above curve No. 1 have been obtained by heating and cooling steels initially at room temperature, when Fe_3C already exists as a structurally stable phase. All the points lying below curve No. 1 (with the exception of those obtained by Carpenter and Keeling which determine curve No. 3) have been obtained by annealing and quenching in order to differentiate the homogeneous from the heterogeneous field. Only the points obtained by Carpenter and Keeling were determined from the melt, in connection with their study of the liquidus and solidus lines of the iron-carbon system.

Although the various values obtained by the Japanese workers are somewhat discordant, yet their loci are all more or less parallel to curve No. 1 as shown in Fig. 1, so that we may legitimately conclude that the disagreement is to be attributed merely to a temperature lag in the observed A_{cm} points. The points obtained by Wark in his careful investigation involve annealing and quenching, and give an A_{cm} line of an entirely different slope (curve No. 2). The Carpenter and Keeling A_{cm} line (No. 3) presents the least slope of the three curves shown in Fig. 1.

The disagreement in the various sets of data (which fall into three classes, as it were) requires some explanation. It occurs to the writer that the influence of the particle-size of the iron carbide (Fe_3C) may adequately account for the disagreement. In the heat treatment by Wark, the samples were first quenched to a fully martensitic structure, (that is, heterogeneous structure in which Fe_3C is colloidally dispersed in the ferrite needles, containing perhaps a small amount of carbide in solid solution) and then heated to successively higher temperatures until the structure is completely homogeneous again, that is, austenitic. Hence, what we really obtain at any temperature, is the equilibrium between iron and Fe_3C particles well within the range in which particle-size affects its solubility—10^{-5} to 10^{-6} cm. in radius.

There are many fine points in the classical work of Carpenter and Keeling on the constitution diagram of the iron-carbon system, which strongly indicate that in the range of temperature lower than, say, 1200 degrees Cent. (2190 degrees Fahr.), their thermal data are quite reliable. Note in Fig. 1 that their A_{cm} curve indicates a higher solubility at any temperature than is commonly accepted. The usual explanation, of course, has been that their samples were considerably undercooled before austenite began to precipitate Fe_3C. The undercooling is in turn attributed to the thermal hysteresis com-

mon to all transitions in which a change of state (phase) is involved. Kaya obtained fairly reliable values, also by cooling down from a fairly high temperature to which the steel sample was heated, initially from room temperature, and his rate of cooling was about the same as that adopted by Carpenter and Keeling in their thermal studies. On the other hand, the A_{cm} line No. 2 was obtained by the method of quenching and annealing and should, therefore, reasonably exclude the probability of undercooling. Yet Wark's A_{cm} line (No. 2) shows supersolubility. In Wark's case, as well as in Carpenter's and Keeling's, the influence of the particle-size of Fe_3C appears to the present writer to be an important factor. In Kaya's case, his steel samples contained only the normal Fe_3C plates (in pearlite) and the proeutectoid Fe_3C practically dissolved and precipitated *in situ* in the austenite grain boundaries, and consequently the problem of nucleation and crystal growth is not such a vital factor in determining the equilibrium A_{cm} line.

The writer has already shown[7] on thermodynamic grounds that the solute in solid γ Fe (austenite) cooled from the melt is elementary carbon which combines to form Fe_3C upon precipitation. Hence, when the steel cools down to the A_{cm} line, the first Fe_3C particles precipitated will be extremely small in size and they will tend to go back into solution again. In this way, undercooling takes place easily, so that, for example, a 1.7 per cent carbon steel shows as much as 158 degrees Cent. (316 degrees Fahr.) retardation in the A_{cm} point (Fig. 1).

The Free Surface Energy of Fe_3C

Thompson[8] was the first one to attempt to measure the free surface energy of Fe_3C by approximating the degree of supersaturation from the change in the specific resistance of the steel samples. In this way, he obtained 1350 dynes per centimeter which, considering the extreme hardness of Fe_3C, appears too small. Aside from the fact that the theoretical basis of his calculations is open to serious question, he used a wrong equation, in which M (the molecular weight of the solid) was omitted,—although his calculated value happens to be of the right magnitude.

---

[7]Op cit, reference No. 1. It may be mentioned here that the writer has gathered enough evidence to warrant a statement that at about 1020 degrees Cent., there appears to occur a transition in the austenite, $\gamma c \rightleftarrows \gamma Fe_3C$, γc being stable above 1020 degrees Cent.

[8]Thompson, "The Interfacial Tension Between Carbide of Iron and Iron," *Transactions*, Faraday Soc., 1922, Vol. 17, p. 391.

As Thompson's experimental data, however, appear to be quite reliable, it is fairly safe to calculate on the basis of his data the magnitude of the free surface energy of Fe_3C. Thompson took two samples of a steel containing about 0.69 per cent carbon and quenched them from 780 degrees Cent. (1435 degrees Fahr.). Then he tempered one sample at 500 degrees Cent. (930 degrees Fahr.) in order to make the structure finely sorbitic. The other piece was annealed for several hours at 650 degrees Cent. (1200 degrees Fahr.), as a result of which the Fe_3C particles were completely spheroidized. The specific resistances of these two samples (at 10 degrees Cent.) were determined to be 17.87 and 16.73 microhms per cubic centimeter, respectively. From these values he calculated the difference in solubility as 0.042 per cent carbon. He assumed the solubility in the second case to be about 0.02 per cent carbon at 500 degrees Cent. (930 degrees Fahr.), so that s_2 (the solubility of the tempered piece) must then be 0.062 per cent. Since the specific resistances of the steels were measured at 10 degrees Cent., we are really dealing with "equilibrium" conditions as obtained at that temperature and not at 500 degrees Cent. as Thompson would have it. The high-temperature treatment is merely to help the colloidally dispersed Fe_3C particles to aggregate to a size within the resolving power of the microscope. It is, therefore, necessary to calculate the solubilities of Fe_3C in ferrite at 10 degrees Cent. (i.e., room temperature).

Yamada[9] has shown that the resistance of steel, θ, at 20 degrees Cent. can be expressed as a linear function of per cent carbon (C) thus

$$\theta = \alpha + \beta C \qquad (15)$$

in which, α the specific resistance of pure iron, is 10.12 microhms per cubic centimeter and β has a value of 0.89. A steel containing 0.69 per cent carbon should then have a specific resistance of about 16.15 microhms per cubic centimeter from which we infer that the second steel sample of Thompson must be supersaturated with Fe_3C. This is as we should expect, because the particle-size of the finely spheroidized cementite is well within the range in which particle-size is a factor of solubility. Using Benedick's value (which Thompson also quoted in his paper) of 2.68 microhms per cubic centimeter increase

[9]Yamada, "On the Solubility of Carbon in Pure Iron," Science Reports, Tohoku Imperial University, Vol. 15, 1926, p. 851.

in resistance per 0.1 per cent dissolved carbon (carbide), the difference between 16.73 and 16.15 microhms gives 0.023 per cent carbon as the increase in the solubility of Fe_3C in the ferrite[10]. Accepting 0.007 per cent as the normal solubility of carbon in ferrite at room temperature the annealed sample, therefore, contained about 0.030 per cent carbon, while the tempered sample contained about 0.072 per cent carbon.

The best datum[11] on the specific gravity of Fe_3C is 7.67. It remains to evaluate r_2 and r_1. Thompson gives 0.5×10^{-5} centimeters as the radius of sorbitic cementite, which is, according to the work of Lucas, a little low. It would be more accurate to assign 10^{-5} centimeters to r_2, and the radius of the finely spheroidized cementite (r_1) should then be of the order of 10^{-4} centimeters. Since the solubilities are so small, no error is introduced in not converting them to mol per cent Fe_3C, so that we can directly substitute all the necessary values in equation (1) thus

$$(8.32 \times 10^7)\ (293)\left(2.3 \ln \frac{0.072}{0.032}\right) = 2\sigma \left(\frac{179.5}{7.67}\right)\left(\frac{1}{10^{-5}} - \frac{1}{10^{-4}}\right)$$

which, solving for σ gives

$\sigma_{20°C}$ = 4,900 ergs per square centimeter (in round figures)

The free surface energy[12] of Fe_3C at room temperature (20 degrees Cent.) is thus calculated to be several times the figure given by Thompson, which the writer had thought to be too low, considering its extreme hardness. On account of the small solubilities involved in the present case, the ratio of solubilities is susceptible to a fairly large error, but inasmuch as the value of r_1 may be a little low (as the exact period of anneal is not given by Thompson and the longer the anneal, the larger the particle-size of Fe_3C), the lower limit of the ratio of solubilities has been used in order to counterbalance it.

[10]Since the temperature coefficient of resistance is small, no appreciable error is introduced in comparing Thompson's values obtained at 10 degrees Cent. with values obtained at 20 degrees Cent.

[11]Consult Iron Oxide Reduction Equilibria by Oliver C. Ralston, Bureau of Mines Bulletin No. 296, p. 218, 1929.

[12]Surface tension is merely a hypothetical tension conceived to be acting in all directions parallel to the surface. Hence, surface tension in dynes acting on a unit area of one square centimeter is equal to surface energy in ergs per square centimeter.

It would be interesting to study the nature of the equilibria obtained by Carpenter and Keeling in their determination of the A_{cm} line (No. 3 in Fig. 1) and incidentally calculate the free surface energy from another source. From the "equilibrium" A_{cm} line (No. 1 in Fig. 1) we obtain at 1136 degrees Cent. (2075 degrees Fahr.) $s_1 = 1.7$ per cent carbon and from the Carpenter and Keeling A_{cm} line, $s_2 = 2.1$ per cent carbon. Converting them to mol per cent, we have 7.43 and 9.05 per cent, respectively. Assuming that 1136 degrees Cent (2075 degrees Fahr.) the specific gravity is about 7.3 and substituting all the necessary values in equation (2) we have

$$(8.32 \times 10^7)\ (1409)\left(2.3 \ln \frac{9.05}{7.43}\right) = 2\frac{\sigma}{r}\left(\frac{179.5}{7.3}\right)$$

$$\frac{\sigma}{r} = 4.7 \times 10^8 \text{ ergs/cm.}$$

If we know the correct value of r, we can easily derive the value of σ. Unfortunately equations (2) and (11) do not permit us to solve simultaneously the values of σ and r. However, if the Carpenter and Keeling A_{cm} line was really obtained under conditions which brought about undercooling, due to the extremely fine particle-size of the Fe_3C involved, equation (9) should give us the same value of σ/r, that is, 4.7×10^8 ergs per centimeter. We must first calculate the heat of solution of Fe_3C in γFe under normal equilibrium conditions. It can be easily shown that from equation (4), the following relationship can be derived, thus

$$\ln \frac{s_2}{s_1} = \frac{Q}{R}\left(\frac{1}{T_2} - \frac{1}{T_1}\right) \qquad (12)$$

in which s_2 and s_1 are the normal solubilities at T_2 and T_1 respectively and $-Q$ is the molal heat of solution. From the A_{cm} curve No. 1 (Fig. 1) we thus calculate Q to be about 4,900 cal./mol of Fe_3C precipitated.[13] Substituting all the necessary values in equation (11),

[13]The value here thermodynamically calculated is at great variance with those derived from experimental data on the heats of reaction upon tempering steels quenched from different high temperatures. The nature of such reactions and the phases involved in the reactions, are quite uncertain and are consequently amenable to several interpretations. The writer has now in course of preparation a paper dealing with this subject.

including the value of T′, which is 978 degrees Cent. (1792 degrees Fahr.) (obtained from Fig. 1) we have

$$1251 = 1409\left[1 - \frac{2\,(179.5)\sigma}{(4900 \times 4.2 \times 10^{7})\,(7.3)\mathrm{r}}\right]$$

$$\therefore \frac{\sigma}{\mathrm{r}} = 4.7 \times 10^{8} \text{ ergs per centimeter}$$

which checks exactly the value derived previously. Equation (11) should, therefore, be very useful in determining the degree of undercooling possible, because if we substitute the value of σ/r obtained from equation (2) in equation (11) knowing, of course, the molal heat of solution of the solute, we can calculate T′ if T is known and *vice versa*.

Thus it is shown for the first time in a quantitative way, that the A_{cm} line obtained by Carpenter and Keeling differs materially from the normal A_{cm} line because of the delayed precipitation of Fe_3C (with the consequent state of supersaturation) due to the influence of its fine particle-size and high surface energy. The former may, therefore, be considered as the *labile* solubility line and the latter (A_{cm} line No. 1) the normal equilibrium solubility line. Equation (11) also enables us to conclude that in Wark's case, the undercooling is much less, because the particle-size of the Fe_3C in his samples must be larger than that in Carpenter's and Keeling's experiments. That this is so, may be inferred from the fact that Wark held his samples at constant temperatures for some time before quenching.

Let us approximate the surface energy at 1136 degrees Cent. (2075 degrees Fahr.). From the work of Lucas[14] the radius of the Fe_3C particles just within the microscopic range is about 8×10^{-6} centimeters, which may be safely used for the value of r,[15] so that

$$\sigma_{1136^{\circ}\mathrm{C}} = (4.7 \times 10^{8})\,\mathrm{r} = (4.7 \times 10^{8})\;(8 \times 10^{-6})$$

[14]For the approximation of the particle-size of the dispersed Fe_3C in quenched steel, consult the various remarkable works by F. F. Lucas: "The Micro-structure of Austenite and Martensite," TRANSACTIONS, American Society for Steel Treating, 1924, Vol. 6, p. 669; "Further Observations on the Microstructure of Martensite," Ibid., Vol. 15, 1929, p. 339; and other papers.

[15]From equation (11) we know that as the temperature decreases the equilibrium radius of the Fe_3C particles also decreases. From Lucas' works, the present writer approximated the stable radius to be between 5×10^{-6} to 10^{-7} cm. so that the mean (in whole number) is 8×10^{-6} cm. It will be shown later that the equilibrium radius of the Fe_3C particles in martensite would be even smaller, due to the high degree of undercooling.

= 3,800 ergs per square centimeter (in round figures)

The calculated value of σ at 1136 degrees Cent. is consistent with the value calculated at 20 degrees Cent. because we know that surface energy decreases as the temperature increases. An indirect method of checking the degree of reliability of the calculated values of σ is available when we recall that the total surface energy U is a constant if we can reasonably consider σ as a linear function of the temperature. It can thus be easily shown by thermodynamics (by means of a Carnot cycle) that

$$U = \sigma + q = \sigma - T\frac{d\sigma}{dT} \qquad (13)$$

in which q is the latent heat of surface tension and is equal to $-T\frac{d\sigma}{dT}$ From the two values of σ calculated at 20 and 1136 degrees Cent., we obtain approximately $\frac{d\sigma}{dT} = -1$ erg per square centimeter per degree Cent. with which we can calculate U in equation (13) thus

$$\left.\begin{aligned} U_{20°C} &= 4{,}900 + 293 = 5{,}193 \\ U_{1136°C} &= 3{,}800 + 1{,}409 = 5{,}209 \end{aligned}\right\} \text{ ergs per square centimeter}$$

The excellent check gives us some assurance at least that the calculated values of σ are of the right magnitude. Moreover, the internal pressure calculated on the basis of these figures is of the relative order compared to the other metals.

Hardening of Steels From the Standpoint of Surface Energy

The writer feels it is not inappropriate to discuss briefly the probable influence of surface energy on the hardness of quenched steels. So many theories of hardening have been advanced by metallurgists in recent years that the present writer hesitates even to express his own views on the subject. On the one hand, we have the colloidal viewpoint represented by Alexander[16] and on the other hand, we have the purely mechanical viewpoint incorporated in

[16] J. Alexander, "Colloidal State in Metals and Alloys," *Chemical and Metallurgical Engineering*, 1922, Vol. 26, 54, 119, 170 and 201.

Jeffries' and Archer's "slip-interference" theory,[17] which is now the most popularly accepted one in this country. The latter, while presenting a captivating picture of hard particles mechanically exerting a keying action that prevents slip in the grains of ferrite composing the matrix, has always been something less than satisfactory to the writer. It appears to him to be an attempt to visualize a very complicated physico-chemical phenomenon in terms of a simple mechanical analogy. Unfortunately, surface energy, like other manifestations of atomic forces, cannot be easily visualized except in its total cumulative effects, and so is not amenable to exact presentation in terms of analogies.

According to the slip-interference theory, the minute cementite particles interfere with the slip of the ferrite grains, already minute. On the general theory of grain-size inheritance, the writer could never quite understand why the ferrite in martensite has ever been considered extremely fine-grained.[18] Recently, Heindlhofer and Bain[19] have shown conclusively that the ferrite grains are coarse. What remains of the slip-interference theory is the so-called "critical dispersion," indeed a happy phrase. Alexander evidently anticipated this in his theory of "maximum colloidality," defined as that state of dispersion in which the specific properties of a colloid are at a maximum.

According to the slip-interference theory, the interference is a purely mechanical action, while Alexander emphasizes the colloidal properties of a dispersed system, e.g., the high surface energy of a dispersed phase. In this, the writer subscribes to Alexander's viewpoint. The high surface energy of Fe_3C[20] shown in this paper can quite adequately account for the great hardness of martensite, as will be shown below. If martensite is an enforced solid solution, as Honda has claimed for a number of years, the high degree of supersaturation

[17] Z. Jeffries and R. S. Archer, "Slip Interference Theory of Hardening of Metals," *Chemical and Metallurgical Engineering*, Vol. 24, 1921, p. 1057.

[18] At the time Jeffries and Archer proposed their theory (1921) we had just begun to use the X-ray spectrometer in metallurgical work. The X-ray spectrograms of martensite show broadening of diffraction lines, which they, perhaps following the lead of Debye and Scherrer, interpreted as refinement of the ferrite grains, whereas Honda interpreted it as distortion of the ferrite lattice, because he found martensite not to be fine-grained as generally assumed.

[19] K. Heindlhoffer and E. C. Bain, "A Study of the Grain Structure of Martensite," TRANSACTIONS, American Society for Steel Treating, Vol. 18, 1930, p. 70.

[20] The slip-interference theory also requires that the dispersed phase must be considerably harder than the matrix. This is merely incidental, as compounds, as indicated by their high hardness, have also high surface energy.

should, of course, result in considerable distortion of the ferrite lattice. It is, however, extremely doubtful if any degree of distortion of the lattice could quite adequately account for the hardness of martensite. Moreover, it is also doubtful if the ferrite in martensite can dissolve more than 0.1 per cent carbon at most.

In the current controversy regarding the nature of martensite, the writer feels that the confusion arises from a misunderstanding of the scope of the terms martensite and troostite. Evidently these terms have been used to define the allotriomorphic forms of the structural phases present in quenched steels, rather than their actual chemical constitution.[21] Thus the acicular structure of martensite is not a specific idiomorphic characteristic of martensite (as a structural phase) but is merely indicative of the high velocity of transition from an extremely labile solid solution. It is, of course, quite probable that in the rapid transformation from a homogeneous phase (austenite) to a heterogeneous system, the internal stress may be so highly localized in places so that a transitional phase[22] may be formed, but the amount of the transitional phase will be very small. This phase, which seemingly has the characteristics of a solid solution, should be considered only as an extremely unstable mesomorphic state of martensite. At the present stage of development of metallographic microscopy, we are only able to detect the presence of Fe_3C particles after the quenched steel has been tempered at 100 degrees Cent.

We do not know at exactly what stage of dispersion of the colloidal Fe_3C[23] we obtain maximum hardness—perhaps at the so-called "critical dispersion" or in the zone of "maximum colloidality"—but we do know that when the Fe_3C particles reach a state of aggregation large enough to be visible under the microscope, the system is not generally at its maximum hardness. On the basis of these facts alone, are we quite justified in assuming that before tempering at,

---

[21]For example, pearlite may be considered loosely as a structural phase, yet from the standpoint of the phase rule, it is composed of two phases, ferrite and Fe_3C.

---

[22]This transitional phase is the body-centered tetragonal ferrite, which Honda calls α-martensite. Some metallurgists have claimed that the keying action (slip interference theory) is due to this phase.

---

[23]According to Honda and h[illegible] school, the first stage of precipitation from martensite is carbon, because they have assum[illegible] that the solute in austenite is also carbon. We know definitely that ΔF of the formation of Fe_3C is positive and is a fairly large quantity at room temperature up to A_1. It would, indeed, be very difficult to conceive the mechanism of their recombination. Hence, the precipitated constituent present in martensite must be Fe_3C; likewise the solute in austenite.

say, 100 degrees Cent., the martensite is a solid solution? Even granting that the transition phase is a solid solution, proof is required that (1) it is very hard and (2) it is present in sufficient quantity to account for the high hardness of quenched steel. Is it not more reasonable merely to conclude from the evidence at hand that the tempering action simply helps to hasten the aggregation of the sub-microscopic particles of Fe_3C?

We shall now attempt to calculate the relationship between the amount of surface energy involved and the increase in the hardness of steel. According to Honda and Takahashi[24] it is more reasonable, from the standpoint of mechanics, to define the hardness as the work required to produce a unit volume of indentation, that is

$$H = \frac{W}{V} = \int_0^h \frac{P\,dh}{V} \qquad (18)$$

Since, however,

$$P = kh\,(1 + ah) \qquad (19)$$

and

$$V = \pi h^2\,(R - \tfrac{1}{3}h) \qquad (20)$$

Therefore,

$$H = \frac{k \int_0^h h\,(1 + ah)\,dh}{\pi h^2\,(R - \frac{1}{3}h)}$$

$$= \frac{k\,(3 + 2ah)}{\pi\,(6R - 2h)} \qquad (21)$$

The measured hardness, therefore, depends upon the load applied, because loading produces a certain amount of cold working. The initial or natural hardness, in which we are more interested in this paper, is then defined by

[24] K. Honda and K. Takahashi, "On the Indentation Hardness of Metals," Science Reports, Tohoku Imperial University, Vol. 16, 1927, p. 357.

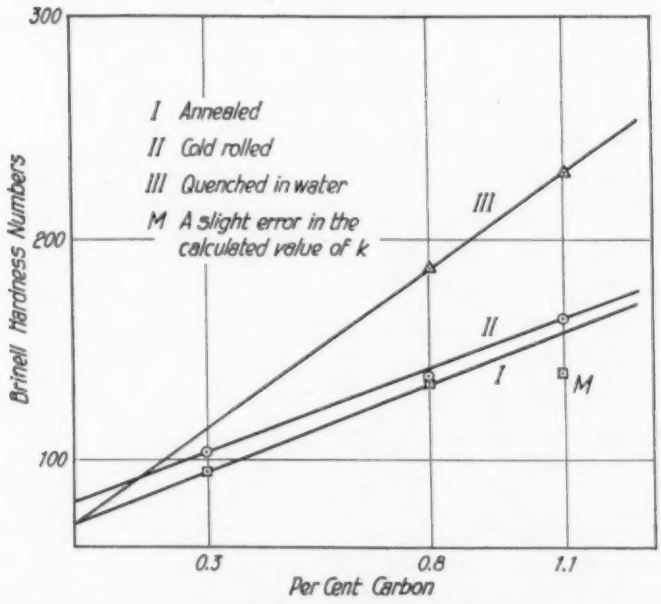


Fig. 2—Natural Hardness (H_0) of Steels in Three States: (I) Annealed; (II) Cold-rolled; and (III) Quenched in Water. (After Honda and Takahashi.)

$$H_0 = \frac{k}{2\pi R} \qquad (22)$$

since, with an infinitely small load, $h = 0$. The value of k can be found from the tangent at the origin, to the P-h curve (Pressure against depth of indentation), or from the value of a, thus

$$k = \frac{P_1}{h_1 (1 + a h_1)} \qquad (23)$$

where

$$a = \frac{P_1 h_2 - P_2 h_1}{P_2 h_1 (h_1 - h_2)} \qquad (24)$$

In Fig. 2 is shown the natural hardness of steels (H_0) after receiving three kinds of treatment, namely: annealing, cold rolling and quenching in water. The points plotted are taken from Honda's and Takahashi's paper *(loc cit)* which the present writer believes to represent work of very high accuracy. There are several conclusions which can safely be drawn from Fig. 2. Thus in the relation between curves I and II, since the amount of hardening by cold working de-

creases with increasing Fe_3C content, we conclude that the cold working affects only the ferrite and not the cementite. This is what we should expect, knowing the extreme hardness (and brittleness) of Fe_3C. Moreover, the two curves intersect each other at about 1.7 per cent carbon, the limit of the true steel range. Lastly, curve I when extrapolated to 6.67 per cent carbon, gives a hardness of about 600 for Fe_3C. This value is in good agreement with that obtained by Tamaru,[25] who found the hardness of Fe_3C to be about 640.

It is, indeed, very interesting to note that curve III intersects pure iron at the same point as curve I. According to the present writer's views, curve III represents the linear increase in hardness of quenched steels due (1) to the increase in the total surface energy of Fe_3C contained in the steels and (2) to the increase in the hardness of the ferrite grains themselves as a result of the distortion of the lattice by the high degree of supersaturation. The dominant factor, however, is the former, although Honda and his school recognize only the second cause. No one has ever paid the slightest attention to the probable influence of surface energy, except Alexander.

The difference then between the Brinell hardness of annealed steels and those quenched in water, that is, $\triangle H_0$, is to be interpreted as the additional amount of energy necessary to produce a unit volume of indentation. Thus, the values of $\triangle H_0$ for the 0.8 and 1.1 per cent carbon steels, are 52 and 72 kg.-mm. respectively. These are equivalent to 5×10^6 and 7×10^6 ergs. Although it is probable that these values of $\triangle H_0$ may be a little high, on account of the residual strain-hardening due to quenching, nevertheless, it should be interesting to determine the magnitude of the surface energy and then compare it with the value of $\triangle H_0$. If the hardening of quenched steels is due to the surface energy of the highly dispersed Fe_3C, then there should be substantial agreement between the two calculated values.

The total free surface (interface) of the dispersed Fe_3C, S, can be obtained from the relationship

$$S = (V/v)s \qquad (25)$$

in which V, the total volume of Fe_3C in a unit volume of steel, divided by v, the volume of a particle of Fe_3C, gives the number of particles, N. Since s is the surface of a particle of Fe_3C, then (V/v) or N

[25] K. Tamaru, "On the Hardness of Different Structures in Steel," Science Reports, Tohoku Imperial University, Vol. 15, 1926, p. 829.

multiplied by s, gives the total surface of the Fe_3C present in a unit volume of steel. Considering the particles to be spheres of radius r, we obtain upon substitution of the formulae for the volume and surface of spheres

$$S = 3V/r \tag{26}$$

The total surface energy, Σ, is then obtained by simply multiplying S by σ, so that

$$\Sigma = S\sigma = \frac{3V\sigma}{r} \tag{27}$$

If we accept the densities of Fe and Fe_3C to be 7.87 and 7.67 grams per cubic centimeter, then in a steel containing 0.8 per cent carbon, the volume percentage of Fe_3C is 12.2 per cent. (In all calculations below we shall only discuss the 0.8 per cent carbon steel, as the values for this steel bear a simple proportional ratio to the values for the 1.1 per cent carbon steel.) We, therefore, know all the terms in equation (27), to calculate Σ except r. It may be conservatively admitted that the smallest particle-size just within the resolving power of our best metallographic microscopes is about 10^{-6} centimeters in radius. This particle-size does not, however, represent the maximum hardness in quenched steels. Although the present writer is not sure that equation (11) can be used to determine the value of r in quenched steels as it is not a normal case of depression in the precipitation temperature on account of the lack of nucleation, nevertheless, we should be able to arrive at some approximate value of r. Let T′ be at room temperature, T, the pearlite transformation temperature, Q, the heat of solution, 4,900 cal./mol; ρ, the density of Fe_3C, 7.67 grams per cubic centimeter and σ, the surface energy 4,200 ergs per square centimeter. Substituting these values in equation (11) we have

$$293 = 993\left[1 - \frac{2 \times 179.5 \times 4200}{(4900 \times 4.185 \times 10^7)\ (7.67)\ r}\right]$$

which, solving for r, gives (in round numbers) 10^{-6} centimeters. This is the particle-size visible upon tempering so-called white martensite at 100 degrees Cent. Hence, the true equilibrium radius of untempered martensite must be somewhat less than 10^{-6} centimeters. In

order then to obtain a value of $\Sigma = 5 \times 10^6$ ergs, we have to assign 3.5×10^{-7} centimeters as the radius of the Fe_3C particles. This is just outside the microscopic range of resolution.[26] We have, as a matter of fact, calculated equation (26) on the assumption that the Fe_3C particles are perfect spheres. If they are not really spherical, then S will be larger than 3V/r (approaching 6V/r as the limit), so that actually the particle-size might be larger than 3.5×10^{-7} centimeters in radius.

If we are to believe with Honda, Bain and others, that the hardness is essentially due to the abnormal solution of carbon (not as Fe_3C, they maintain) resulting in the distortion or overstrain of the ferrite lattice, then thermodynamically we can calculate the energy equivalent of the hardening in terms of the suppressed heat of reaction. Now a cubic millimeter of a 0.8 per cent carbon steel contains 9.35×10^{-4} grams of Fe_3C. According to the present writer's calculations *(loc cit)*, the heat of precipitation of Fe_3C is equal to 27.3 cal./g. of Fe_3C, so that the suppressed heat of precipitation is equal to 2.55×10^{-2} cal. or 1.1×10^6 ergs. This figure is only one-fifth of the experimental value, which we have just seen, agrees with the value obtained if the hardening of quenched steels is assumed to be due to the surface energy of Fe_3C.

In the case of austenite preserved by quenching from a high temperature, we have the additional heat of transition of γ to αFe suppressed. According to Tamaru (*loc cit*) the hardness of austenite containing 0.8 per cent carbon is about 155, so that from Fig. 2 $\triangle H_0$ is equal to 21 kilogram millimeters per cubic millimeter or 2×10^6 ergs. The energy equivalent of the total suppressed heats of reactions should then be of this magnitude also. A cubic millimeter of a 0.8 per cent carbon steel contains 6.9 milligrams of ferrite. According to Umino[27] the heat of transition from γ to αFe is about 5.35 cal./g. The suppressed heat of transition of 6.9 milligram of γFe is equal to 3.7×10^{-2} cal. or 1.5×10^6 ergs. Adding to this the energy equivalent of the suppressed heat of precipitation as calculated above, 1.1×10^6 ergs, we have finally 2.7×10^6 ergs, which is in good

[26] Particles of this size should contain about 1000 molecules of Fe_3C each. Incidentally, the value of Σ obtained from equation (27) is for a cm.^{3} volume, so that it must first be divided by 10^3 for a cubic millimeter volume, as H_0 is expressed in kilogram millimeter per cubic millimeter.

[27] S. Umino, "On the Heat of the A_2 and A_3 Transitions in Carbon Steels," Science Reports, Tohoku Imperial University, Vol. 16, 1927, p. 1009.

agreement[28] with the value calculated from $\triangle H_0$, that is, 2×10^6 ergs.

Thus we see that the calculated equilibrium radius of the Fe_3C particles in martensite is of the order of $3 - 4 \times 10^{-7}$ centimeters. The question then arises: "Although not visible microscopically, is it so unreasonable to believe in the presence of Fe_3C particles of this size, even though particles three times larger are already visible?" It does not appear to the present writer as reasonable to conclude that because we cannot see the Fe_3C particles in white martensite, they are, *ipso facto* in solid solution. Unfortunately, due to the dominant influence of the physical metallurgists who have taken up the study of X-ray crystal analysis, almost all our theories of hardening today have been limited to variations of two concepts, namely: (1) that ferrite is very fine and (2) that the carbon in solid solution distorts the ferrite lattice. These concepts are the outgrowth of the physical interpretation of the broadening of the diffraction lines in the X-ray spectrogram of quenched steels. The first concept has been more or less completely exploded by the work of Heindlhoffer and Bain *(loc cit)*. We know that the substitutional type of solid solutions increases in hardness with increasing amount of solute, up to a certain point. If the stress on the lattice exceeds a certain degree, a new lattice may be formed, such as a body-centered tetragonal lattice from a body-centered cubic lattice or a body-centered cubic lattice from a face-centered cubic lattice. The presence of a body-centered tetragonal ferrite in quenched steel is to the writer evidence that the great internal stress has been relieved by the formation of a new lattice, however unstable. Proof that this body-centered tetragonal ferrite is extremely hard is totally lacking. It appears to the writer that the presence of a tetragonal ferrite is merely indicative of the quenching conditions which produce maximum hardness, and is rather the symptom than the cause.

One point brought up in support of the solid solution theory is that in quenched steels we cannot detect the A_0 point. This argument has always seemed unconvincing, because it has never been shown that the magnitude of the A_0 (either by magnetic or thermal analysis) does not decrease with particle-size. The present writer

---

[28]Although these calculations are true only qualitatively, nevertheless, from thermodynamic point of view, we gain an insight as to the relative hardness of α solid solution and of austenite in terms of the suppressed heats of reactions. The only way we can conceive the α solid solution to possess more potential energy than austenite quenched from the same temperature, is to assume that the heat capacity of the former is very much less than that of austenite. This is, however, not true, according to available experimental evidence.

believes that with decreasing particle-size A_0 will become increasingly difficult to detect, just as the heat of solution decreases with particle-size.

It has been shown by Mehl[29] that in spite of the great difference in hardness between an 0.89 per cent carbon steel in the annealed and the quenched states, yet their compressibilities in the two states are identical. This was also true of a 1.35 per cent carbon steel. This is, indeed, very remarkable and it was this fact which has led the writer to the study of the influence of surface energy of Fe_3C on the hardening of alloys. Aside from other sources of evidence, Mehl's observation constitutes strong evidence that the phases present in the annealed and quenched steels are the same, that is, ferrite and Fe_3C. If the hardness of martensite were due to lattice distortion as a result of abnormal solution of carbon in ferrite, the hardness could only have been produced by an alteration in the interatomic forces. In this case, the compressibility of the quenched steel should show an appreciable difference from that of the annealed state.

The writer presents the views expressed in this paper merely for the consideration of others who in the future may formulate new theories of hardening.[30] It appears to him that the physico-chemical interpretation of the rôle of the highly dispersed Fe_3C in terms of surface energy is more consistent than the purely mechanical concept of slip-interference emphasized by Jeffries and Archer. Moreover, the line of attack shown in this paper is applicable to all cases of precipitation hardening, whether the precipitated constituent is a compound or a simple metal. A compound will, of course, possess higher surface energy per unit area, but the total surface energy per unit volume is primarily a function of the degree of dispersion (that is, of the particle-size) as shown in the calculations above.

Summary

1. The theoretical relations between particle-size and solubility have been developed, together with certain equations governing normal and labile solutions.

[29] R. F. Mehl, "Interatomic Forces in Metals and Alloys," A.I.M.E. Technical Publication No. 57, 1928.

[30] It must be mentioned here that the writer is not the first one to advance an essentially chemical interpretation of hardening. Edwards and later Hanemann and Schrader advanced a theory that hardening is due to the formation of a compound, $Fe_{24}C$. Another variation of this theory of pseudo-molecule formation was proposed by Dean and Gregg. In their preoccupation with the concept of "shared" electrons, they overlooked the presence of unbalanced atomic forces at the interface.

2. The quantitative applications to the A_{cm} lines of the equations developed, result in a rational explanation of the difference in the various A_{cm} lines obtained. It is believed this is the first time an attempt has been made to apply quantitatively the laws of surface energy to metallic systems.

3. The surface energy of Fe_3C has been calculated and found to be about 4,900 and 3,800 ergs per square centimeter at 20 and 1136 degrees Cent. respectively. Considering the hardness of Fe_3C these values are not excessive.

4. The hardening of steels is discussed theoretically from the standpoint of surface energy of Fe_3C. Calculations are then made which indicate that the main factor in the hardening of quenched steels is the surface energy of the highly dispersed Fe_3C. The particle-size of the Fe_3C present in martensite is calculated to be of the order of $3 - 4 \times 10^{-7}$ centimeters in radius—just beyond the range of microscopic resolution. The hardness of austenite is theoretically discussed from the standpoint of the energy equivalent of the suppressed heats of reaction, and the calculated figures agree in the main with the experimental values.

5. It is suggested that the cause of precipitation hardening in metallic alloys lies in the surface energy of the dispersed phase. If the dispersed phase is a compound, the surface energy will be large; hence, the hardening will also be more pronounced than when the dispersed phase is a simple metal. However, the main factor is the degree of dispersion, that is, the size of the particles dispersed.

Acknowledgment

The writer acknowledges the kindness of his friend, Dr. Joseph T. Shipley, in helping him prepare this paper for publication.

DISCUSSION

Written Discussion: By F. C. Thompson, The Victoria University of Manchester, England.

The paper by Yap, Chu-Phay is one of the very greatest interest and value. His reference to my earlier attempt to measure the surface tension of iron carbide and his use of my own experimental data for his redetermination naturally afford me considerable satisfaction. I should like to take this opportunity of congratulating both the author and the Society through which this publication comes on a piece of work of fundamental importance.

I am not surprised that the author has found a value for the surface tension some three times as high as that given in my determinations published in the *Transactions* of the Faraday Society, Vol. 17, p. 392. I pointed out in

there that my calculation could only give a *minimum* value for this constant. So far as I can see, the treatment which Yap, Chu-Phay has adopted is more likely to lead to the real value than my own, and I should imagine that his value must be fairly close to the truth.

Written Discussion: By F. G. Sefing, metallurgist, Michigan State College, East Lansing, Mich.

The correlation between the surface energy of Fe_3C and some of the properties of steel is particularly interesting as presented by the author.

The abnormality of carbon steel as discussed by Harder and Johnson* may be partly explained by the discussion of the author of his Fig. 1.

About the middle of page 310 reference is made to the so-called body-centered tetragonal lattice of the transitional martensite which is recognized by Phragmen, Honda, and others. According to the simplest principles of crystallography such a crystal cannot exist in steels and irons. For a substance crystallizing in a particular system (isometric in the case of steel) cannot crystallize in a new system and if it is found to do so it is a pseudomorph and is always unstable, which is the case of the tetragonal martensite. Let us be careful to hold to the principles of crystallography in interpreting our X-ray spectograms.

On page 297 the middle paragraph explains the lowering of the A_{cm} line 158 degrees Cent. in connection with the production of extremely small Fe_3C particles, which tend to go back into solution even below the A_{cm} line. This is inconsistent with our present conception of energy and physical metallurgy inasmuch as an unstable solid solution such as austenite below the A_{cm} line could not possibly dissolve any Fe_3C particles however small.

Whether the hardness of heat treated steel is caused by: 1. Surface energy of Fe_3C; or 2. Distortion of Ferrite grains (page 307) is merely one of opinion, as each group of scientists can prove its cause satisfactorily to itself. Attention is called to the results published by the Michigan Engineering Experiment Station bulletin 37, "Thermodynamics of a Heat Treated Steel," where the hardness of a steel was directly associated with the energy content of the metal and also the energy content was shown to be surprisingly close to the work done on the steel by expanding it during the hardening process.

Author's Closure

I am very grateful for the kind words of encouragement from Professor Thompson, particularly in view of the fact that my colleagues have ignored my paper. I had thought that the concept of surface energy playing a large rôle in the precipitation hardening of alloys, should be of challenging interest to those who have one time or another proposed some theory of hardening.

It is a little difficult for me to grasp the substance of Mr. Sefing's comments; nevertheless, I appreciate his interest in my paper. I cannot quite see the validity of his objection to the theory that a solution may behave as an unsaturated one towards particles smaller than the equilibrium particle-size and as a supersaturated one towards particles larger than the equilibrium particle-size. To deny this is to deny the occurrence of two well-known phenomena: undercooling and supersaturation.

*TRANSACTIONS, American Society for Steel Treating, Vol. XV, p. 54 et seq.

COMPARATIVE STUDY OF LOW CARBON BESSEMER AND BASIC OPEN-HEARTH WIRES BY X-RAY DIFFRACTION METHODS

By Norman P. Goss

Abstract

A comparative study was made of annealed low carbon bessemer and basic open-hearth steel wires given small plastic deformations and then reannealed at various temperatures.

The X-ray spectrograph was used because of its ability to detect the effect of small plastic deformations given annealed wires. The results found were as follows:

1. *The bessemer steel wires given the same mechanical and heat treatments as the basic open-hearth wires were more sluggish to recrystallization.*
2. *In bessemer and basic-open hearth steel wires reduced 10 per cent in area by wire drawing dies and annealed at 1300 degrees Fahr., no grains recrystallized in the bessemer wire, while large grains grew in the open-hearth wire.*
3. *In general this paper shows how impurities inherent in all bessemer steels influence the grain structure when heat treated.*

IN this investigation low carbon steel rods produced from basic open-hearth steel and bessemer steel were used. The green hot-rolled rods $\frac{7}{16}$ inch in diameter were drawn down to $\frac{3}{8}$ inch wires in one draft through wire drawing dies, and then pot annealed at 1250 to 1300 degrees Fahr. (675 to 705 degrees Cent.) for 6 hours. This included the time required to bring the wires up to temperature and the cooling time.

X-ray diffraction patterns were made of the annealed wire specimens, and in every specimen examined, the wires were completely recrystallized. The grains in the low carbon steel basic open-hearth wires were larger than those in the bessemer steel wires. In addition the grains were found to be uniform in size and distributed at random.

The author, Norman P. Goss, a member of the society, is research physicist for the Cold Metal Process Co., Youngstown, Ohio. Manuscript received March 19, 1932.

The chemical analysis of the wire samples are given below.

Basic Open-Hearth	Per Cent	*Bessemer Steel*	Per Cent
Carbon	0.09	Carbon	0.11
Manganese	0.37	Manganese	0.41
Sulphur	0.041	Sulphur	0.044
Phosphorus	0.018	Phosphorus	0.102
Silicon	0.006	Silicon	0.006

Comparing the chemical analysis of the wires, it is seen that the phosphorus content of the bessemer wire is nearly six times greater than that of the basic open-hearth wire. This is characteristic of all bessemer steel, and it may influence the recrystallization properties of such wires.

The annealed wires were given area reductions as follows:

Per Cent Area Reduction	*Reduction in Diameter* Inches
5	0.375 to 0.365
10	0.375 to 0.356
15	0.375 to 0.345

The object of this investigation was to determine the effect of heat treatment on the grain structure of bessemer and open-hearth steel wires given slight plastic deformations. X-ray examination of the wires with area reductions of 5 per cent showed the grains to be completely fragmented, but no directional characteristics were developed. An area reduction of 15 per cent was sufficient to produce preferred orientation of the grain fragments, but it was not very intense. From the nature of these X-ray diffraction patterns it would appear that the bessemer steel wires had received more cold work, but this is due to the difference in grain size. These observations would lead one to believe that the bessemer steel wires should respond more readily to heat treatment than the basic open-hearth wires. The experimental results are contrary to these deductions.

The cold-worked wires were cut into short lengths and annealed for one hour at 1000, 1100, 1200, 1300 and 1600 degrees Fahr. (540, 595, 650, 705 and 870 degrees Cent.). The specimens of bessemer steel wires and open-hearth steel wires given the various area reductions were annealed together at these temperatures.

When these wires were annealed at 1000 degrees Fahr. for one hour no recrystallization resulted. Longer annealing periods were tried, but the results were the same as before.

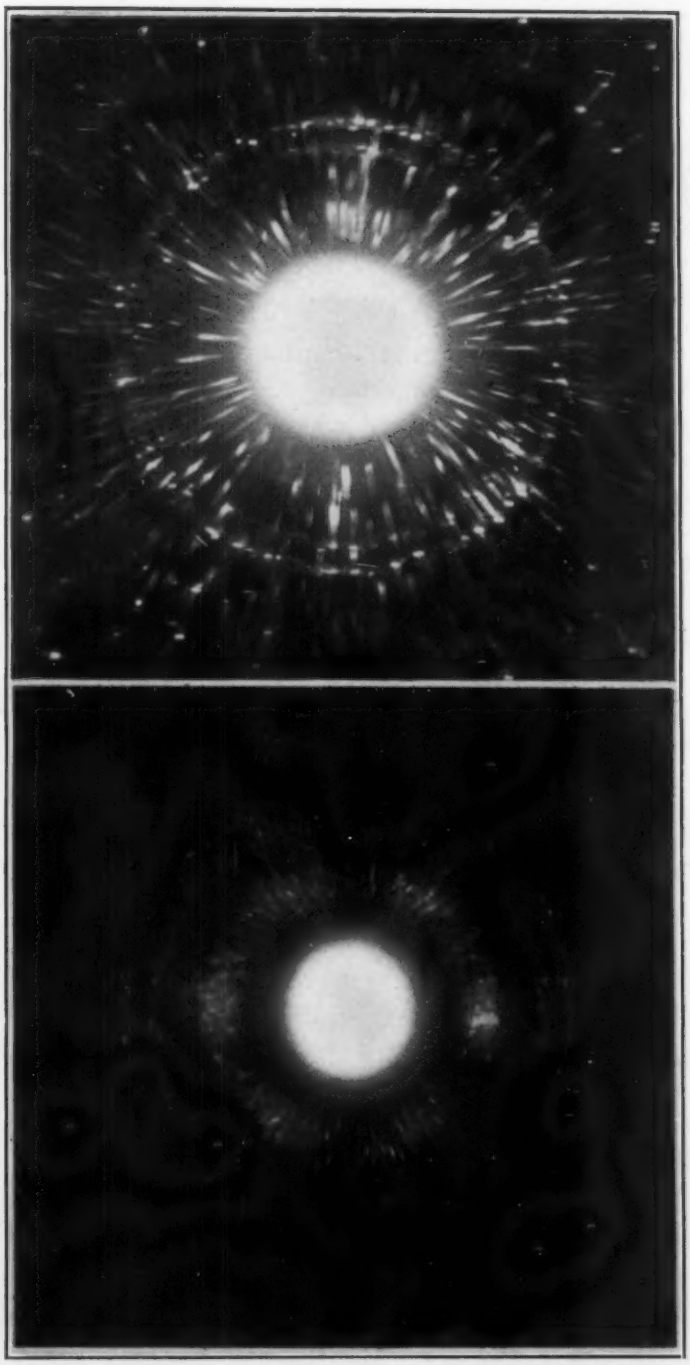


Fig. 1 (Upper)—Low Carbon Basic Open-hearth Steel Wire Given an Area Reduction of 15 Per Cent and Annealed at 1100 Degrees Fahr. (595 Degrees Cent.) for One Hour.

Fig. 2 (Lower)—Low Carbon Bessemer Steel Wire, Area Reduction 15 Per Cent and Annealed at 1100 Degrees Fahr. (595 Degrees Cent.) for One Hour. Compare with Fig. 1.

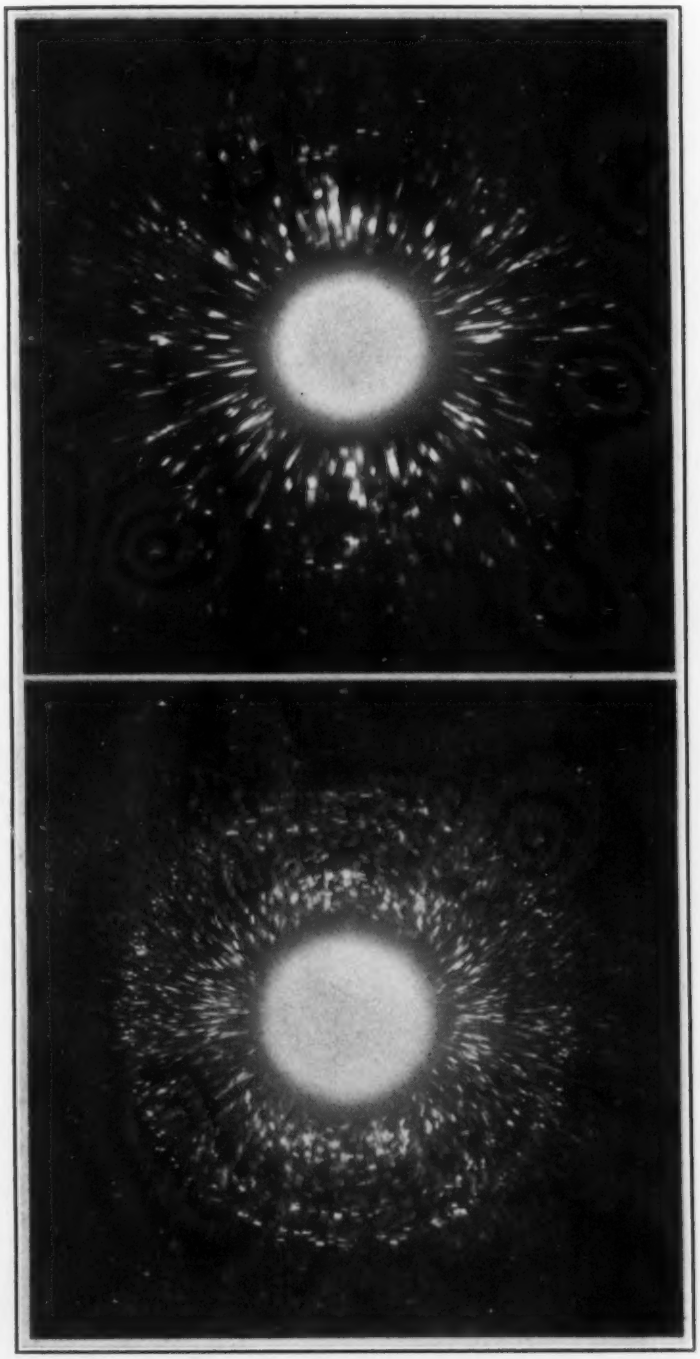


Fig. 3 (Upper)—Basic Open-hearth Steel Wire Given an Area Reduction of 15 Per Cent and Annealed at 1200 Degrees Fahr. (650 Degrees Cent.) for One Hour.

Fig. 4 (Lower)—Bessemer Steel Wire, Area Reduction 15 Per Cent; Annealed at 1200 Degrees Fahr. (650 Degrees Cent.) for One Hour.

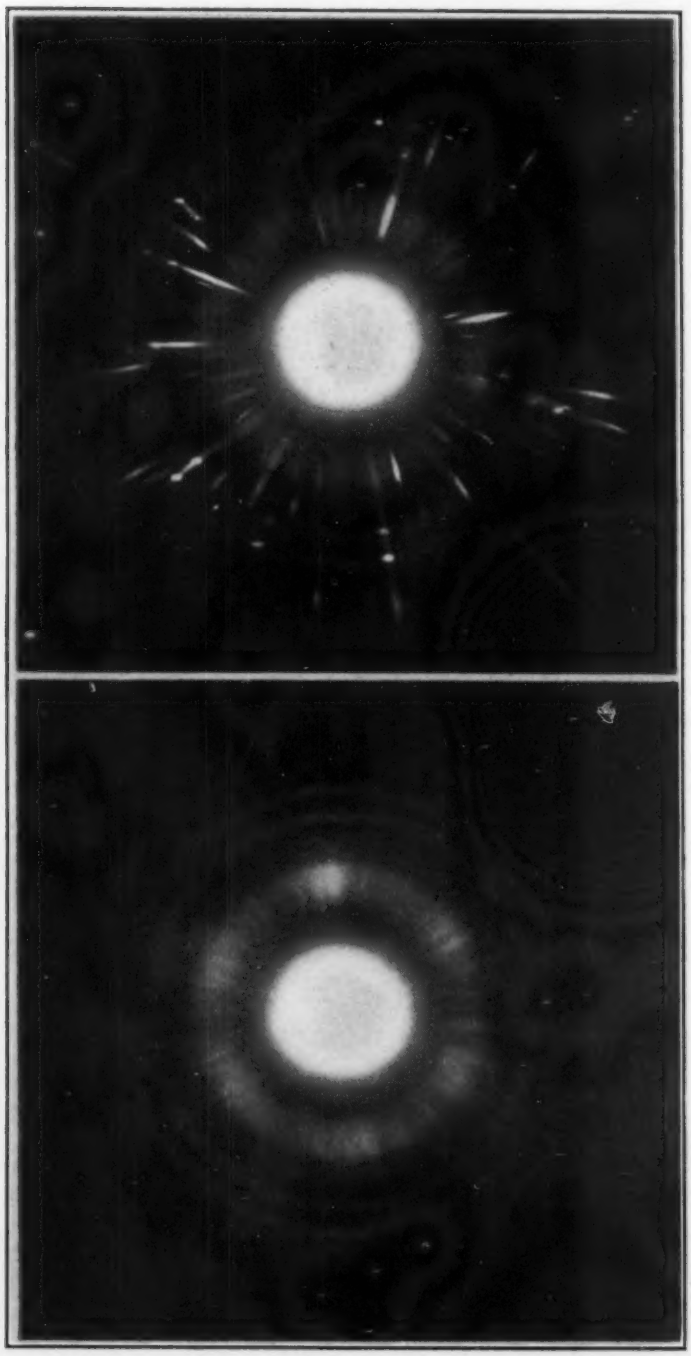


Fig. 5 (Upper)—Basic Open-hearth Steel Wire Given an Area Reduction of 10 Per Cent and Annealed at 1300 Degrees Fahr. (705 Degrees Cent.) for One Hour.

Fig. 6 (Lower)—Bessemer Steel Wire, Area Reduction 10 Per Cent and Annealed at 1300 Degrees Fahr. (705 Degrees Cent.) for One Hour. No Recrystallization.

Annealing at 1100 degrees Fahr. (595 degrees Cent.) did not recrystallize the wires with 5 and 10 per cent area reductions, but marked grain growth appeared in the wires with 15 per cent area reductions. Recrystallization was more marked in the basic open-hearth steel wires. Figs. 1 and 2 are X-ray diffraction patterns of these wires, and the distinct difference can be seen. These X-ray spectra show that the grains which started to grow in the open-hearth steel wires possessed a wealth of growth inertia, but due to the fact that all of the grains did not recrystallize, they did encounter resistance from the inert fragments and were distorted. In other words, a single grain viewed under the microscope in reality is not a true single crystal, but is made up of laminations. We can liken a nearly perfect single crystal to a pack of playing cards, and the distorted crystal likened to a pack of cards piled in a disorderly fashion.

On the other hand, grain growth in the bessemer steel wires was much more sluggish, perhaps due to the impurities inherent in such steels. As these grains did not have as great a grain growth inertia as the grains in the basic open-hearth steel wires, naturally at this stage not much grain distortion is in evidence. If the recrystallized grains continue to grow and the inert grains would not start to recrystallize, then distortion would result in the growing grains.

No recrystallization could be detected in wires with area reductions of 5 per cent and annealed at 1200 degrees Fahr. (650 degrees Cent.). Incomplete recrystallization occurred in the wires drafted 10 per cent and annealed at the same temperature. A longer time of annealing would be required for complete recrystallization. In the case of the wires with 15 per cent area reductions, one hour annealing at 1200 degrees Fahr. (650 degrees Cent.) completely recrystallized the cold-worked grain structure. As before the basic open-hearth steel wires had the larger grains, and they were distorted more than the grains in the bessemer steel wires, annealed under exactly the same conditions. (See Figs. 3 and 4.)

Specimens of the wires with the area reductions of 5 per cent and annealed at 1300 degrees Fahr. (705 degrees Cent.) failed to recrystallize. Perhaps a longer time of annealing would have induced recrystallization in the basic open-hearth wires.

In the case of the wires drafted 10 per cent and annealed at 1300 degrees Fahr. (705 degrees Cent.) for one hour, a rather strange phenomena occurred, in that the bessemer steel wires failed to recrystallize. At least 25 different specimens were examined with

the X-ray, and in every case without exception, no recrystallization was found. All of the specimens were given the same heat treatment, and at different times. The open-hearth steel wires in some instances did not recrystallize completely; in fact, portions of the same wires were found to be completely recrystallized, and other parts only beginning to show signs of grain growth. One hour annealing is not long enough to effect complete recrystallization.

To check these results short (about 1 inch long) specimens of bessemer steel wire and open-hearth steel wire with 10 per cent area reductions were annealed together in a small electric furnace. To prevent oxidation during heat treatment the specimens were sealed in an air-tight pipe. The temperature never exceeded 1300 degrees Fahr. (705 degrees Cent.) and the time of heat treatment was one hour. Figs. 5 and 6. The bessemer wire failed to recrystallize and the basic open-hearth wire partially recrystallized. As stated above, all the X-ray diffraction patterns made of these wires in the cold-worked state would imply that the bessemer steel had received more grain fragmentations, yet they resist recrystallization.

Annealing at 1600 degrees Fahr. (870 degrees Cent.) for one hour recrystallized the cold-worked structure of all the wires. Those given an area reduction of 5 per cent recrystallized with very small grains distributed at random. Even smaller grains were found in the wires with 10 per cent area reductions. The wires with 15 per cent area reductions recrystallized in a similar way but the grains in the open-hearth steel wires were larger and more perfect in structure than the corresponding bessemer steel wire. Bessemer steel wires given the same mechanical and heat treatments as the corresponding basic open-hearth steel wires, are much more sluggish to recrystallization. Another important observation is the great irregularity of grain recrystallization in the basic open-hearth wires, in that one portion would be completely recrystallized and another only partially, this illustrates the importance of "uniformity" of structure.

The failure of the bessemer steel wires with area reductions of 10 per cent and annealed at 1300 degrees Fahr. (705 degrees Cent.) to recrystallize, was a striking result, as it is a well established fact that exceedingly large grains are grown in basic open-hearth steel wires given the same treatment. The high phosphorus content combined with the regular slag inclusions found in all bessemer steels may be responsible for this abnormal state of affairs. No doubt "dirty" basic open-hearth steels may behave in a similar manner.

BRITTLENESS IN LOW CARBON STEEL

By H. H. Bleakney

Abstract

The fact that a mixture of martensite and ferrite grains constitutes the structure of hypoeutectoid steel drastically quenched from a temperature within the critical range has long been recognized.

This paper attempts to evaluate the influence of such martensite on the dynamic properties of the steel.

Evidence is presented, which indicates that brittleness in the cores of single quenched carburized parts is due to the martensite formed, and not to a coarse grain structure. It is also indicated that cyanide brittleness is attributable to this martensite.

It is suggested that a fine-grained carburizing steel, rapidly quenched from a temperature slightly higher than the Ac_3 of the core would have superior core properties without an injuriously coarsened grain in the case.

MORE than twenty years ago Osmond and Stead[1] demonstrated the occurrence of martensite particles in a ferrite matrix when hypoeutectoid steel is quenched from within its critical range. Of recent years several investigators have discussed the phenomena encountered in the various heat treatments to which low carbon steel has been subjected. Crook[2] stressed the fact of martensite formation and the change in its character, as found in low carbon steel quenched from increasing temperatures within its critical range. It is therefore astonishing that no one had inferred the embrittling effect of such martensite until Pulsifer's valuable discussion on low carbon steel[3] drew attention to its deleterious influence on the properties of the steel.

One of the clearest explanations of the structural changes tak-

[1]F. Osmond and J. E. Stead, "The Microscopic Analysis of Metals," p. 208 to 214 inclusive.

[2]W. J. Crook, "Heat Treatment of Low-carbon Steel," *Metal Progress*, Vol. 18, 1930, p. 47.

[3]H. B. Pulsifer, "Low-carbon Steel," Iron and Steel Division, American Institute of Mining and Metallurgical Engineers (1931). Technical Publication No. 426.

The author, H. H. Bleakney, a member of the society, is ferrous metallurgist, Mines Branch, Department of Mines, Canada. Manuscript received October 28, 1931.

ing place in steel when heated through its critical range was given by Davenport and Bain[4]. Their description was so concise and lucid that, with the kind permission of the authors, it is here quoted as follows:

"When annealed carbon or low alloy steels are suitably heated, the ferrite (alpha iron solid solution) and the carbide of which they are composed react together to form a single solid solution of carbon (and other elements) in gamma iron (austenite). This reaction may begin only at a certain minimum temperature called the eutectoid temperature. The first ferrite and carbide thus to react together do so in definite proportions known as the eutectoid composition. With further heating, the original constituent that is present in excess is dissolved in the austenite until exhausted. Whether the excess constituent be ferrite (hypoeutectoid steels) or carbide (hypereutectoid steels) the procedure is much the same and upon slow cooling the homogeneous austenite expels the excess of either (proeutectoid ferrite or carbide) until the eutectoid composition is reached. Thus the reaction upon heating is strictly reversed upon cooling and accordingly an equilibrium diagram of this process may be constructed."

From these facts, it must follow that for every temperature within the critical range of a hypoeutectoid steel, a definite quantity of austenite is in equilibrium with a definite quantity of ferrite, these quantities being determined by the analysis of the steel and the actual temperature employed. And it also must be obvious that the volume of austenite is a minimum at the Ac_1 but increases at the expense of the ferrite until the steel becomes completely austenitic at the Ac_3. And since the carbon is practically all in the austenite, the carbon concentration in the austenite must become steadily less with the increasing volume of that austenite. Quenching such a steel from a temperature within its critical range does not greatly affect the ferrite but serves to convert the austenite to martensite, provided the quenching is sufficiently drastic. The hardness of the martensite so formed must vary directly as its carbon concentration, and hence must vary inversely as the quenching temperature.

Since almost all steels which are case-hardened by the cyanide process, and some carburized steels are thus quenched from within their critical range, consideration of the above facts should lead, at

---

[4]E. S. Davenport and E. C. Bain, "Transformation of Austenite at Constant Subcritical Temperatures," *Transactions*, Iron and Steel Division, American Institute of Mining and Metallurgical Engineers, 1930, p. 117.

least to the suspicion, that the hard brittle martensite particles thus formed should have a somewhat more serious embrittling effect than a slightly coarsened grain structure or an excessively hard case. It is the object of this investigation to evaluate that effect and to offer a quantitative measure of the relative embrittlement produced when low carbon steel is quenched from various temperatures within its critical range.

Experimental Methods and Results

In order to obtain the necessary information and data, a number of similar sections of low carbon steel were quenched into water from various temperatures within the critical range of the steel, commencing with a temperature just over the Ac_1 and increasing by increments of 25 degrees Fahr. until the last pair were quenched from a temperature well over the Ac_3. The samples were then tested on the Izod impact machine, and the results taken as a measure of the brittleness induced by the quenching treatments.

All test pieces were cut from a single length of 5/8 inch round steel of the following analysis:

	Per Cent
Carbon	0.16
Manganese	0.55
Phosphorus	0.015
Sulphur	0.019
Silicon	0.09

The test pieces were all cut to 3-inch lengths and turned in a lathe to one half inch diameter. Before proceeding further with the experiment, the position of the critical points was determined on a transformation point apparatus. From the curve obtained and shown in Fig. 1 it can be seen that the Ac_1 occurs just under 1340 degrees Fahr. (725 degrees Cent.), and the Ac_3 at about 1530 degrees Fahr. (830 degrees Cent.). These figures agree with those given in the iron-carbon equilibrium diagram.

The furnace employed was an electrically heated box type, with pyrometric control. Before commencing the experiment the furnace thermocouple and pyrometer were checked against a standard and found to be correct. The furnace was then heated to 1350 degrees Fahr. (730 degrees Cent.) and that temperature maintained until the brickwork was well soaked, after which two test pieces were placed in the chamber close to the couple and held at $\pm$ 5 degrees Fahr. of the indicated temperature for twenty minutes. In quench-

ing, each sample was seized with the tongs close to the end, transferred from the furnace to the quenching medium with the utmost rapidity, and quenched by stirring vigorously in a large tank of slowly circulating cold water. Except for the increasing temperatures employed, each pair was treated identically as the preceding

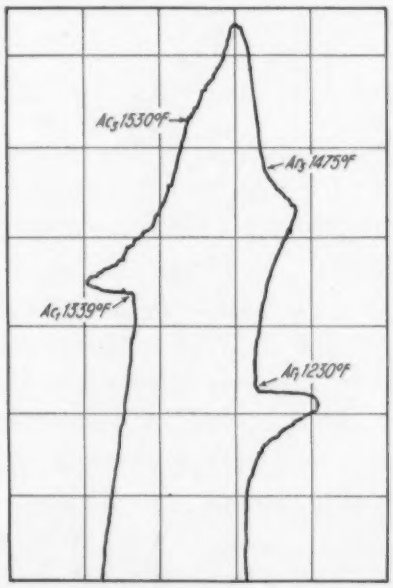


Fig. 1—Critical Point Curve of Steel Used in this Experiment.

pair, and in subsequently machining the pieces to standard Izod test bar dimensions, the notch was invariably cut in the end opposite that gripped in the tongs. After breaking the tests, Brinell hardness values were determined on each pair and these with the results of the Izod tests are presented in Table I.

These results were most surprising to the author, being widely

Table I
Impact and Hardness Tests

Quenching Temperature	Izod Value		Brinell Hardness Number	
	Test No. 1	Test No. 2	Test No. 1	Test No. 2
1350° F.	6	6	207	207
1375° F.	7	7	228	228
1400° F.	9	9	241	241
1425° F.	19	18	248	248
1450° F.	29	29	255	255
1475° F.	20	18	262	269
1500° F.	25	25	277	277
1525° F.	29	30	293	293
1550° F.	29	29	311	302
1575° F.	30	28	311	311
1600° F.	27	26	311	311

at variance with those anticipated. It is apparent that the Brinell hardness of the steel increases with increasing quenching temperature and hence with an increasing volume of martensite. That result was not unexpected, and in fact is by no means new. But it was thought at the time that the steel would show increasing brittleness with increasing hardness. Pulsifer appears to have been misled here, for he states that "It will probably be granted that the harder the core, the greater the tendency toward brittleness." But he goes on to say that "this is only a general consideration" and cites some exceptions. However, it appears that the examples he suggests as exceptions are actually examples of the rule.

The peculiar backsliding shown by the samples quenched from 1475 and 1500 degrees Fahr. (800-815 degrees Cent.) was so inexplicable as to demand verification. To that end a length of similar steel from a different heat was treated in precisely the same manner as the preceding tests. The analysis of this bar is as follows, and the Izod impact results obtained are presented in Table II.

	Per Cent
Carbon	0.08
Manganese	0.35
Phosphorus	0.018
Sulphur	0.043
Silicon	0.08

Table II
Izod Impact Tests

Quenching Temperature Degrees Fahr.	Degrees Cent.	Izod Value Test No. 1	Izod Value Test No. 2
1350	730	12	15
1375	745	22	17
1400	760	30	31
1425	775	28	29
1450	787	24	23
1475	800	23	25
1500	815	30	31
1525	830	76	96

The comparative toughness of this steel as compared with that used in the preceding test is of decided interest as giving a measure of the effect of carbon content on the dynamic properties of the quenched samples. The remarkable increase in the Izod value of the 0.08 per cent carbon steel quenched from temperatures in excess of 1500 degrees Fahr. (815 degrees Cent.) should be of distinct commercial importance. It is not surprising that this material displayed much poorer agreement between duplicate tests than the 0.16 per cent

carbon steel, since the substantially lower carbon content of the bar used in the second test would greatly exaggerate its sensitivity to even the slightest variations in heat treatment. Nevertheless, allowing for the difference in carbon content, the similarity of the results obtained in the two tests is convincing, particularly with respect to the irregular behavior noted in the pieces quenched from temperatures in the middle of the critical range. Hence it must be concluded that that

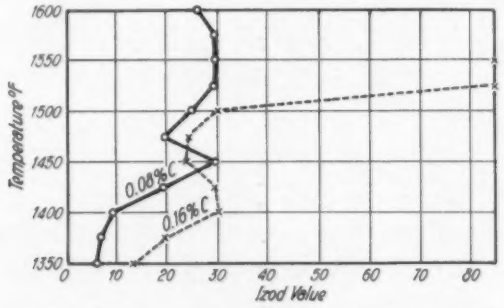


Fig. 2—Curve Showing the Relationship Between Izod Value and Quenching Temperature of the Steels Tested.

behavior is an intrinsic characteristic of these steels. Fig. 2 illustrates graphically the relation of brittleness to quenching temperature in the two steels tested, and demonstrates the general similiarity in the results obtained.

Microstructure

The photomicrographs presented in Figs. 3 to 13 inclusive illustrate the changes occurring when mild steel is heated through its critical range, and which were so well described by Davenport and Bain (loc cit). The martensite areas seen in the photomicrographs obviously were austenite at the quenching temperature, and the gradual growth of the austenite grains with increasing temperature can be readily visualized. The concurrent elimination and final disappearance of the ferrite is also clearly apparent.

In order to find an explanation for the variations in the degree of embrittlement imparted to the steel by the various quenching temperatures employed, it is necessary to study the structures at a higher magnification. Figs. 14 to 21 inclusive represent at a magnification of one thousand diameters, the same structures as were illustrated in Figs. 3 to 10 respectively at one hundred diameters. The higher magnifications adequately expose the structure of the individual martensite and ferrite grains so that by correlating these struc-

tures with the Izod values obtained, an explanation for the brittleness phenomena may be constructed. Such an explanation is proposed below, not as a statement of fact but simply as an argument supporting a theory which appears to be in agreement with the facts.

It is reasonable to believe that the ferrite can have no material influence in promoting the embrittlement which is the subject of this discussion. Any explanation of that embrittlement seemingly should attribute it to the martensite, and the word martensite is used here to designate the product of the decomposition of the austenite, present at the quenching temperature, and which is transformed on quenching. It is clearly understood that the characteristics of this martensite vary with the quenching temperature, and that formed by quenching the steel from 1350 degrees Fahr. (730 degrees Cent.) is widely different from that formed by quenching it from 1500 degrees Fahr. (815 degrees Cent.). Indeed, these differences must form the basis for the explanation of the varying degrees of brittleness encountered.

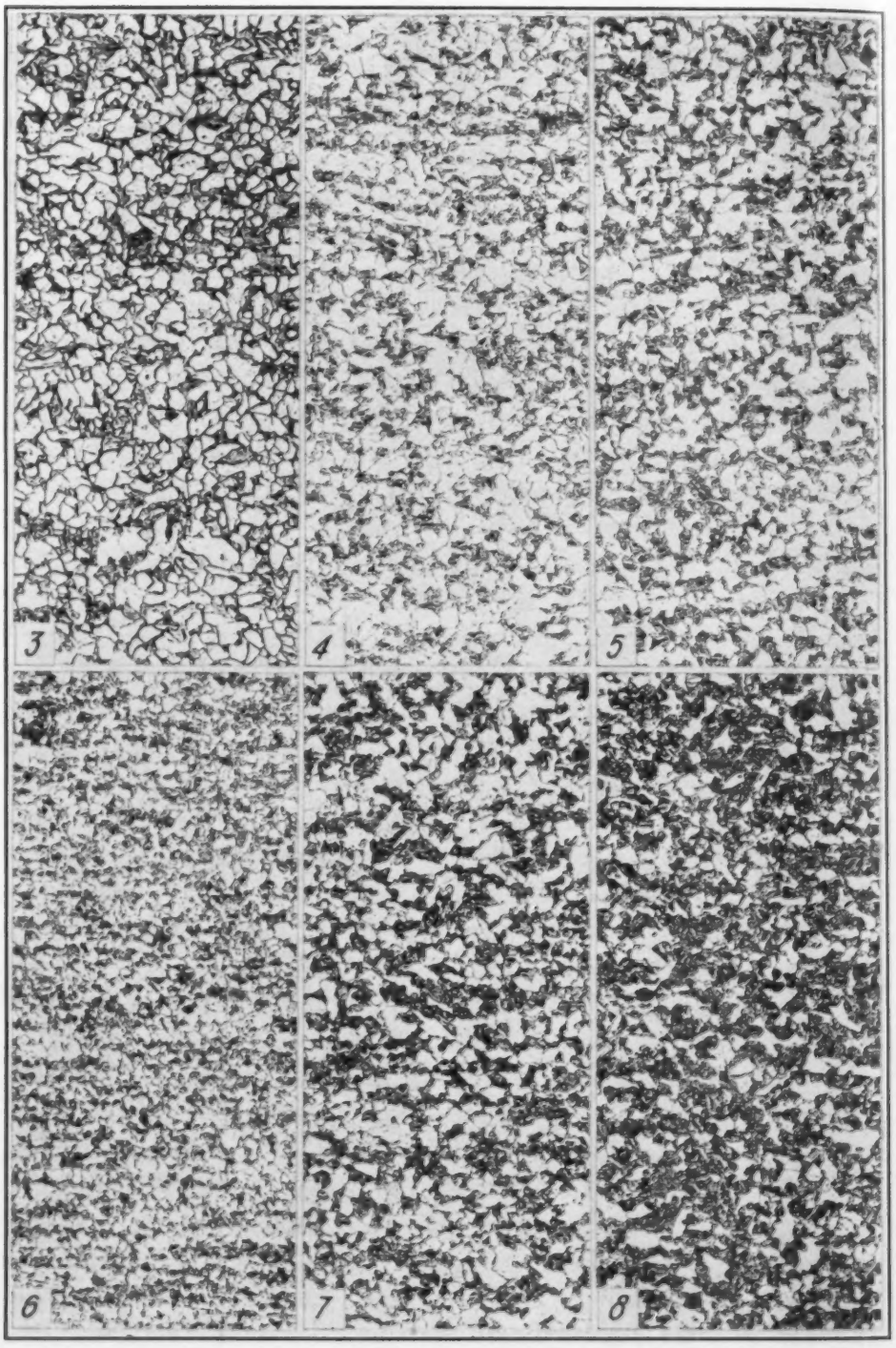
It is believed that there are four main factors governing the effect of the martensite on the dynamic properties of the steel, and that they affect the properties as follows:—

(1) *Disposition of the martensite*—Where the martensite is present in massive, rounded particles, as found in the samples quenched from the middle and upper temperatures of the critical range, its effect should be much less deleterious than where it shows a tendency to envelope the ferrite grains, as found in samples quenched from the lower temperatures of the range.

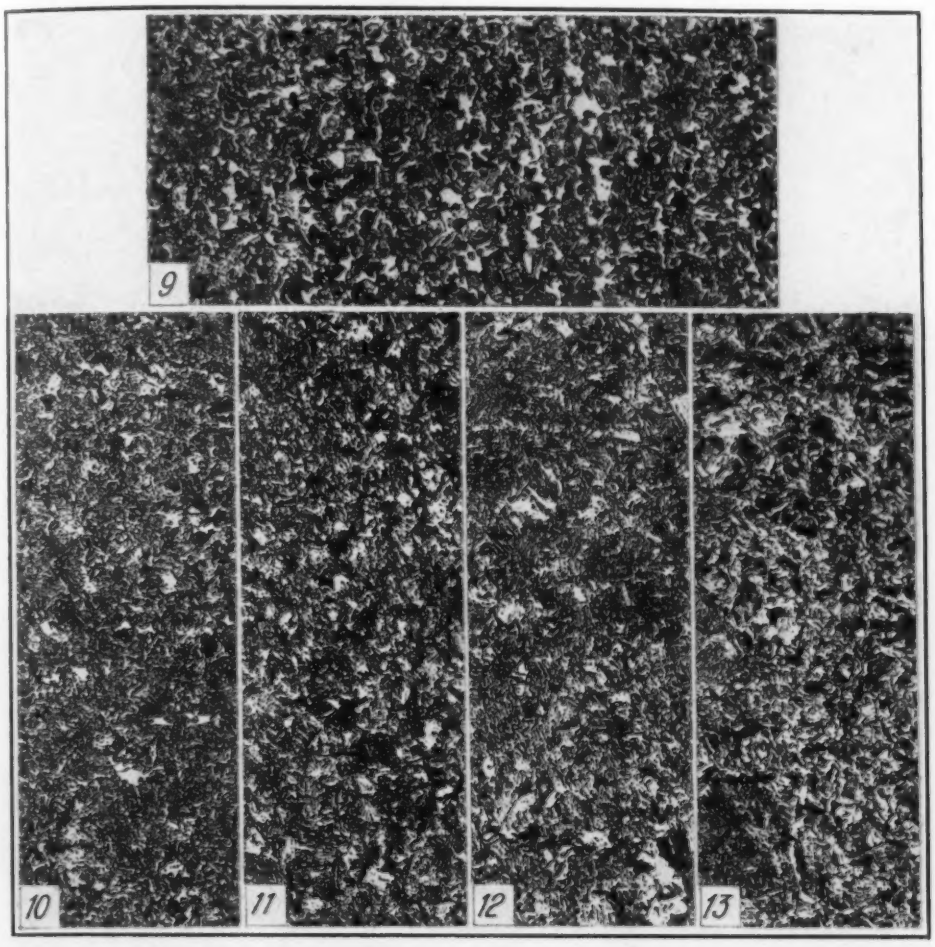
(2) *Intrinsic hardness and brittleness of the martensite*—The brittleness of the steel should vary directly as the hardness and brittleness of the martensite it contains.

(3) *Volume of the martensite*—The brittleness of the steel should vary directly as the volume of the martensite it contains.

(4) *Surface condition of the martensite particles*—The effect of this element is not so obvious as the preceding three, but it is believed that it has an influence on the dynamic properties of the steel. Where the surface of the martensite particles is smooth and its area a minimum in relation to the volume, its embrittling effect should seemingly be greater than where the surface is highly irregular and fringed with troostite. In the latter case any shock could conceivably be transmitted fairly readily from the ferrite to the martensite, and the latter could thus exert such intrinsic toughness as it possesses.



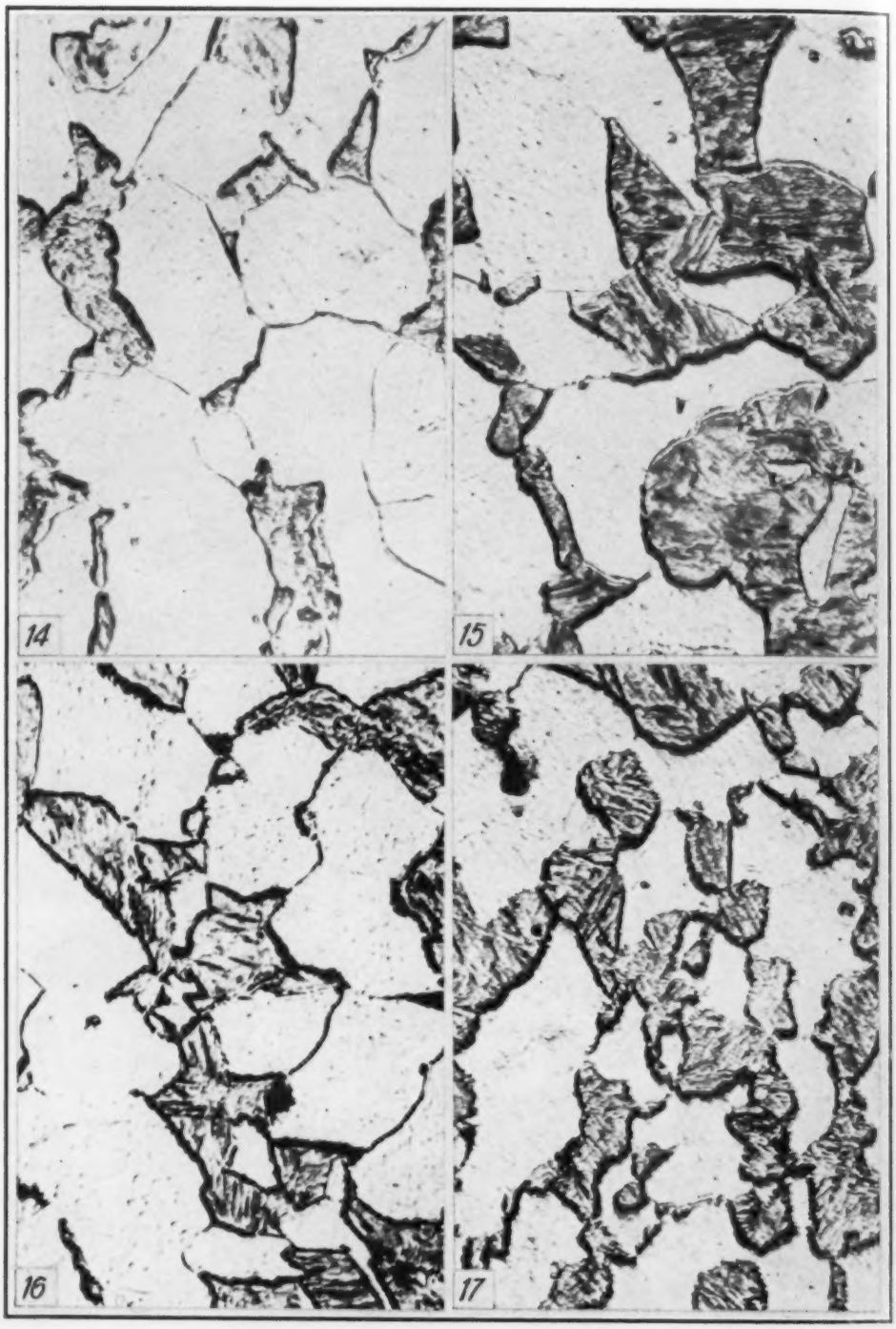
Figs. 3 to 8—Microstructure of 0.16 Per Cent Carbon Steel Quenched from the Following Temperatures, Respectively. × 100. 1350, 1375, 1400, 1425, 1450, 1475 Degrees Fahr.



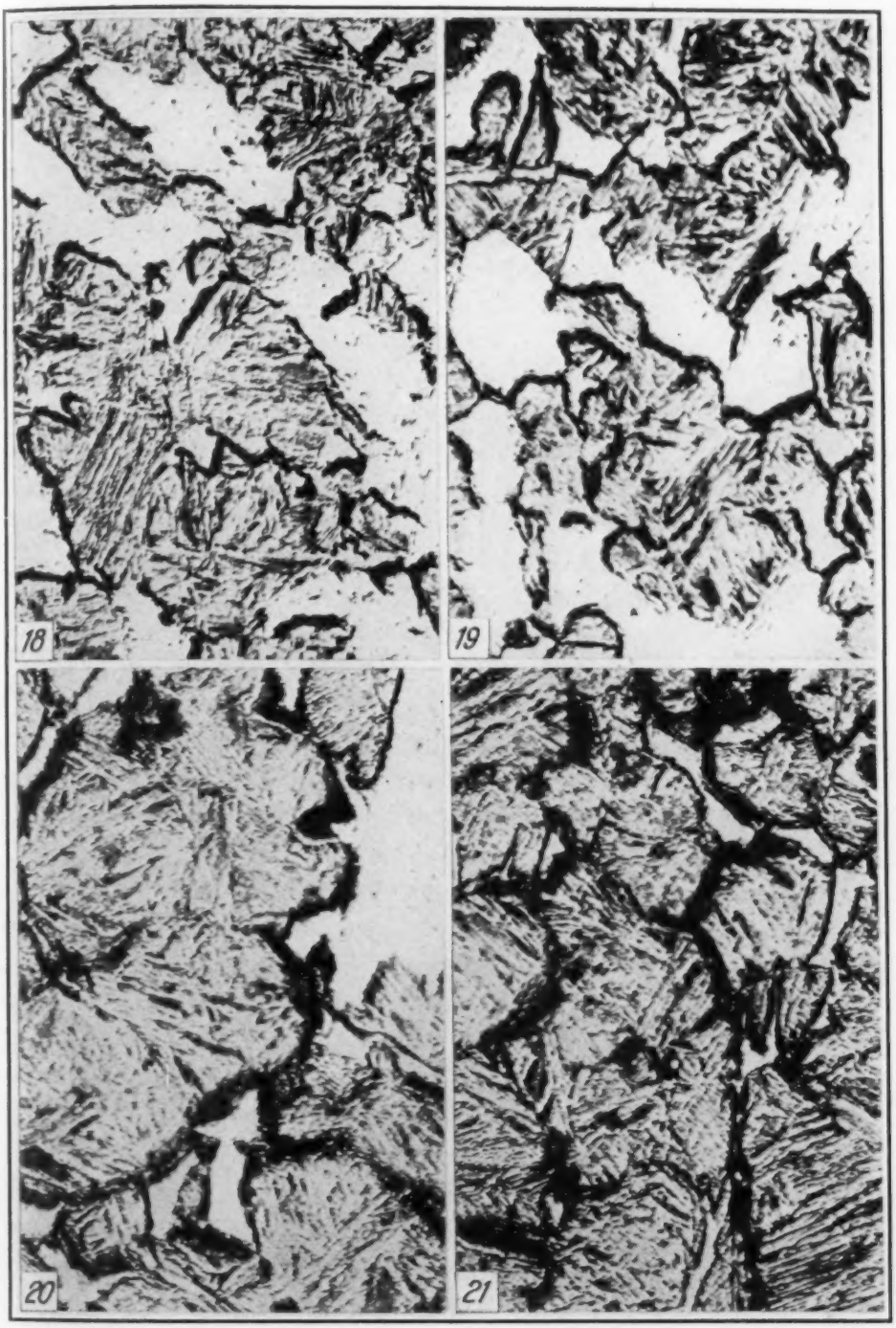
Figs. 9 to 13—Microstructure of 0.16 Per Cent Carbon Steel Quenched from the Following Temperatures, Respectively. × 100. 1500, 1525, 1550, 1575, 1600 Degrees Fahr.

But where the surface of the martensite particles is smooth it might be expected to act as an inclusion, and hence have a purely negative effect on the toughness of the steel.

If it be granted that the dynamic properties of the steel are governed by these factors, then their application, in conjunction with a study of the microstructure, should lead to an explanation of the reaction of the steel to the various treatments imposed. After quenching from the lowest temperature employed, i.e., 1350 degrees Fahr. (730 degrees Cent.), it will be seen that the martensite formed is such that the three factors of disposition, intrinsic brittleness and surface condition are exerting their maximum embrittling effect, while the volume of the martensite is a minimum, and it is apparent that the



Figs. 14 to 17—Microstructure of 0.16 Per Cent Carbon Steel Quenched from the Following Temperatures, Respectively. × 1000. 1350, 1375, 1400, 1425 Degrees Fahr. Izod Value 6, 7, 9, 18 Respectively.



Figs. 18 to 21—Microstructure of 0.16 Per Cent Carbon Steel Quenched from the Following Temperatures, Respectively. × 1000. 1450, 1475, 1500, 1525 Degrees Fahr. Izod Value 29, 19, 25, 30 Respectively.

effect of the first three factors so far exceeds that of the last as to leave the steel as a whole in its most brittle condition. Quenching from increasing temperatures serves progressively to modify the disposition, hardness, and surface condition of the martensite so as to render the steel decreasingly brittle. The growing volume of martensite is not sufficiently influential to counteract that effect, and the net result of increasing the quenching temperature is to lessen the embrittlement up to a temperature of about 1425 to 1450 degrees Fahr. (775-787 degrees Cent.). The recurring brittleness found just above those temperatures, and illustrated in the curves of Fig. 2, is difficult to understand in the absence of any apparent change of trend in the microstructures. However, it is probable that at these temperatures the effect of the martensite disposition and surface factors has become negligible, and that the degree of brittleness encountered is a product of the opposing influences of growing martensite volume and decreasing martensite hardness. And it would appear that at these temperatures the embrittling effect of increased martensite volume is greater than the toughening effect of decreased martensite hardness. At higher temperatures the effect of the latter factor becomes greater than the effect of the former, and again the trend for the steel becomes one of increasing toughness with increasing quenching temperatures, up to the temperature of the Ac_3. Above that point toughness decreases with increasing temperature, due to a coarsening of the grain structure.

The accuracy or inaccuracy of the explanation presented above does not alter the fact that the presence of martensite particles in low carbon steel is a source of distinct embrittlement, and that fact is one which must be recognized and overcome if such brittleness is to be eliminated. The author has encountered this phenomenon at different times, in cyanided work, carburized work, and various other occasions where low carbon steel has been quenched from a temperature low in its critical range. He believes that it is a sinister and undetected influence in many of our plants today, and hopes that the present work may be helpful in exposing and combating that influence.

Discussion

The structures obtained in the experiments recorded in this paper probably cover, fairly generally, the possible degrees of embrittlement imparted to low carbon steel by treatments which trans-

form the pearlite grains to martensite. But these results were produced under a set of fixed conditions, closely approximating equilibrium. The same effects could be obtained by a variety of methods, and a survey of the conditions governing the results produced leads to the conclusion that the following are the predominating factors.

(1) Analysis of the steel
(2) Quenching temperature
(3) Time at temperature
(4) Quenching medium
(5) Size of piece quenched.

The broad effect of each of the above factors is sufficiently self-evident as to require no experimental support. In general it may be said that in order to produce the brittleness indicated in this work, the quenching medium must be sufficiently drastic and the section of the steel treated sufficiently small to produce martensite on quenching. Consequently, where pieces are quenched into oil, or where their least dimension is in excess of about one inch, no serious embrittlement need be anticipated. As regards the factor of time at temperature, it must be apparent that where a piece is quenched from a certain temperature before equilibrium has been established, the result is the same as would be obtained by quenching the piece from a lower temperature under equilibrium conditions.

Practical Applications

Cyanide Brittleness

In 1926 Hillman and Clark[5] offered an explanation for the occurrence of cyanide brittleness which was generally accepted at that time and which since has not been seriously contested. They attributed that brittleness entirely to the extreme brittleness of the case, and stated that the core, per se, was tough. Their experiments were convincing, but it must be apparent, from this work, that such cores may be distinctly brittle. And it is contended that the main cause of cyanide brittleness is actually the presence of martensite grains in the core, produced by quenching the steel into water from the cyaniding temperature. Were this form of brittleness due to the case alone,

[5] V. E. Hillman and E. D. Clark, "Cyanide Brittleness," Transactions, American Society for Steel Treating, Vol. 10, 1926, p. 954.

then it should vary directly with the thickness of the case. But the author has found decided brittleness in a cyanided piece having only 0.002 inches of case, but having martensite grains in the core, while a piece having 0.006 inches of case, but troostite grains in the core, was tough. Both samples had been water-quenched, and both cases were file-hard. The difference in the core structures was due to the fact that the tough sample had reached equilibrium at 1500 degrees Fahr. before being quenched, while the brittle one had not. Hence the latter received the effect of being quenched from a lower, and more embrittling temperature.

It is not within the province of this paper to propose any set rules for counteracting the brittleness just described. It is extremely doubtful if there is any rule which would have a general application. However, the following three methods of attack may be of interest.

1. *Quenching into oil.* Due to the retarded speed of cooling of pieces quenched in this manner, the austenite grains in the core are transformed to troostite rather than martensite. As a consequence, the core does not display the brittleness which has been shown to be associated with the presence therein of martensite particles. However, where a file-hard case is desired, quenching into oil is quite unsatisfactory.

2. *Raising the quenching temperature.* The curves illustrated in Fig. 2 indicate, that for the lower carbon carburizing steels at least, raising the quenching temperature tends to minimize the tendency toward brittleness. Unfortunately this practice is accompanied by the serious disadvantages of a coarsened grain structure in the case, the danger of spalling the case and an increased rate of deterioration of the cyanide bath.

3. *Utilization of lower carbon steels.* It appears that the only sure and satisfactory way to avoid the brittleness under discussion is to use a steel so low in carbon that its influence is negligible. Just how low the carbon content should be is not known, but it seems that even 0.08 per cent carbon renders the steel susceptible to a considerable measure of embrittlement. An investigation of the influence of various carbon contents upon the core brittleness of cyanided steels should yield information of the greatest interest and value to industries employing this method of case hardening. In fact it is believed that a knowledge of that influence is essential to the making of a good quality product.

Heat Treatment of Carburized Steel

When carburized steel which has been slowly cooled from the carburizing temperature is reheated above the critical point of the case and quenched into water, the core becomes brittle in a measure depending on its carbon content, the section of the piece, and the quenching temperature. This fact has long been recognized and erroneously attributed to the coarse grain structure which the carburizing treatment produces in the core. Since the double quenching treatment which is applied to carburized work was evolved to eliminate the supposed embrittling effect of the coarse grain structure of the core, and since that coarseness is not primarily responsible for the brittleness encountered, as may be seen by comparing Fig. 17 with Fig. 22, the beneficial results of such a double treatment must be attributed to some other cause. It was thought desirable to provide some measure for the actual increase in toughness produced by the double quenching treatment as compared with the single quenching treatment, and to that end, the following experiment was made. Six test bars, three inches long and one half inch in diameter, were turned from a hot-rolled one inch round bar of steel of the following composition.

	Per Cent
Carbon	0.16
Manganese	0.43
Phosphorus	0.010
Sulphur	0.039
Silicon	0.22

Two of these bars were heated to 1425 degrees Fahr. (775 degrees Cent.), held at that temperature for twenty minutes, and quenched in water. The other four were heated to 1600 degrees Fahr. (870 degrees Cent.) and quenched in water after holding for twenty minutes at temperature. These four bars were then placed in a furnace which was at a temperature of 1425 degrees Fahr. (775 degrees Cent.), and just as soon as the bars reached the temperature of the furnace, one pair was quenched in water. The other pair was similarly quenched after holding at temperature for twenty minutes. The six bars were then machined to round Izod test bar dimensions, notched and broken. The results obtained are shown in Table III.

The microstructure of the single-quenched pieces is the same as

Table III

Izod Tests

Heat Treatment 1st Quenching Temperature		2nd Quenching Temperature			Izod Value	
Degrees Fahr.	Degrees Cent.	Degrees Fahr.	Degrees Cent.	Time at Temperature	Test No. 1	Test No. 2
		1425	775	20 minutes	16	16
1600	870	1425	775	none	41	49
1600	870	1425	775	20 minutes	41	42

that shown in Figs. 6 and 17, consisting of martensite and ferrite. The microstructures of the two sets of tests which were double quenched are illustrated in Figs. 22 and 23. These again consist of martensite and ferrite and since there is rather close agreement between both the Izod values and microstructures of both the sets of double quenched bars it would appear that equilibrium was quickly established at that temperature.

Two other sets of tests were treated in a similar manner, except that the temperature of the second quench was 1375 degrees Fahr. (745 degrees Cent.). The Izod values obtained are given in Table IV and the microstructures illustrated in Figs. 24 and 25.

Table IV

Izod Tests

Heat Treatment 1st Quenching Temperature		2nd Quenching Temperature			Izod Value	
Degrees Fahr.	Degrees Cent.	Degrees Fahr.	Degrees Cent.	Time at Temperature	Test No. 1	Test No. 2
1600	870	1375	745	none	109	92
1600	870	1375	745	20 minutes	66	70

From a consideration of the Izod values and microstructures obtained in these double treatment experiments, a general picture may be drawn of the structural changes taking place in the steel. In slowly cooled low carbon steel, the carbon is concentrated in pearlite grains of eutectoid composition, and when heated over the Ac_1, these grains are converted quickly and easily to austenite. But in the case of the samples under discussion, which were water-quenched from 1600 degrees Fahr. (870 degrees Cent.), the carbon is fairly homogeneously dispersed throughout the steel as extremely fine carbides. Reheating such samples for a case-refining quench progressively softens and toughens the core up to the Ac_1. It is in effect a draw-

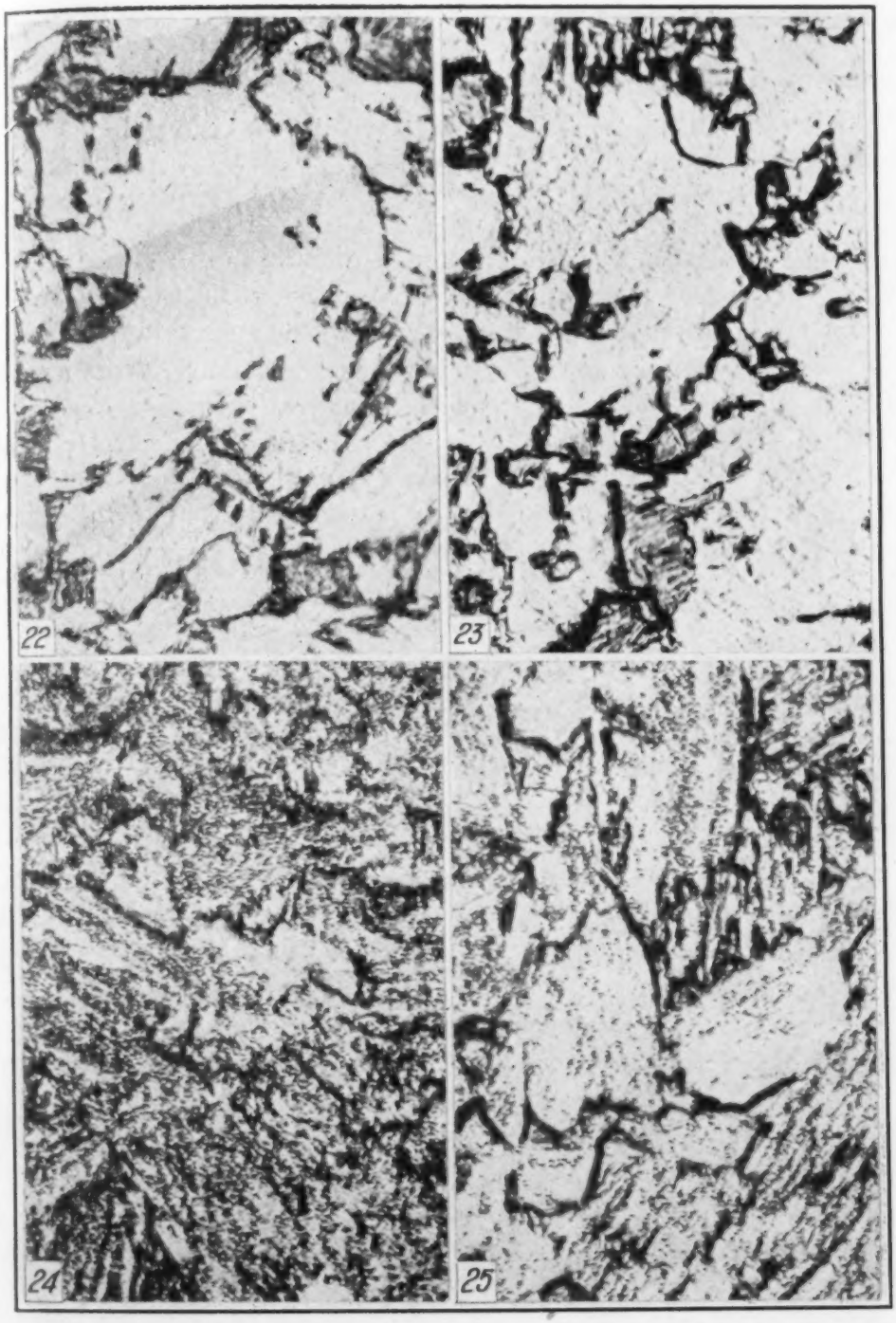


Fig. 22—0.16 Per Cent Carbon Steel Quenched from 1600 and 1425 Degrees Fahr. without Holding at the Latter Temperature. × 1000. Izod Value 45.

Fig. 23—0.16 Per Cent Carbon Steel Quenched from 1600 and 1425 Degrees Fahr. after Holding at the Latter Temperature for Twenty Minutes. × 1000. Izod Value 42.

Fig. 24—0.16 Per Cent Carbon Steel Quenched from 1600 and 1375 Degrees Fahr. without Holding at the Latter Temperature. × 1000. Izod Value 100.

Fig. 25—0.16 Per Cent Carbon Steel Quenched from 1600 and 1375 Degrees Fahr. after Holding at the Latter Temperature for Twenty Minutes. × 1000. Izod Value 68.

ing operation. After passing the Ac_1 however, the formation of austenite is not the simple occurrence which was noted when the pearlitic samples were reheated. In that case, grains of eutectoid composition transformed to austenite at the Ac_1 and the carbon diffused outward, as the austenite grew at the expense of the ferrite with increasing temperature. In reheating samples prequenched from over the Ac_3 however, the austenite must form at a number of nuclei, and the carbides must diffuse inward to dissolve in that austenite. It is apparent that this diffusion toward austenite nuclei must result in the disappearance of all free carbides in the steel, and the formation of a structure composed entirely of austenite and ferrite at any temperature over the Ac_1. But the fact that the steel is a fairly homogeneous low carbon alloy should result in the effectual raising of the Ac_1. That such is the case is indicated by the fact that even after a twenty minute soak, the pieces quenched from 1375 degrees Fahr. (745 degrees Cent.) did not show complete elimination of the previous structure.

The Izod values obtained in the double quenching treatments described above are not at all reassuring to those engaged in the heat treatment of carburized work. While the core is obviously toughened by the double treatment, its toughness is not comparable with that of the untreated steel and there is no doubt that, as pointed out by Hillman and Clark (loc cit) the brittleness of such a steel would be greatly increased by the super-imposition of a hard and brittle case. Obviously, the optimum condition is one where a fully hard case is obtained with a core having the toughness of the reheated sample quenched in water from 1375 degrees Fahr. without soaking. From the figures submitted, it is obvious that the lowest possible temperature which will produce a hard case is the best temperature, since the toughness of the core decreases rapidly with increasing quenching temperature. It may be noted that this tendency is the opposite of that shown by single quenched pieces.

Regarding the improvement in the Izod value of the double quenched tests over those single quenched from 1425 degrees Fahr. (775 degrees Cent.), it must be attributed to the disposition of the martensite. In both cases the structures are a mixture of martensite and ferrite and hence it must be concluded that in the double quenched sample, the martensite is so disposed in the ferrite matrix that its embrittling effect is greatly minimized.

If a method could be devised whereby a carburized part, previously water-quenched from over the Ac_3 of the core, could be so treated as to give the case the effect of being quenched from a temperature in excess of 1400 degrees Fahr. (760 degrees Cent.), while the core did not receive the effect of a temperature higher than 1375 degrees Fahr. (745 degrees Cent.), the resulting product should have a uniform fully hard case, combined with a core of maximum toughness. To bring about such a condition the piece would require to be heated at such a rate that the case would reach a temperature of 1425 degrees Fahr. (775 degrees Cent.) before the transfer of heat from case to core allowed the latter to reach a temperature higher than 1375 degrees Fahr. (745 degrees Cent.). In effect, the rate of heating should be the fastest practicable. A possible method would be to heat for quenching in a continuous furnace, the furnace temperature being about 1600 to 1700 degrees Fahr. (870-925 degrees Cent.) and the speed of the work such that the case would just reach a temperature of 1425 degrees Fahr. (775 degrees Cent.) when the piece was discharged into the quenching medium. Under such conditions the core should be decidedly tougher than under the usual practice of soaking the whole piece thoroughly at 1400 to 1425 degrees Fahr. (760-775 degrees Cent.).

The only considerable objection to the treatment described above would be the difficulty of keeping the quenching temperature of the carburized pieces within the desired limits of about 1400 to 1425 degrees Fahr. (760-775 degrees Cent.). However, that difficulty is by no means insurmountable and the rewards for successfully applying such a method would well repay some effort to do so. In any case, it is the author's sincere hope that the facts to which he has called attention in this paper may prove of some benefit to industries engaged in the carburization of steel, and that they may stimulate further research in a field which contains so much that is not yet known.

The data and conclusions presented in this paper are the result of an investigation confined solely to plain carbon steel. A further study of the effect of alloys on the core properties of carburizing steel should yield information of the greatest value, as it is possible, and even probable, that the consequent improvement in those properties might be much greater than is generally recognized.

The author wishes gratefully to acknowledge the kind help, en-

couragement and advice which he received from Messrs. W. P. Benter and A. P. Terrile of the Pittsburgh Crucible Steel Co., and Mr. T. W. Hardy of the Mines Branch, Canadian Government Department of Mines. He must also express his indebtedness to Mr. Howard Adair, student assistant in the Mines Branch, Canadian Government Department of Mines, for most valuable help in the heat treatment and photomicrography of the tests.

Brittleness in Low Carbon Steel—Part II

In Part I of this discussion the author demonstrated that a 0.15 per cent carbon steel of one half inch round section, prequenched in water from over its Ac_3 point, displayed much higher impact resistance if the second quenching treatment were carried out from 1375 degrees Fahr. (745 degrees Cent.) rather than 1425 degrees Fahr. (775 degrees Cent.) which is the temperature customarily employed in treating carburized parts. From purely theoretical considerations a method of heating for the case refining quench was proposed which was designed to produce full hardness in the case and maximum toughness in the core. That method, in brief, was to heat the steel for the second quench in a furnace held at 1600 degrees Fahr. (870 degrees Cent.) or over, and to quench in water as soon as the surface of the piece had attained a temperature of 1425 degrees Fahr. (775 degrees Cent.). It was believed that by such a treatment, the surface temperature would be sufficiently high to produce full hardness in the case, while the core, due to the rapidity of heat application, would be at some lower temperature, which would ensure greatly improved toughness.

Since writing the above paper, the author devised a plan by which to check the practicability of the method proposed. And it is the purpose of this paper to report the results obtained, the conclusions drawn from those results, and to offer what is believed to be a more practicable modification of the previously proposed method.

Three photomicrographs of Part I are herewith considered. Fig. 24 illustrates the structure of the 0.15 per cent carbon steel after quenching in water from 1600 degrees Fahr.; reheating to 1375 degrees Fahr (745 degrees Cent.) and quenching in water immediately upon attaining that temperature. This sample gave an Izod impact value of 100 foot-pounds.

Fig. 25 illustrates the structure of the same steel after quench-

ing in water from 1600 degrees Fahr. (870 degrees Cent.), reheating to 1375 degrees Fahr. (745 degrees Cent.) and quenching in water after holding at temperature for 20 minutes. This sample gave an Izod impact value of 68 foot-pounds.

Fig. 22 illustrates the structure of the same steel after the following treatment: quenching in water from 1600 degrees Fahr., requenching in water from 1425 degrees Fahr. after holding at temperature for 20 minutes. This sample had an Izod impact value of 42 foot-pounds.

From these photomicrographs it is apparent that at 1375 degrees Fahr. (745 degrees Cent.) there is a tendency for the carbides to migrate to centers forming grains of austenite, but that this movement is relatively slow. At slightly higher temperatures, however, this effect is greatly accelerated. In the experiment described below, an effort was made to heat small carburized test pieces at such a rate as to produce, on quenching, full hardness in the case while the core was at a temperature sufficiently lower that its structure would be similar to that shown in Fig. 24. It was assumed that if such a structure were found, then the toughness of the core would be of the same order as was found in the steel from which Fig. 24 was photographed. No attempt was made to measure the temperature of the pieces at quenching. As the temperature of the pieces was a function of the length of time they remained in the furnace, the latter was taken as a relative measure of the former.

Several round test pieces of a 0.15 per cent carbon steel, about two inches long and one half inch in diameter, were carburized to a depth of about 3/64 inches, cooled in the pot and then reheated and quenched in water from 1600 degrees Fahr. (870 degrees Cent.). One of these pieces was placed in a furnace which was held at 1800 degrees Fahr. (980 degrees Cent.), and then quenched in water after holding in the furnace for 90 seconds. Similar test pieces were similarly treated, except that they were held in the furnace for 100 seconds, 110 seconds, and 120 seconds respectively. The case hardness of the samples was measured on the Rockwell hardness tester, and the core structures examined on the microscope. The results obtained are shown in Table V.

This experiment was repeated several times, using higher and lower furnace temperatures, and varying the time of holding the test pieces in the furnace to correspond. In all cases the results were sub-

Table V

Rockwell Hardness Tests

Time in Furnace	Rockwell "C" Hardness of Case	Structure of Core
90 seconds	15 to 20	good—see Fig. 24
100 seconds	45 to 55	good—see Fig. 24
110 seconds	60 to 65	fair —see Fig. 25
120 seconds	65 to 67	poor—see Fig. 22

stantially the same, and it is evident that at temperatures sufficiently high to fully harden the case, the core temperature is sufficiently high to produce the relatively brittle martensite-ferrite structure on quenching. It is also apparent that the structural change taking place in the core is very rapid, being a matter of seconds only. Hence any treatment designed to produce tough cores must be so conducted that the temperature of the core before quenching will not exceed 1375 degrees Fahr. (745 degrees Cent.) for more than a few seconds, as that temperature appears to be about the one at which such structural change has its inception.

Although the temperature of the steel was not measured in the preceding experiment, its appearance on quenching indicated a temperature of not less than 1400 degrees Fahr. (760 degrees Cent.) in all the samples except the one held for 90 seconds, which sample might have been a little lower. It was concluded therefore that the failure to obtain the desired result by the method employed was the result of imperfect solution of the case constituents due to an insufficiency of time for complete solution to be effected. In order to obtain a carburized piece which exhibits full case hardness together with the desired core toughness, the following three factors are evidently essential.

1. Sufficient time at a temperature higher than the critical point of the case to ensure complete solution of the structural constituents of the case.

2. A sufficiently high temperature of the case to ensure full hardness on quenching.

3. A method of heating such that the temperature of the core does not exceed 1375 degrees Fahr. (745 degrees Cent.) for more than a very few seconds.

Can the case of a carburized piece be fully hardened by quenching from a temperature of 1375 degrees Fahr. (745 degrees Cent.) or less? Such a treatment would be in line with that suggested by

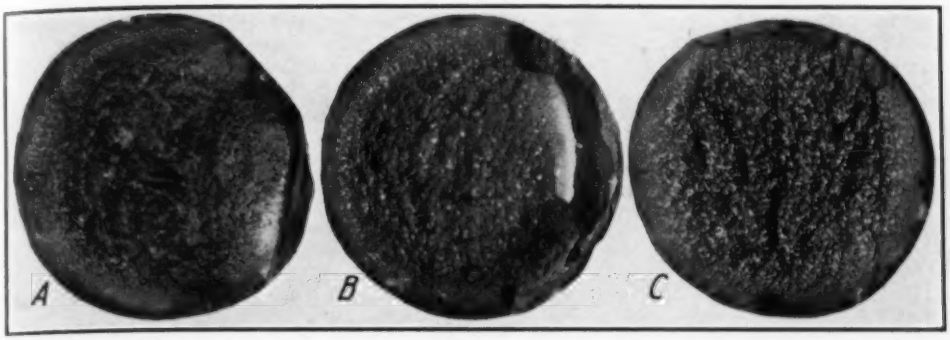


Fig. 26—Photograph of the Fractured Surfaces of Three Samples Treated as Described in the Text. × 3.

Pulsifer[6], and if successful would satisfy the three factors listed above. The author believes that it could be successfully performed if the transference of the piece from the furnace to the quenching medium were very rapid, and if it were protected from cooling influences during that transference. However he was unable to obtain a satisfactory result by quenching a sample from 1375 degrees Fahr. (745 degrees Cent.) without those precautions, and he is convinced that the method is not practicable for commercial operations. Since the temperature employed was high enough to ensure complete solution of the case constituents, failure to obtain hardness in the case must be attributed to an insufficient degree of superheat. One possible method of achieving the desired result remained. That was to effect complete solution of the case constituents by holding the steel between 1340 degrees Fahr. (725 degrees Cent.), the Ac point of the case, and 1375 degrees Fahr. (745 degrees Cent.), the apparent Ac_1 of the core for a few minutes, and to follow that treatment by a rapid application of heat so that the case would reach a sufficiently high temperature to harden fully on quenching, while the core was sufficiently unaffected as to retain its toughness.

To test the practicability of the proposed method, four carburized samples prequenched from 1600 degrees Fahr. (870 degrees Cent.) were heated to 1360 degrees Fahr. (737 dgrees Cent.) and held at temperature for five minutes. Two of the pieces were then quickly removed and immersed for four seconds in a lead bath which was maintained at a temperature of 1600 degrees Fahr. (870 degrees Cent.). These pieces were then quenched in cold water. The

[6]H. B. Pulsifer, "Low Carbon Steel," *Transactions*, American Institute of Mining and Metallurgical Engineers, 1931, Iron and Steel Division, p. 375.

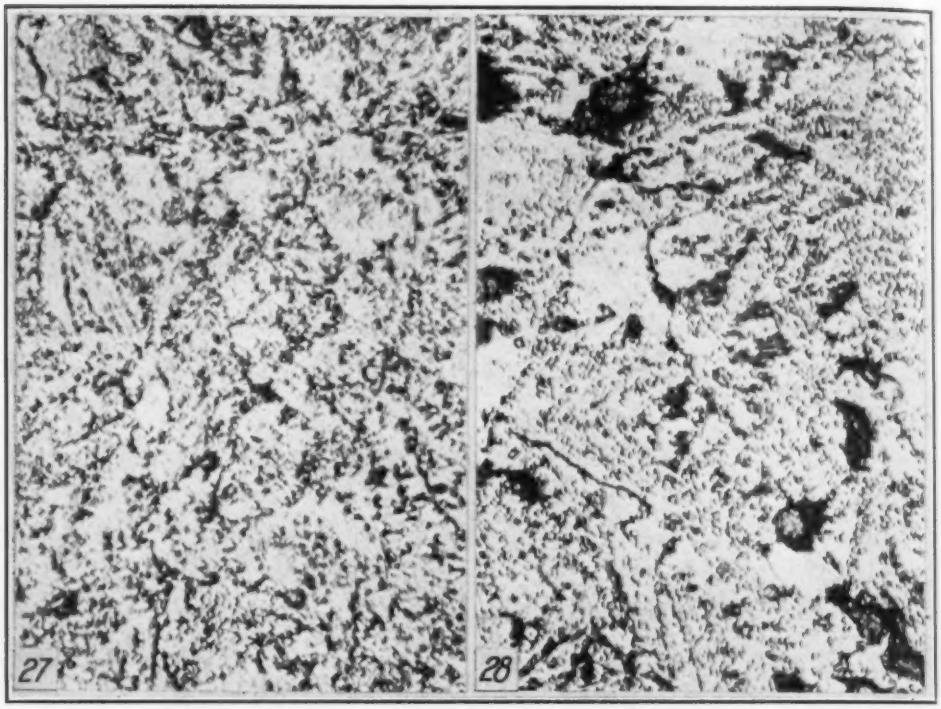


Fig. 27—Microstructure of Sample Marked A in Fig. 26. × 1000.
Fig. 28—Microstructure of Sample Marked B in Fig. 26. × 1000.

remaining samples were treated identically except that they were held in the lead for eight seconds. All the samples proved to be fully case-hardened when tested on the Rockwell hardness tester. Fig. 26 illustrates the appearance of the fractured surfaces of the pieces treated as described above, together with that of a piece treated in the conventional manner. The example marked A which displays the tough fibrous fracture was one of the pieces which was held in the lead for four seconds, and the microstructure of its core is illustrated in Fig. 27. The example marked B of Fig. 26 was one of the pieces which was held in the lead for eight seconds, and the structure of its core is illustrated in Fig. 28. The appearance of this fracture indicates a fairly tough core condition, but the crystallinity shown proves that some embrittlement had occurred in the last four of the eight seconds during which it was held in the lead. The example marked C of Fig. 26 shows the relatively brittle, crystalline fracture of pieces quenched in the usual way, and its core structure is practically identical with that already noted in Fig. 22.

Rockwell hardness tests of the cores of the three pieces shown in

Fig. 26 proved that each had about the same hardness as the others, being between B90 and B95.

Summary

1. In part one of this paper it was shown that the conventional treatment of carburized parts develops in the cores less than half their potential resistance to impact.

2. Rapid heating for the case refining quench does not produce a satisfactory combination of case hardness and core toughness.

3. While a case refining quenching temperature of 1375 degrees Fahr. (745 degrees Cent.) would produce a tough core, it is probably too low to produce full case hardness under practical operating conditions.

4. To obtain carburized parts having full case hardness and maximum core toughness, the following treatment is proposed: Carburize; Quench from the pot, or; Cool in the pot and reheat to 1600 degrees Fahr. (870 degrees Cent.) and quench. Reheat to 1360 degrees Fahr. (737 degrees Cent.) and hold at temperature for about five minutes.

Remove rapidly and place in a heating medium held at an elevated temperature. Hold for just sufficient time to permit the case to receive sufficient superheat to ensure full hardening on quenching. Quench in cold water or a more drastic medium.

In the treatment proposed above, neither the medium for rapid heat application nor the time for which the steel should be held in it are specified. It was found that lead was satisfactory as a medium, but it is certainly not the only one. However, it is probable that the medium should be liquid, since in a furnace containing air the rate of heat transfer might not be sufficiently rapid to provide the temperature necessary for the case without overheating the core.

The time for which the steel should be held in that medium would depend largely on the section of the piece and on the rapidity of heat transfer from the medium to the piece. In a liquid medium the time would probably vary from 5 to 10 seconds.

Discussion

As a general rule maximum toughness is developed in carbon and low alloy steels by quenching from over the upper critical point, reheating to just under the lower critical point and quenching again.

In effect that is the treatment which the cores of carburized parts would receive by the method proposed in the summary above; and it is the treatment applied to the sample illustrated in A of Fig. 26. The completely fibrous structure of the core of that sample, and the absence of any martensite in the microstructure prove it to be in its toughest condition. Hence it is safe to conclude that the treatment employed not only produces full hardness in the case but develops all the potential toughness of the core.

Whether or not such a degree of core toughness would warrant the extra refinements of treatment necessary to obtain it is open to question, since it could be argued that if the case is cracked, a piece is unfit for service even though the core remains intact. That is really an engineering question outside the scope of this paper. But if the conventional treatment produces adequate core toughness in carburized parts, then the use of a fine-grained steel should effect approximately the same result by a single quenching treatment. In Part I it was shown that a single quench from just over the Ac_3 of the core produced an Izod impact resistance value of about 30, while the conventional double treatment produced an Izod value of about 40. With a fine-grained steel the Izod value of the core would probably be higher than 30, while the case would not be seriously coarsened by the higher quenching temperature employed. At the same time, the core hardness of the single quenched steel would be about half as much again as that of the double quenched steel, which is a very important consideration. And as these comparisons are made on the assumption that the steels are of similar analysis, it should be quite possible, by lowering the carbon content, to produce by a single quench a core toughness equal to that obtained by double quenching, and equal or superior core hardness.

In conclusion the author wishes to express the hope that the facts which have been presented in these papers will prove of value to engineers. The various combinations of dynamic and hardness properties which it is possible to produce in carburized parts by various heat treatments have been indicated, and it is believed that this should be useful in producing the desired properties for the various applications for which such parts are designed.

THE CHEMISTRY OF LIQUID HARDENING BATHS

By George Barsky

Abstract

This paper discusses the chemistry of the reactions occurring between steel objects placed in molten salt hardening baths and the bath.

It was found that case hardening with liquid salt baths may be regarded as a reaction of the bath with the surface of the steel to form iron carbide which in turn diffuses into the steel.

Oxygen and oxygen-containing compounds have an influence on hardening with sodium cyanide.

Reactions of iron with sodium cyanide are discussed as is also the reactions taking place in the calcium cyanide bath.

IN liquid hardening baths a chemical reaction takes place between the compounds in the bath and the surface of the immersed steel part, resulting in the formation of iron carbide at the surface. At the temperatures used, iron carbide is soluble to a certain extent in the steel and consequently, as it forms, it diffuses into the steel and gives an outside shell of higher carbon content than the core. Reactions may also occur as a result of which nitrogen is also absorbed by the steel. These, however, are not considered in this paper, which is concerned with the reactions involved in the formation of iron carbide.

The reactions occurring in liquid hardening baths are somewhat obscure. In the case of sodium cyanide, not only does a reaction take place resulting in the transference of carbon from sodium cyanide to the iron, but, in addition to this reaction, there are other reactions resulting in depletion of the cyanide content of the bath, as, for example, oxidation of the cyanide by the air.

$$2\ NaCN + 2\ O_2 \rightarrow Na_2CO_3 + CO + N_2 \qquad (I)$$

A paper presented before the Cleveland Chapter of the American Society for Steel Treating in March, 1931. The author, George Barsky, is connected with the experimental laboratory of the American Cyanamid and Chemical Corporation, Linden, New Jersey.

Volatilization of cyanide also takes place as well as oxidation to cyanate.

Investigation of the mechanism of hardening in the cyanide bath is of great interest, especially to the chemist, but the experimental difficulties involved are many. In our laboratory we have attempted to throw some light on the reactions in liquid baths, with a view to improving methods of case hardening in such baths. While we cannot yet claim to have the final answers to the many questions that arise, results obtained so far are of interest and are presented with the qualification that much of this work is still under way.

Sodium Cyanide Bath

Several observations seem to indicate that oxygen or oxygen-containing compounds have a marked effect on the case hardening properties of sodium cyanide. For example, the following experiment is cited. A wire, 0.080 inch in diameter, was suspended vertically in a sodium cyanide bath containing 30 per cent NaCN and treated at 1600 degrees Fahr. (870 degrees Cent.) for one hour. The wire was then removed from the bath, quenched and broken at about 2-inch intervals and the case depth at the fractures measured with a Brinell glass. The pieces were then analyzed for carbon content by combustion, the figure obtained being, of course, the average of the whole section. The results are shown in the following table as well as in Fig. 1. Evidently the oxygen of the air

Inches from Bottom of Wire	Case Depth In.	Per Cent Carbon
2	0.004	0.17
4	0.008	0.19
8	0.011	0.29
14	0.012	0.34

either directly or indirectly influenced the case hardening reaction. The effect is not very pronounced at 1550 degrees Fahr. (845 degrees Cent.). To determine more quantitatively this influence of oxygen or oxygen-containing compounds, the depth of case produced in steel treated for one hour in sodium cyanide baths in the presence of air, nitrogen and sodium carbonate has been determined at 1550 and 1600 degrees Fahr. (845-870 degrees Cent.).

The sodium cyanide baths of various compositions were contained in a small steel bomb fitted with a cover which contained an

inlet tube dipping below the level of the melt for the passage of gas through the melt and also a small hole through which the test piece was suspended in the bath. The steel bomb was maintained at the desired temperature by immersion in a small pot furnace.

The cyanide baths were prepared from the 96-98 per cent sodium cyanide which contained on fusion about 2 per cent sodium

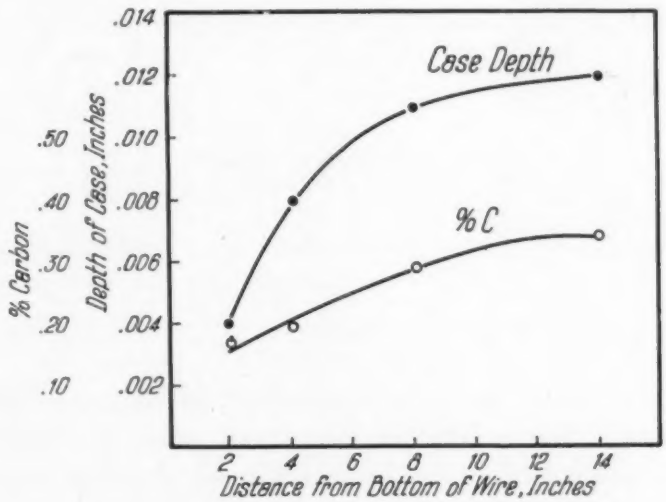


Fig. 1—Graph Showing the Case Hardening Properties of 30 Per Cent NaCN Bath for 1 Hour at 1600 Degrees Fahr. (870 Degrees Cent.)

carbonate. In a number of experiments to decrease the influence of the carbonate present in the cyanide, sodium chloride was added to the cyanide. In all experiments either dry air or dry oxygen-free nitrogen was bubbled through the melt. Nails as test pieces were treated for one hour and then quenched in water. The case was read with a Brinell glass on the polished and etched section. The results are presented in Table I.

Since the sodium cyanide used in these experiments contained 2 per cent of sodium carbonate, the case hardening properties of sodium cyanide absolutely free from oxygen or oxygen-containing compounds could not be determined. However, an approximation to an oxygen-free bath was obtained by the use of 20 per cent NaCN —80 per cent NaCl and 10 per cent NaCN—90 per cent NaCl mixtures in an atmosphere of nitrogen. Using these mixtures, case depths of 0.008 and 0.006-0.008 inch in one hour at 1600 degrees Fahr. (870 degrees Cent.) were obtained. Using the above mixtures with additions of 5 per cent Na_2CO_3 in an atmosphere of nitro-

Table I
Temperature 1600 Degrees Fahr.

	Composition	Depth of Case in Inches With Air	Nitrogen
1	96% NaCN	0.012	0.010
2	30% NaCN 70% Na_2CO_3	.....	0.012
3	20% NaCN 80% NaCl	.....	0.008
4	19% NaCN 76% NaCL 5% Na_2CO_3	.....	0.012
5	10% NaCN 90% NaCL	.....	0.006-0.008
6	9% NaCN 84% NaCl 5% Na_2CO_3	.....	0.012
	Temperature 1550 Degrees Fahr.		
7	30% NaCN 70% NaCl	0.010	0.006-0.008
8	28% NaCN 65% NaCl 7% Na_2CO_3	.....	0.010

(Compare 1 with 2; 3 with 4; 5 with 6; 7 with 8.)

gen and the 96 per cent NaCN in the presence of air, case depths of 0.012 inch in one hour at 1600 degrees Fahr. (870 degrees Cent.) were obtained in each case. The following reactions may be written for sodium cyanide:

$$3\,Fe + 2\,NaCN \rightarrow \underset{\text{(Sodium Cyanamide)}}{Na_2CN_2} + Fe_3C \qquad (a) \qquad (II)$$

$$Na_2CN_2 + 3/2\ O_2 \rightarrow \underset{\text{(air oxidation)}}{Na_2CO_3} + N_2 \qquad (b)$$

Reaction IIa is quite interesting as it is the reverse of one reaction used in the manufacture of sodium cyanide. The reactions taking place in the synthesis of sodium cyanide are:

$$2\,Na + 2\,NH_3 \rightarrow 2\,Na\,NH_2 + H_2 \qquad (a) \qquad (III)$$

$$2\,NaNH_2 + C \rightarrow Na_2CN_2 + 2\,H_2 \qquad (b)$$

$$Na_2CN_2 + C \rightarrow 2\,NaCN \qquad (c)$$

In the case of the sodium compounds in the presence of carbon, the cyanide is the more stable form. In the case of the calcium compounds, in the absence of solvents, which may be molten salts, the more stable form is the cyanamide.

In an effort to prove that the reaction IIa takes place, a small charge of case hardening compound, containing 43 per cent NaCN, was placed in a boat along with some iron filings. These were heated in a tube furnace at 1600 degrees Fahr. (870 degrees Cent.)

for thirty minutes, with nitrogen passing through the tube. When cool, the mass was analyzed for sodium cyanamide, but none was found.

The experiment was repeated using a closed iron crucible in which was placed a nickel crucible containing the charge. Inlet and outlet pipes were connected to the iron crucible for the passage of nitrogen. This was done in a large muffle furnace. The temperature was again 1600 degrees Fahr. (870 degrees Cent.) for about 1½ hours. Analysis of the cooled sample failed to show the presence of any sodium cyanamide.

These negative results, however, do not disprove that in actual case hardening sodium cyanamide is not formed. It may be that the decarburizing action of the sodium cyanamide is so great that unless it is removed by oxidation (equation IIb), the formation of iron carbide is prevented. This theory would explain readily the necessity for the presence of oxygen or oxygen-containing compounds on the activity of sodium cyanide.

Another theory of the reaction between iron and sodium cyanide is that the carbon reacts with the iron and that metallic sodium is volatilized with the evolved nitrogen.

$$2\ NaCN + 6\ Fe \rightarrow 2\ Na + N_2 + 2\ Fe_3C \qquad (IV)$$

Bucher, during an investigation of the formation of sodium cyanide by the reaction which is catalyzed by metallic iron, actually

$$Na_2CO_3 + 4C + N_2 \rightarrow 2\ NaCN + 3\ CO \qquad (V)$$

prepared metallic sodium and metallic potassium by heating a mixture of the cyanides with powdered iron. There is also the possibility that the iron reacts with nitrogen formed in this decomposition.

Guernsey and Sherman showed that sodium cyanide is dissociated into sodium carbide as well as to sodium, nitrogen and carbon on heating to about 1800 degrees Fahr (980 degrees Cent.).

We attempted to follow the reaction with iron quantitatively by using known amounts of cyanide and iron, and determining the increase in carbon content of the iron, the decrease in amount of cyanide and the amount of metallic sodium formed. A charge of 43 per cent NaCN case hardener and iron was placed in a nickel

crucible which in turn was placed in a closed iron crucible. The iron crucible was provided with inlet and outlet pipes for the passage of nitrogen. An iron condenser was connected to the outlet pipe of the crucible. The end of the condenser dipped into kerosene. No sodium was collected. The experiment was repeated in a tube furnace at 1600 degrees Fahr. (870 degrees Cent.) in a current of nitrogen. No metallic sodium could be detected in the mass on cooling in a current of nitrogen. The cooled mass showed no trace of sodium cyanamide.

Still another possibility with sodium cyanide is oxidation of the cyanide to cyanate followed by reaction of the cyanate with iron.

$$NaCN + 1/2\ O_2 \rightarrow NaCNO \qquad (VI)$$
$$2\ NaCNO + 3\ Fe \rightarrow Fe_3C + NaCN + Na_2CO_3 \qquad (VII)$$

We have found that potassium cyanate will actually produce a case.

This theory serves to explain readily the results obtained with the wire immersed vertically in the sodium cyanide bath. Sodium cyanide is oxidized at the surface of the bath to sodium cyanate which is carried into the bath by the circulation of the molten salts.

Calcium Cyanide Bath

This bath is remarkably different from the sodium cyanide bath in that very small concentrations of the cyanide are required, a special combination of molten salts being used. We attribute the difference in activity to properties of calcium cyanide. This cyanide is formed by fusion in an electric furnace under special conditions from calcium cyanamide, which is, as is generally known, made from carbide and nitrogen.

$$CaC_2 + N_2 \rightarrow CaCN_2 + C \qquad (a) \qquad (VIII)$$
$$CaCN_2 + C \rightleftarrows Ca(CN)_2 \qquad (b)$$

As we noted in our earlier discussion, the more stable form for the calcium salts is the cyanamide. In fact, calcium cyanide in fairly pure state, made by an indirect method will, on heating to a moderate temperature (about 400 degrees Fahr.), revert quantitatively to the cyanamide (reverse of equation VIIIb). In the presence of molten salts, the tendency for reversion may be reduced to a point depending on the composition of the salt mixture, the temperature, and the concentration in the salt mixture.

Oxygen seems to have no part in the case hardening reaction of the calcium cyanide bath. In an experiment with a wire immersed vertically in the bath, similar to the one performed with the sodium cyanide bath, the depth of case obtained and the carbon content were uniform from the top to the bottom of the wire.

In order to follow the chemistry of this bath closely and to

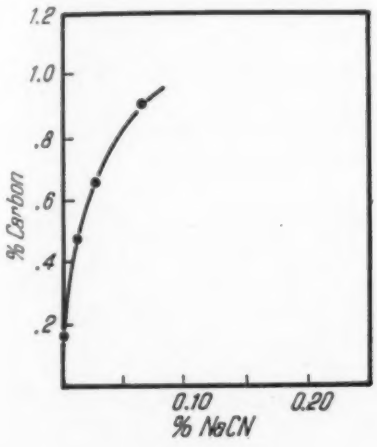


Fig. 2

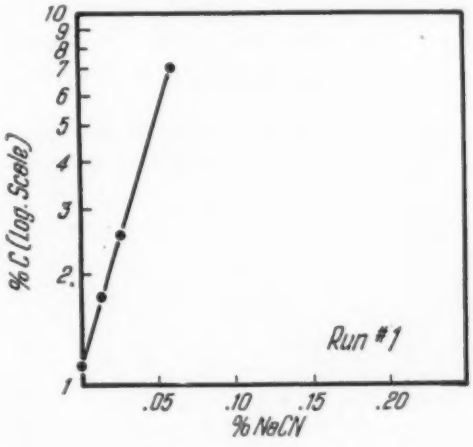


Fig. 3

Fig. 2—Graph Showing Carbon Absorption Plotted Against Cyanide Concentration.
Fig. 3—Graph Showing Rate of Carbon Absorption Plotted Against Cyanide Concentration. Run No. 1.

permit rapid comparisons to be made on a quantitative basis, a short and rapid method for the determination of the activity of case hardening baths was developed in our laboratory.

The method generally used for the determination of the activity of case hardening baths involves the lengthy procedure of machining special test bars, hardening these bars over periods of time varying from one hour to three hours, cooling the bars, accurately turning off successive cuts in a lathe and analyzing the individual cuts for carbon content. This elaborate procedure does not allow the determination of activities of the bath over relatively short periods and gives the average activity over the time during which the specimen was immersed.

The new method consisted in immersing thin steel strips in the bath for 15-minute intervals, quenching the strips and determining the carbon content by combustion. By this method interesting information has been obtained on the correlation of the cyanide content of the bath and the absorption of carbon by steel.

The bath was prepared for each run with the necessary addition

of the cyanide compound and no additions of cyanide were made during a run. Thin steel strips, 0.0065 ± 0.002 of an inch in thickness and of 0.16 per cent carbon content, were treated in the bath for 15 minutes and then analyzed for carbon. Samples of the bath were taken throughout the run and their cyanide content determined. The temperature was 1580 degrees Fahr. (860 degrees Cent.).

The per cent cyanide was plotted against time. From these curves by interpolation the average cyanide content of the bath was

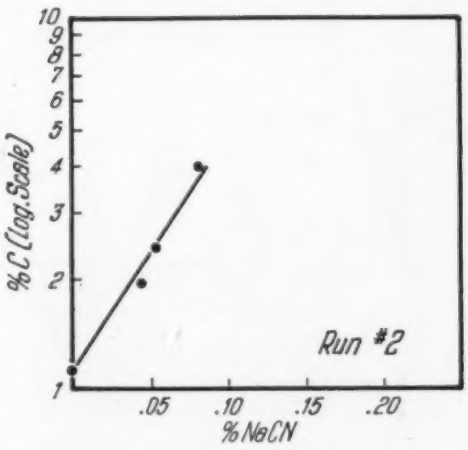


Fig. 4

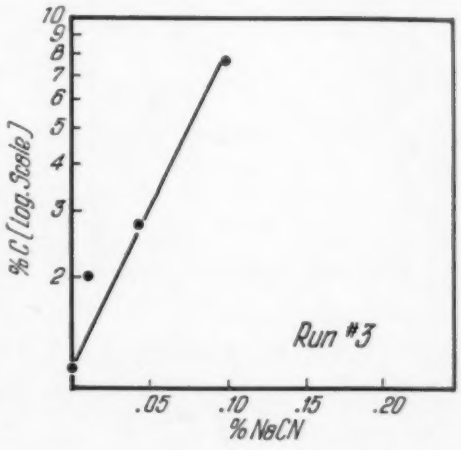


Fig. 5

Fig. 4—Graph Showing Rate of Carbon Absorption Plotted Against Cyanide Concentration. Run No. 2.
Fig. 5—Graph Showing Rate of Carbon Absorption Plotted Against Cyanide Concentration. Run No. 3.

calculated for each steel strip. Carbon absorption was then plotted against cyanide concentration.

(Fig. 2). The shape of this curve is quite significant. We would expect, of course, that at any fixed temperature the rate of carbon absorption is dependent upon the carbon content of the steel, and would be directly proportional to the degree of unsaturation, that is to C_e—C where—

C_e is the carbon content at equilibrium at 1580 degrees Fahr. according to the iron-carbon diagram.
C is the carbon content at any time.

Expressing this mathematically we have—

$$\frac{dc}{dt} = a\,(C_e - C) \qquad \text{(IX)}$$

The rate of carbon absorption is also some function of the cyanide concentration. If the reaction involves one mol of calcium cyanide per mol of Fe_3C formed as in the equation—

$$Ca(CN)_2 + 3\ Fe \rightarrow Fe_3C + CaCN_2 \qquad (X)$$

the rate of absorption should be directly proportional to the cyanide concentration.

$$\frac{dc}{dt} = a\ Cy \qquad (XI)$$

Combining equation IX and XI, we have—

$$\frac{dc}{dt} = k,\ Cy\ (C_e - C) \qquad (XII)$$

or

$$\frac{dc}{C_e - C} = k,\ Cy\ dt \qquad (XIII)$$

Integrating, we have—

$$\text{Log}\ (C_e - C) = k,\ Cy\ t + k_2 \qquad (XIV)$$

$$\text{Log}\ \frac{1}{C_e - C} = k,\ Cy\ t + k_2 \qquad (XV)$$

When Cy = o, c = 0.16. C_e from the iron-carbon equilibrium diagram is 1.05.

$$k_2 = \log \frac{1}{C_e - C} = \log \frac{1}{.89} = \log 1.12$$

This gives us—

$$\log \frac{1}{C_e - C} + k,\ Cy\ t + \log 1.12 \qquad (XVI)$$

Since t is the same for all tests with strips, if we plot $\log \frac{1}{C_e - C}$ against cyanide concentration, we should obtain a straight line passing through the point 0, 1.12.

We have plotted $\log \frac{1}{C_o - C}$ against cyanide concentration (expressed as sodium cyanide) for three runs. These are shown in Figs. 3, 4 and 5. In the case of Run No. 1, the curve is quite definitely a straight line. For Run No. 2, the same is true. From the plot of Run No. 3, the same conclusion can be drawn, if we assume one point to be in error.

This evidence, while not absolutely positive proof, is consistent with the theory that the reaction is—

$$Ca(CN)_2 + 3\ Fe \rightarrow Fe_3C + CaCN_2$$

In conclusion the author wishes to express his thanks to Dr. Eli Lurie for valuable cooperation and to the American Cyanamid and Chemical Corporation for permission to publish these results.

Summary

1. Case hardening in liquid baths may be regarded as a reaction of the bath with the surface of the steel to form iron carbide which diffuses into the steel.

2. Oxygen or oxygen-containing compounds are shown to have an influence on hardening with sodium cyanide.

3. Possible reactions of iron with sodium cyanide are discussed.

4. The reaction in the calcium cyanide bath has been discussed and the theory advanced that it is—

$$Ca(CN)_2 + 3\ Fe \rightarrow CaCN_2 + Fe_3C$$

DIVISION OF THE IRON-VANADIUM-OXYGEN SYSTEM INTO SOME OF ITS CONSTITUENT BINARY AND TERNARY SYSTEMS

By C. H. Mathewson, E. Spire and C. H. Samans

Abstract

An X-ray analysis of briquetted and sintered mixtures prepared in vacuo indicates that there are four oxide phases which can appear separately in equilibrium with iron, viz., FeO (solid solution), FeV_2O_4, V_2O_3 and V_2O_2. FeV_2O_4 is an iron-vanadium spinel, described for the first time, which is sufficiently soluble in iron to form well crystallized inclusions. The other oxides, aside from FeO, are practically insoluble in iron, so that they may even be used as crucible materials in preparing clean metal (in vacuo) free from inclusions. The ternary systems reaching into the iron corner of the constitutional diagram are Fe-V-V_2O_2, Fe-V_2O_2-V_2O_3, Fe-V_2O_3-FeV_2O_4 and FeV_2O_4-FeO. Some metallographic data, particularly on the binary system FeO-FeV_2O_4, are included. This system is especially characterized by an eutectic of the approximate composition 18 mols. FeO to 1 mol. FeV_2O_4. The crystal structure of V_2O_2 is similar to that of FeO with a parameter value, $a_o = 4.08$ Å.

No oxide of vanadium lower than V_2O_2 was observed and this oxide reduces ferrous oxide.

Acicular structures of Widmanstätten character, due presumably to separation of vanadium from its solid solution in V_2O_2, were observed in vanadium-oxygen alloys of suitable composition.

VERY little is known concerning the conditions of equilibrium in the system iron-vanadium-oxygen notwithstanding their great importance in any effort to explain the action of vanadium as an alloying ingredient in iron or steel. Complicated equilibria of this character must first be systematically analyzed so that the compounds

---

This is a communication from the Hammond Metallurgical Laboratory of Yale University. Dr. C. H. Mathewson is a member of the Society and is Professor of Metallurgy. Messrs. Spire and Samans are graduate students in the Department of Metallurgy. The X-ray studies will be incorporated in a report to be presented to the faculty of the graduate school of Yale University by Mr. Samans in partial fulfillment of the requirements for the degree of Master of Science. Manuscript received July 3, 1931.

or solid solution lattice types which actually function as components within the desired concentration range may be recognized and a closer study of their interrelationship planned in accordance with the character of the information desired.

Iron-Vanadium and Iron-Oxygen

In the present case, due to the definite results from recent researches, it is now possible to summarize the essential constitutional features of two of the boundary systems, namely, Fe-O and Fe-V, with considerable accuracy. The iron-oxygen system was reviewed this past year by one of the present authors and associates[1]. In rapidly cooled mixtures a ferrous phase, substantially FeO, occurs in the form of globular inclusions in equilibrium with iron containing a trifling amount of oxygen in solid solution. This ferrous phase possesses a homogeneity range extending to about 24.5 per cent of oxygen in the direction of Fe_3O_4 and at about 570 degrees Cent. (1060 degrees Fahr.) the saturated solid solution breaks down into Fe(O) + Fe_3O_4 if the cooling is very slow or if annealing is conducted below the transformation temperature. In the present investigation, the cooling conditions were such as to maintain the composition of the ferrous phase, and the conditions brought about by annealing to equilibrium at comparatively low temperatures were not investigated. The ferrous solution and magnetite form an eutectic mixture* at about 25 per cent oxygen, but in our survey of the iron-vanadium-oxygen system only those phases which occur in equilibrium with metal in rapidly cooled mixtures were considered and magnetite thus fell beyond the limit of the present undertaking.

The constitutional diagram of the iron-vanadium system originally presented by Vogel and Tammann[2] has been amplified by Oya[3]

[1]C. H. Mathewson, E. Spire, and W. E. Milligan, "Evolution of the Iron-Oxygen Constitutional Diagram." Transactions, American Society for Steel Treating, Vol. 19, 1931, p. 66.

[2]R. Vogel and G. Tammann, "Uber Vanadin-Eisenlegierungen," *Z. Anorg. Chem.*, Vol. 58, 1908, p. 73.

[3]M. Oya, "On the Equilibrium Diagram of the Iron-Vanadium System," Science Reports, Tohoku Imperial University, Vol. 19, 1930, p. 235; "On the Equilibrium Diagram of the Iron-Vanadium-Carbon System," *do*, Vol. 19, 1930, p. 449. See also A. Osawa and S. Oya; "X-ray Analysis of Iron-Vanadium Alloys," *do*, Vol. 18, 1929, p. 729.

*Recently, L. B. Pfeil, *Journal*, Iron and Steel Inst., No. 1, 1931, p. 237, has ascribed the eutectic appearance of these mixtures to characteristic separation of the Fe_3O_4 phase from a primary or secondary (peritectic) ferrous phase and more recently Schenck and Hengler, *Archiv für das Eisenhüttenwesen*, Vol. 5, 1931-2, p. 209, have found both a minimum and a maximum of the liquidus-solidus curves above the field of ferrous solid solution. The presence of an eutectic is thus questionable and a further attempt to overcome the difficulties, (crucible and thermocouple attack) which have beset all of these thermal studies would be welcome.

who studied the effect of vanadium on the critical points of iron and also reported confirmation by X-ray methods of solid solubility in the full range of concentration between iron and vanadium. Quite recently Wever and Jellinghaus[4] have shown that iron-vanadium alloys in the concentration region, 29 to 60 per cent of vanadium react on slow cooling to form a compound of the formula FeV. This phase was not encountered in our rapidly cooled mixtures, and the effect of this complication in ternary system was not investigated.

Concerning the third system little can be said except that the melting point of vanadium-oxygen mixtures rises continuously from vanadium at least as far as the composition, V_2O_3.[5]

The present experiments are restricted solely to the question of the identity of the oxides which are found in equilibrium with the metals iron and vanadium and no attempt has been made to work out any of the individual binary and ternary constitutional diagrams encountered. Table I contains a description of all materials used during the course of the investigation.

It was considered advisable to use the X-ray powder method in this survey since it offers the most positive means of identifying the various constituents of the alloys. Furthermore, the extremely baffling problem of producing crucibles in which these mixtures of metals and oxides may be melted without contamination may be avoided by the simple expedient of utilizing compressed powder mixtures which have been heated in vacuo just short of the melting point. The powder for these briquets, amounting to 5 to 10 grams, was passed through a 100-mesh screen and compressed in a cylindrical mold one inch in diameter at a pressure of 20,000 pounds. Mixtures containing the very fine V_2O_3 powder available needed no binder. Others were moistened with a little alcohol. Under these conditions complete reaction may be expected to occur and the product can then be pulverized for X-ray examination along with a sample of pure sodium chloride in the other half of the specimen tube. In other surveys of this sort great difficulty has been experienced in preparing uncontaminated alloys and identifying the various structure elements under the microscope.

The well known X-ray diffraction equipment supplied by the

[4]F. Wever and W. Jellinghaus, "Zur Kenntniss des Zweistoffsystems, Eisen-Vanadium," *Mitt. aus dem K. W. Institut fur Eisenforschung.* Dusseldorf, Vol. 12, Lieferung, Vol. 19, 1930.

[5]O. Ruff and W. Martin, "Uber Reines Vanadin," *Z. Angew. Chemie,* Vol. 25, 1912, p. 49.

Table I

List of Materials Used for X-Ray Analysis or Microscopic Examination

A—Oxides of Vanadium

No.	Kind of Material	Notes	X-Ray Table	Photo
1	V_2O_4	Heated in vacuo 30 minutes at approx. 1600 degrees Cent.		
1a	V_2O_4	As received		
2	V_2O_3	Heated in vacuo 1 hour at 14-1500 degrees Cent.	2	
2a	V_2O_3	As received	2	
3	V_2O_2	Briquet—67% V_2O_3+33% V cont'g 7.22% O, sintered in vacuo	3	Fig. 1
4	V_2O	Sintered briquet representing hypothetical compound	4	Figs 3-4

B—Percentage Composition of Mixtures Shown in Fig. 7

No.	% V Containing 7.22% O	% V_2O_2	% V_2O_3	% Fe	% FeO	X-Ray Table	Photo
1	100					4	Fig. 5
2	100*					4	
3					100	6	
4				100		6	
5			73.45	26.55		7	
5a		65.65			34.35	7	
6		39.00			61.00	8	Fig. 7
7		55.50			44.50	9	
8		29.82		70.18		11	
9	80.10			19.90		11	
10	23.75			5.50	70.75	8	
11			68.15		31.85		
12			41.75		58.25		Fig. 10
13		78.82			21.18	7	
14			48.07	51.93		12	
15	51.22				48.78	13	
16	21.48				78.52	8	Fig. 11
17	38.47				61.53	12	
18			29.88	70.12		12	
19		80.00		20.00		13	
23	10.20		89.80			5	
24			67.62		32.38	10	
25		55.50		44.50		11	
26			29.46		70.54	9	
27			34.29		65.71		
28			41.04		58.96	10	Fig. 9
29			20.70		79.30	9	
30			45.50		54.50		
31			67.60		32.40	6	
32			58.19		41.81		
33			10.39		89.61		Fig. 8
34			51.25		48.75		
35			80.69		19.31	10	
36	48.42		51.58			5	Fig. 2
37	31.40		68.60			5	

*This sample was 99.5% pure.

General Electric Company was used in this work. In Tables II to XIII listing the results, the spacing as read on the General Electric scale[6], after the best possible adjustment of the film so as to indicate correct spacings for the NaCl line series adjacent to the unknown series, are given in the first column, followed by a simple designation of the observed intensities. The interpretation of the pattern is then

[6]W. P. Davey, "A Study of Crystal Structure and Its Applications," *General Electric Review*, Vol. 29, 1926, p. 128.

given in the remaining columns by designating the substances considered responsible for the different groups of spacings and showing the theoretical spacings calculated from the most probable parameter values as listed below.

Quite a number of weak lines and occasionally a strong one could not be identified as belonging to any substance within the range of the investigation. These are, of course, attributed to impurities contained in the original vanadium preparations or to unforeseen contamination during preparation. It was generally possible to obtain a very complete line series, within the range of measurement, of any constituent listed as present in these mixtures. Only the information considered most essential for identifying the various constituents is included in the tables. Thus, in order to save space, the indices of planes producing the diffraction pattern are not included. It is expected that a more detailed presentation of some of the more important X-ray data will be given elsewhere.

Vanadium-Oxygen

Attention was first directed to the behavior of vanadium with relation to its own oxides. These occur in an ascending series beginning with V_2O_2, or perhaps V_2O, and ending with V_2O_5. It may confidently be expected that the higher oxides are reduced by the metal itself at temperatures in the vicinity of the melting point so that only V_2O_2 (or V_2O) will exist in a metallic matrix.

For these experiments, it was possible to obtain, through the courtesy of Jerome Strauss of the Vanadium Corporation of America, samples designated C.P. of the oxides V_2O_3, V_2O_4 and V_2O_5 and also a liberal sample of metallic vanadium containing 91.85 per cent of vanadium with impurities as follows: Fe 0.36, Al 0.16, Si 0.28 and C 0.11, the remainder amounting to 7.22 per cent doubtless being oxygen. A small quantity of much purer material from the same source was also available. This contained 99.55 per cent of vanadium, about 0.2 per cent of iron and silicon, a trace of carbon and probably about 0.2 per cent oxygen. As in the work with iron and its oxides*, it was desired to conduct the experiments in vacuum of the general order of 1 millimeter and it was expected that such lower oxide as might be in equilibrium with the metal would possess an extremely

*Loc. Cit. (1)

low dissociation pressure at the temperature of incipient fusion of the briquetted powder. However, no data on the dissociation pressure of these oxides could be discovered and a few preliminary experiments were undertaken as follows:

(1) 10 grams of V_2O_4 heated to approximately 1600 degrees Cent. (2910 degrees Fahr.) in a platinum crucible lost approximately 7 per cent of its weight during a 30 minute period of heating.

(2) 10 grams of V_2O_3 treated similarly for 1 hour lost less than 1 per cent of its weight but no accurate estimate of the temperature reached in this experiment or of the conditions responsible for this small loss of weight could be made on account of a reaction resulting in local perforation of the crucible. The same result was obtained on repeating this experiment.

X-ray examination of the heated V_2O_3 powder, No. 2 of Table IA, gave the data shown in Table II in comparison with data from untreated oxide, 2a.

The pattern obtained from material No. 1a, V_2O_4 as received, shows extraneous lines probably due to contamination with V_2O_3. After heating in vacuo (Material No. 1) the line series of V_2O_3 could no longer be recognized and the lines of the principal series representing the (undetermined) structure of V_2O_4 had shifted perceptibly and developed a certain complexity which denotes some form of alteration in the lattice structure. It is concluded that the loss of oxygen on heating in vacuo has brought about an absorption of molecules of the lower oxide into the lattice by some form of solid solution, but has not produced any structurally free V_2O_3.

Subsequent work made it clear that no oxide mixture corresponding to the patterns obtained from materials 1 and 1a appeared in equilibrium with either iron or vanadium and no detailed analysis of these patterns was therefore attempted.

The spacings from material 2 do not differ appreciably from those of 2a and are compatible with the hexagonal structure of V_2O_3 reported[7] by Goldschmidt, Barth and Lunde and later in greater detail by Zachariasen.[8]

It is evident from the conditions just described that oxides of vanadium lower in the scale than V_2O_4 may be heated in vacuo in the

[7]Cf. Wyckoff in *International Critical Tables*, Vol. 1, p. 343.

[8]W. H. Zachariasen, "Untersuchungen über die Kristalstruktur von Sesquioxyden und Verbindungen ABO_3." Skrifterutgitt au det Norske Videnskops-Akademi I Oslo, 1928, p. 17.

Table II

X-Ray Data on Materials Listed in Table I-A

Specimen 2a, (V_2O_3 As Received)				Specimen 2, (V_2O_3 Heated in Vacuo)			
Observed Pattern	Observed Intensity	Theoretical Due to	Theoretical Pattern	Observed Pattern	Observed Intensity	Theoretical Due to	Theoretical Pattern
3.680	vs	V_2O_3	3.642	3.680	s	V_2O_3	3.642
2.705	vs	V_2O_3	2.698	2.705	vs	V_2O_3	2.698
2.480	vs	V_2O_3	2.466	2.480	vs	V_2O_3	2.466
2.345	vw	V_2O_2	2.358	2.345	vw	V_2O_2	2.358
2.195	s	V_2O_3	2.179	2.195	s	V_2O_3	2.179
2.045	w	V_2O_2	2.041	2.045	vw	V_2O_2	2.041
1.912	vw	....	.....	1.828	s	V_2O_3	1.821
1.830	s	V_2O_3	1.821	1.698	vs	V_2O_3	1.689
1.698	vs	V_2O_3	1.689	1.612	vw	V_2O_3	1.612
1.612	vw	V_2O_2	1.612	1.578	w	....	.....
1.580	vw	....	.....	1.470	s	V_2O_3	1.465
1.470	s	V_2O_3	1.465	1.443	vw	V_2O_2	1.443
1.445	vw	V_2O_2	1.443	1.428	vs	V_2O_3	1.423
1.429	vs	V_2O_3	1.423	1.328	m	V_2O_3	1.324
1.328	m	V_2O_3	1.324	1.230	m	{V_2O_2} {V_2O_3}	1.231–1.233
1.235	w	{V_2O_2} {V_2O_3}	1.231 1.233	1.220	m	V_2O_3	1.214
1.223	vw	V_2O_3	1.214	1.195	vw	V_2O_2	1.191
1.195	vw	V_2O_3	1.191	1.175	w	{V_2O_3} {V_2O_2}	{1.171} {1.178}
1.175	w	{V_2O_2} {V_2O_3}	1.178–1.171	1.168	m	V_2O_3	1.167
1.170	s	V_2O_3	1.167	1.125	m	V_2O_3	1.121
1.125	m	V_2O_3	1.121	1.092	s	V_2O_3	1.088
1.092	s	V_2O_3	1.088	1.057	s	V_2O_3	1.055
1.059	s	V_2O_3	1.055	1.020	w	V_2O_2	1.020
1.021	w	{V_2O_3} {V_2O_2}	1.020	1.001	vw	V_2O_3	1.001
1.003	vw	V_2O_3	1.001				

$a_0 = 4.081$ gives values listed as theoretical pattern for V_2O_2.

Pattern given as theoretical for V_2O_3 is that of W. H. Zachariasen. (8)

Composition of original briquets: 100% V_2O_2 (As Received)

$a_0 = 4.081$ gives values listed as theoretical pattern for V_2O_2.

Pattern given as theoretical for V_2O_3 is that of W. H. Zachariasen. (8)

Composition of original briquets: 100% V_2O_3 (As Received)

region of the melting point of vanadium* substantially without decomposition and it thus appears a simple matter to determine just which oxide is in equilibrium with vanadium at such temperature by preparing, sintering in vacuo and examining various briquetted mixtures of V and V_2O_3.

This was done inside of a 3-inch quartz tube using the Ajax-Northrup high frequency furnace with a ring and cover of sintered tungsten around the preparations in order to obtain the requisite electrical coupling and heat effect. The simplicity of the apparatus makes it unnecessary to add further details.

It was straightway found that V and V_2O_3 mixed in the proportions necessary to produce V_2O_2 appeared to react quantitatively. Under the microscope a rather homogeneous grey-brown metallic powder was seen, with occasional specks of a brighter metallic con-

*1715 degrees Cent. according to O. Ruff and W. Martin. L. c. (5).

stituent, obviously metallic vanadium which had separated on cooling. This structure is shown in Fig. 1. It recalls the precipitation of iron from a preparation approximating the composition, FeO.*

The X-ray pattern reveals a line series, Table III, unlike that of vanadium or any of the higher oxides. This is a face-centered cubic series with a scale of intensities closely approximating that observed in the case of FeO and it is therefore probable that V_2O_2 conforms to the space group (NaCl, 4b, 4c) assigned by Wyckoff and Crittenden[9] to FeO.

The method adopted to serve the general purpose of this investigation cannot be expected to yield final heat treated products corresponding exactly to predetermined compositions. There is accordingly some doubt as to the parameter of the unit cell composed entirely of pure compound, V_2O_2. A homogeneity range corresponding to parameter values from 4.04 to 4.14 Å was actually observed, the former from the compound in association with vanadium and the latter from the compound mixed with the trioxide. The material (No. 3, Table IA) prepared as V_2O_2 gave the value 4.08 Å. Assuming the

Table III

X-Ray Data on Materials Listed in Table I-A

Specimen 3, (V_2O_2) I				Specimen 3, (V_2O_2) II				Specimen * (V_2O_2) III			
Observed Pattern	Observed Intensity	Due to	Theoretical Pattern	Observed Pattern	Observed Intensity	Due to	Theoretical Pattern	Observed Pattern	Observed Intensity	Due to	Theoretical Pattern
2.355	s	V_2O_2	2.358	2.355	s	V_2O_2	2.358	2.380	s	V_2O_2	2.378
2.050	vs	V_2O_2	2.041	2.050	vs	V_2O_2	2.041	2.060	vs	V_2O_2	2.059
1.625	vw	....	.....	1.628	vw	....	.....	1.452	vs	V_2O_2	1.455
1.441	vs	V_2O_2	1.443	1.440	vs	V_2O_2	1.443	1.238	m	V_2O_2	1.240
1.230	m	V_2O_2	1.230	1.230	m	V_2O_2	1.230	1.188	m	V_2O_2	1.187
1.177	m	V_2O_2	1.178	1.179	m	V_2O_2	1.178	1.028	m	V_2O_2	1.028
1.021	w	V_2O_2	1.020	1.019	m	V_2O_2	1.020	0.944	w	V_2O_2	0.944
0.938	w	V_2O_2	0.937	0.938	w	V_2O_2	0.937	0.920	m	V_2O_2	0.920
0.912	m	V_2O_2	0.913	0.914	m	V_2O_2	0.913	0.840	m	V_2O_2	0.840
0.832	m	V_2O_2	0.833	0.832	m	V_2O_2	0.833				
a_o = 4.082 gives values listed as theoretical pattern for V_2O_2.				a_o = 4.082 gives values listed as theoretical pattern for V_2O_2.				a_o = 4.115 gives values listed as theoretical pattern for V_2O_2.			

Average of these two films gives $a_oV_2O_2 = 4.08 \pm 0.01$.

Composition of original briquets:

67.0% V_2O_3
33.0% V

*This specimen came from a crucible of the composition, V_2O_2, after it had been used for melting a sample of electrolytic iron.

*Loc. cit. (1).

[9]R. W. G. Wyckoff and E. D. Crittenden, "The Preparation and Crystal Structure of Ferrous Oxide," *Journal*, American Chemical Society, Vol. 47, 1925, p. 2876.

presence of 8 atoms in the unit cell, as in the case of FeO, a density of 6.5 would be required. This is somewhat greater than the density of pure vanadium (6.0). The maximum a_o value observed, 4.14, would require a density of 6.2. The density of the very porous briquetted material (Cf. Fig. 1) was found to be 5.6, which might not unreasonably be considered at least 15 per cent too low.

There appears to be no doubt, that it is the oxide V_2O_2 which is normally found in association with metallic vanadium, while V_2O, if indeed capable of existence at all, does not form under these conditions. It is of interest to note in this connection* that early observers notably Berzelius apparently mistook preparations containing enough oxygen to be composed substantially of V_2O_2 for the metal itself. It was also alleged that the suboxide or hemioxide, V_2O, was present in metal prepared by the aluminothermic process and indeed occurred in the oxide film formed by slow oxidation of vanadium in the air. Koppel and Kaufmann[10] have shown that the alleged suboxide is probably a mixture of V and V_2O_2.

X-ray examination of three briquetted mixtures located in the concentration region between V and V_2O_2 substantiates this contention. All of these reveal the line series of these two components, corresponding to a_o values which indicate a substantial degree of mutual solid solubility. The presence of oxygen in the vanadium lattice causes contraction as may be seen by comparing the results (Table IV) obtained from our purest vanadium, $a_o = 3.024$, with those obtained from the inferior grade containing 7 per cent of oxygen, $a_o = 2.987$.

Samples containing 13.5, 15, and 20 per cent of oxygen, respectively, the first corresponding to a hypothetical V_2O, contain vanadium whose a_o value has been reduced to 2.928 and V_2O_2 possessing a parameter value, $a_o = 4.036$ (Tables IV and V), substantially less than the value, $a_o = 4.082$, obtained from the pure preparation (Table III).

Under the microscope these specimens are characterized by the presence of an acicular structure, obviously denoting the separation of vanadium from solution in V_2O_2. In Fig. 2, representing sample No. 36 containing 20 per cent oxygen, the separated phase may be

*A good summary of the literature on this subject is contained in the recent "Comprehensive Treatise on Inorganic and Theoretical Chemistry," Vol. IX, Longmans, 1929, by J. W. Mellor.

[10]J. Koppel and A. Kaufmann, *Z. Anorg. Chem.*, Vol. 45, 1905, p. 352.

Table IV

X-Ray Data on Materials Listed in Table I

Specimen 2, Table I-B, (99.5% V)

Observed Pattern	Observed Intensity	Due to	Theoretical Pattern
2.410	m	....	.....
2.150	vs	V	2.140
1.820	vw	....	.....
1.688	w	....	.....
1.512	s	V	1.511
1.388	vw	....	.....
1.232	vs	V	1.235
1.149	vw	....	.....
1.070	s	V	1.070
1.046	w	....	.....
0.957	vs	V	0.958
0.871	w	V	0.874
0.808	vs	V	0.809

a_o = 3.024 gives values listed as theoretical pattern for Vanadium.

Composition of original samples:
99.5% V
0.5% ?

Specimen 1, Table I-B, (91.85% V)

Observed Pattern	Observed Intensity	Due to	Theoretical Pattern
2.235	s	....	.....
2.110	vs	V	2.112
1.682	w	....	.....
1.496	m	V	1.494
1.311	m	....	.....
1.242	w	....	.....
1.230	s	V	1.220
1.148	vw	....	.....
1.110	m	....	.....
1.053	w	V	1.056
0.942	m	V	0.945
0.887	m	....	.....

a_o = 2.987 gives values listed as theoretical pattern for Vanadium.

Composition of original samples:
91.85% V
0.36% Fe
0.18% Al
0.28% Si
0.11% C
7.22% O_2 (?)

Specimen 4, Table I-A, (V_2O) Hypothetical

Observed Pattern	Observed Intensity	Due to	Theoretical Pattern
2.340	w	V_2O_2	2.330
2.260	s	from Comm. V	
2.080	vs	V	2.070
2.020	m	V_2O_2	2.019
1.948	vw	....	.....
1.890	w	....	.....
1.800	w	....	.....
1.702	vw	....	.....
1.462	s	V	1.465
1.424	s	V_2O_2	1.427
1.356	w	....	.....
1.331	vw	....	.....
1.261	vw	....	.....
1.229	s	....	.....
1.218	w	V_2O_2	1.216
1.191	vw	V	1.195
1.165	vw	V_2O_2	1.165
1.132	w	....	.....
1.037	m	V	1.035
1.007	vw	V_2O_2	1.009
0.945	vw	....	.....
0.928	w	V-V_2O_2	0.926
0.898	vw	V_2O_2	0.902
0.848	vw	V	0.846
0.820	w	V_2O_2	0.824

a_o = 2.928 gives values listed as theoretical pattern for Vanadium.

a_o = 4.036 gives values listed as theoretical pattern for V_2O_2.

Composition of original briquet:
74.5% V (91.85%)
25.5% V_2O_3

seen both as a network in the boundaries and a segregate of Widmanstätten characteristics inside of the original grains of V_2O_2. With brilliant white illumination and a 4-millimeter objective, the separated particles of metal have a dazzling white lustre and the residual oxide a brownish tint. Figs. 3 and 4 show the microstructure of sample No. 4, Table IA, corresponding to hypothetical V_2O, before and after quenching* from 1350 degrees Cent. (2460 degrees Fahr.). At this quenching temperature much of the previously precipitated acicular vanadium has dissolved. The X-ray pattern after this treatment remained substantially unaltered.

*This operation was performed by heating the briquetted material for a period of two hours in a quartz tube connected to the vacuum line and quenching in water. Quenching after annealing 1 hour at 1200 degrees Cent. (2190 degrees Fahr.) produced no change in the appearance of the "needles."

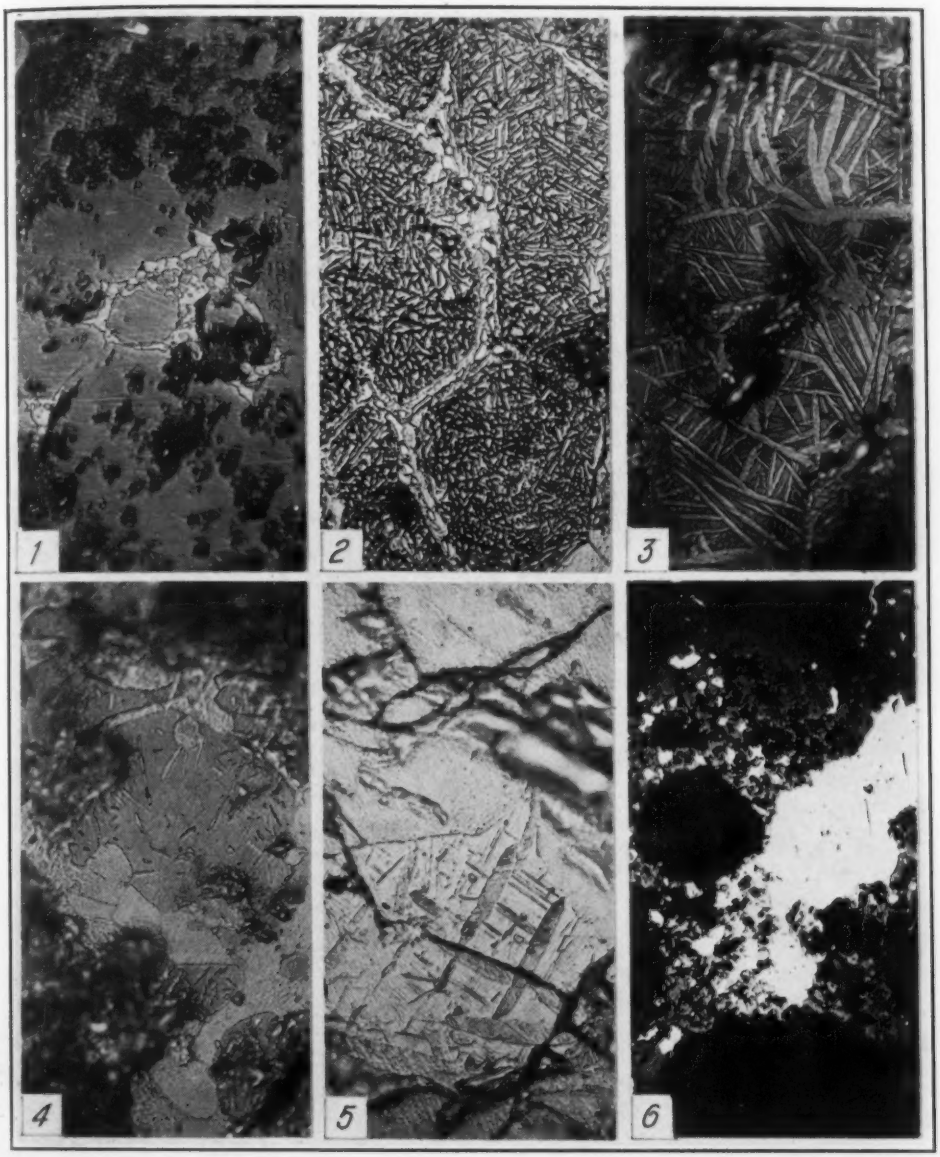


Fig. 1—No. 3 Table I-A, V_2O_2. Shows Network of Precipitated Vanadium. Etched with $HNO_3 + H \cdot C_2H_3O_2$. × 250.

Fig. 2—No. 36 Table I-B. Vanadium Containing Twenty Per Cent Oxygen. Precipitated Vanadium in Matrix of V_2O_2. Etched with $HNO_3 + H \cdot C_2H_3O_2$. × 500.

Fig. 3—No. 4 Table I-A. Preparation Corresponding to Formula V_2O. Needles or Plates of V in V_2O_2. Etched with $HNO_3 + H \cdot C_2H_3O_2$. × 500.

Fig. 4—No. 4 Table I-A. Preparation Corresponding to Formula V_2O Quenched in Water from 1350 Degrees Cent. Etched with $HNO_3 + H \cdot C_2H_3O_2$. × 500.

Fig. 5—Vanadium Containing About 7 Per Cent Oxygen. Etched with $HNO_3 + H \cdot C_2H_3O_2$. × 500.

Fig. 6—No. 6 Table I-B. Reduction of FeO by V_2O_2. Unetched. × 75.

The vanadium patterns (Table IV) are complicated by the presence of lines, some of them quite intense, which cannot be referred to

Table V

X-Ray Data on Materials Listed in Table I-B

Specimen 37, (15% O in V)				Specimen 36, (20% O in V)				Specimen 23, (V_3O_4) Hypothetical			
Observed Pattern	Observed Intensity	Due to	Theoretical Pattern	Observed Pattern	Observed Intensity	Due to	Theoretical Pattern	Observed Pattern	Observed Intensity	Due to	Theoretical Pattern
2.340	m	V_2O_2	2.330	2.340	s	V_2O_2	2.330	3.650	m	V_2O_3	3.642
2.270	s	(From 91.85 V)		2.270	w	(From 91.85 V)		2.700	m	V_2O_3	2.698
2.075	s	V	2.071	2.075	s	V	2.071	2.470	m	V_2O_3	2.466
2.020	m	V_2O_2	2.019	2.020	vs	V_2O_2	2.019	2.390	m	V_2O_2	2.392
1.942	vw	....	.....	1.895	vw	....	.....	2.180	w	V_2O_3	2.179
1.894	vw	....	.....	1.798	vw	....	.....	2.075	vs	V_2O_2	2.071
1.800	vw	....	.....	1.696	vw	....	.....	1.822	w	V_2O_3	1.821
1.700	vw	....	.....	1.655	vw	....	.....	1.695	s	V_2O_3	1.689
1.650	vw	....	.....	1.598	vw	....	.....	1.614	vw	....	.....
1.598	vw	....	.....	1.508	vw	....	.....	1.462	vs	$\{V_2O_3\}$ $\{V_2O_2\}$	1.465
1.510	vw	....	.....	1.463	s	V	1.465				
1.463	s	V	1.465	1.428	vs	V_2O_2	1.427	1.422	m	V_2O_3	1.423
1.420	s	V_2O_2	1.427	1.355	vw	....	.....	1.326	w	V_2O_3	1.324
1.353	w	....	.....	1.260	vw	....	.....	1.250	m	V_2O_2	1.249
1.321	vw	....	.....	1.218	s	V_2O_2	1.216	1.232	w	V_2O_3	1.233
1.262	vw	....	.....	1.180	w	....	.....	1.192	m	$\{V_2O_3\}$ $\{V_2O_2\}$	1.195
1.221	s	V_2O_2	1.216	1.161	m	V_2O_2	1.165				
1.163	vw	V_2O_2	1.165	1.032	vw	V	1.035	1.175	w	V_2O_3	1.171–1.167
1.138	w	....	.....	1.010	vw	V_2O_2	1.009				
1.035	w	V	1.035					1.121	vw	V_2O_3	1.121
1.008	vw	V_2O_2	1.009					1.089	w	V_2O_3	1.088
								1.055	w	V_2O_3	1.055
								1.035	m	V_2O_2	1.035
								1.023	w	V_2O_3	1.020

a_o = 2.928 gives values listed as theoretical pattern for Vanadium.
a_o = 4.036 gives values listed as theoretical pattern for V_2O_2.

Composition of original briquets:
68.6% V (91.85)
31.4% V_2O_3

a_o = 2.928 gives values listed as theoretical pattern for Vanadium.
a_o = 4.036 gives values listed as theoretical pattern for V_2O_2.

Composition of original briquets:
51.58% V_2O_3
48.42% V (91.85)

a_o = 4.142 gives values listed as theoretical for V_2O_2.
Pattern given as theoretical for V_2O_3 is that of W. H. Zachariasen (8).

Composition of original briquets:
89.8% V_2O_3
10.2% V (91.85)

any known substance encountered in this investigation. This condition is particularly pronounced in the case of the material, believed to contain about 7 per cent of oxygen, generally used in the preparation of our briquetted mixtures. This material is brittle and under the microscope shows predominantly a single phase, with an occasional area of the kind shown in the central portion of Fig. 5, which is believed to represent precipitation of oxide from locally saturated areas. The extraneous lines are probably due to segregated impurities which have increased the brittleness in these regions causing them to break away completely during grinding and polishing. The purer sample of vanadium was obtained in the form of shot-like pellets which could be flattened under the hammer and rolled cold into thin strips. It may be noted that even this malleable material gave a few extraneous

Table VI
X-Ray Data on Materials Listed in Table I-B

Specimen 4, (Elect. Fe)				Specimen 3, (FeO)				Specimen 31, ($FeO.V_2O_3$ made in Pt Crucible)			
Observed Pattern	Observed Intensity	Due to	Theoretical Pattern	Observed Pattern	Observed Intensity	Due to	Theoretical Pattern	Observed Pattern	Observed Intensity	Due to	Theoretical Pattern
2.020	vs	Fe	2.012	2.480	m	FeO	2.479	3.680	vw	V_2O_3	3.642
1.424	m	Fe	1.423	2.145	s	FeO	2.146	3.000	m	FeV_2O_4	2.994
1.161	s	Fe	1.161	1.930	vw	....	.....	2.705	w	V_2O_3	2.698
1.006	m	Fe	1.006	1.513	s	FeO	1.517	2.560	vs	FeV_2O_4	2.552
0.900	m	Fe	0.901	1.428	vw	....	.....	2.470	w	V_2O_3	2.466
0.822	w	Fe	0.822	1.293	m	FeO	1.294	2.190	w	V_2O_3	2.179
0.761	w	Fe	0.761	1.240	m	FeO	1.239	2.110	m	FeV_2O_4	2.118
0.710	w	Fe	0.712	1.073	m	FeO	1.072	1.820	w	V_2O_3	1.821
				1.015	vw	....	.....	1.725	m	FeV_2O_4	1.728
a_o = 2.846 gives values listed as theoretical pattern for Fe.				0.985	w	FeO	0.985	1.688	m	V_2O_3	1.689
				0.960	s	FeO	0.960	1.615	s	....	.....
				0.878	m	FeO	0.876	1.494	vs	FeV_2O_4	1.496
								1.462	w	V_2O_3	1.465
				a_o = 4.291 gives values listed as theoretical pattern for FeO.				1.426	w	V_2O_3	1.423
								1.323	w	V_2O_3	1.324
								1.279	m	....	.....
								1.231	w	V_2O_3	1.233
								1.212	vw	V_2O_3	1.214
								1.170	vw	V_2O_3	1.171
								1.128	m	FeV_2O_4	1.131
								1.096	s	FeV_2O_4	1.102
								1.052	m	FeV_2O_4	1.058
								0.998	w	FeV_2O_4	0.998
								0.970	s	FeV_2O_4	0.972
								a_o = 8.468 gives values listed as theoretical pattern for FeV_2O_4.			
								Pattern given as theoretical for V_2O_3 is that of W. H. Zachariasen (8).			
Composition of original briquets: Approx. 100% Fe				Composition of original briquets: 96% FeO solid solution (23.17% O) 4% Fe				Composition of original briquets: 32.3% FeO 67.7% V_2O_3			

lines and a parameter value, $a_o = 3.02$, appreciably less than the one, $a_o = 3.04$, reported by Hull[11] from a sample of unspecified purity, but more than that, $a_o = 3.011$, reported more recently by G. Hägg* from a sample of the same purity.

A mixture (No. 23) containing equal molecular proportions of VO and V_2O_3 exhibited the line series of both of these compounds (Table V), the former corresponding to an a_o value of 4.14 and the latter approximately to the theoretical pattern of the pure compound (Table II). These oxides do not therefore combine directly to form a compound of the spinel type as is the case with the corresponding oxides of iron and similarly with ferrous oxide in combination with vanadium trioxide (See Table VI).

[11] A. W. Hull, "Crystal Structure of V, Ge and Graphite," *Physical Review*, Vol. 20, 1922, p. 113.

*G. Hägg, "Röntgenuntersuchungen über die Hydride von Titan, Zirkonium, Vanadin und Tantal," *Zeit. Physikalische Chem.*, B Vol. 11, 1931, p. 433.

Iron Oxide and Vanadium Oxides

(a) FeO-V_2O_2. Having verified the earlier constitutional evidence* that iron at temperatures above 560 degrees Cent. (1040 degrees Fahr.) is found in equilibrium with a ferrous oxide, possessing however a homogeneity range of several per cent of oxygen in the direction of the magnetic oxide, and having established the fact that

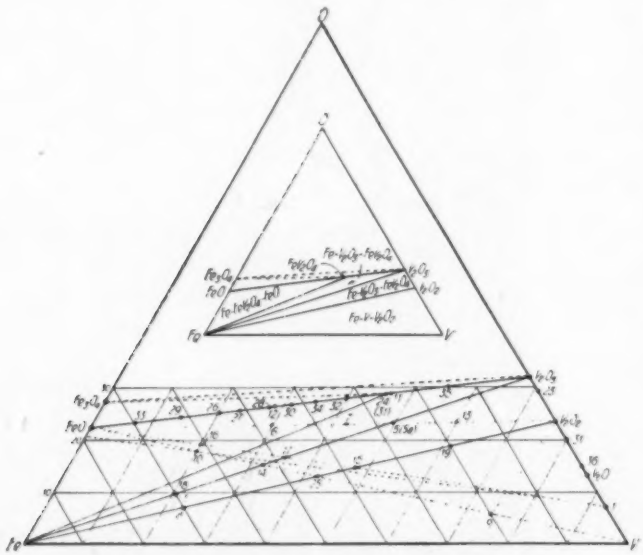


Fig. 7—Partial Survey of Ternary System: Iron-Vanadium-Oxygen.

vanadium occurs in association with its dioxide, experiments were devised to determine whether these two oxides are stable in the presence of one another, viz., can appear as components in a binary system.

A simple scheme of surveying the ternary system Fe-V-O in the vicinity of the pure metal components is outlined in Fig. 7 in which the mixture numbers of Table IB appear.

Mixtures 5, 6, 7 and 13 applying to this part of the investigation were prepared as follows:

An iron oxide containing about 23 per cent of oxygen, made by burning electrolytic iron in oxygen, was brought to the exact composition FeO by melting in a platinum crucible in vacuo together with a calculated amount of electrolytic iron, quenched in water immediately after solidification, pulverized in an agate mortar and dressed with a magnet to remove the small quantity of magnetic oxide formed

*Loc. Cit. (1).

at the surface of the regulus when air was admitted prior to quenching.

Vanadium dioxide was prepared by mixing calculated weights of vanadium and ignited vanadium trioxide, pressing into a briquet and firing to approximately the melting point in vacuo.

The mixtures designated above were then made by mixing these relatively pure oxides in the proportions shown in Table I and firing as described above.

The rate of cooling after this treatment, which varied from about 250 degrees per minute between 1500 and 1000 degrees Cent. to 80 degrees per minute between 1000 and 850 degrees Cent., was found to be sufficiently rapid to prevent the decomposition of FeO into a mixture of Fe and Fe_3O_4, normally encountered in the pure ferrous preparation at 650 degrees Cent. (1200 degrees Fahr.).

The results of the X-ray examination of these mixtures are contained in Tables VII, VIII and IX and the following definite conclusions may be recorded.

The most significant statement which can be made concerning these mixtures is that all of them contain metallic iron, as revealed by the presence of strong iron lines in the X-ray pattern and the occurrence of bright metallic particles (Fig. 6) in the microstructure.

It is thus evident that ferrous oxide is reduced to metal, not alone by elementary vanadium, but also by the lowest oxide of vanadium. Depending upon the proportions of FeO and V_2O_2, the reduced iron was found in contact with V_2O_2 and V_2O_3 (mixture No. 13), V_2O_3 (mixture No. 5), V_2O_3 and a new compound of the spinel type which will be described directly (mixture No. 5a), and this compound together with FeO (mixture No. 6). The presence of FeO in the last mixture was detected in the microstructure but not in the X-ray pattern. We have invariably found it difficult to obtain the pattern of FeO unless this oxide is present in very considerable amount. The mixtures designated 5 and 5a were calculated to produce the same concentration, the former from Fe + V_2O_3 and the latter from FeO + V_2O_2. The latter, however, developed a weak pattern of FeV_2O_4 in addition to the predominant Fe and V_2O_3 patterns, thus indicating an appreciable shift into the ternary region, Fe-FeV_2O_4-V_2O_3.

The full development of the above evidence calls for partition of the Fe-V-O system according to the scheme adopted in Fig. 7. Subsequent work produced further evidence in favor of this interpretation.

Table VII

X-Ray Data on Materials Listed in Table I-B

Specimen 5				Specimen 5a				Specimen 13			
Observed Pattern	Observed Intensity	Due to	Theoretical Pattern	Observed Pattern	Observed Intensity	Due to	Theoretical Pattern	Observed Pattern	Observed Intensity	Due to	Theoretical Pattern
3.640	m	V_2O_3	3.642	3.650	m	V_2O_3	3.642	3.650	m	V_2O_3	3.642
2.705	w	V_2O_3	2.698	2.990	vw	FeV_2O_4	2.994	2.700	m	V_2O_3	2.698
2.470	w	V_2O_3	2.466	2.705	m	V_2O_3	2.698	2.470	m	V_2O_3	2.466
2.180	w	V_2O_3	2.179	2.550	m	FeV_2O_4	2.552	2.340	vw	V_2O_2	2.351
2.045	m	Fe	2.018	2.470	m	V_2O_3	2.466	2.180	w	V_2O_2	2.179
1.823	w	V_2O_3	1.821	2.180	w	V_2O_3	2.179	2.040	s	V_2O_2	2.038
1.689	vs	V_2O_3	1.689	2.110	w	FeV_2O_4	2.118	2.020	s	Fe	2.018
1.606	w	....	.....	2.020	s	Fe	2.018	1.820	w	V_2O_3	1.821
1.575	w	....	.....	1.822	m	V_2O_3	1.821	1.689	m	V_2O_3	1.689
1.465	m	V_2O_3	1.465	1.690	m	V_2O_3	1.689	1.610	vw	....	.....
1.425	s	{Fe} {V_2O_3}	{1.427} {1.423}	1.614	vw	....	.....	1.460	m	V_2O_3	1.465
1.322	vw	V_2O_3	1.324	1.575	w	....	.....	1.438	w	V_2O_2	1.440
1.234	w	V_2O_3	1.233	1.488	vw	FeV_2O_4	1.496	1.423	m	{Fe} {V_2O_3}	{1.427} {1.423}
1.215	vw	V_2O_3	1.214	1.465	w	V_2O_3	1.465	1.320	w	V_2O_3	1.324
1.192	vw	V_2O_3	1.191	1.426	m	{Fe} {V_2O_3}	{1.427} {1.423}	1.230	w	{V_2O_3} {V_2O_2}	{1.233} {1.228}
1.170	w	V_2O_3	1.171	1.322	w	V_2O_3	1.324	1.212	vw	V_2O_3	1.214
1.165	w	{V_2O_3} {Fe}	{1.167} {1.165}	1.282	vw	....	.....	1.191	vw	V_2O_3	1.191
1.122	w	V_2O_3	1.121	1.233	vw	V_2O_3	1.233	1.172	w	{V_2O_2} {V_2O_3}	{1.176} {1.171}
				1.213	w	V_2O_3	1.214				
1.087	m	V_2O_3	1.088	1.191	vw	V_2O_3	1.191	1.166	s	{V_2O_3} {Fe}	{1.167} {1.165}
1.055	m	V_2O_3	1.055	1.171	vw	V_2O_3	1.171	1.120	w	V_2O_3	1.121
1.020	vw	V_2O_3	1.020	1.166	s	{V_2O_3} {Fe}	{1.167} {1.165}	1.088	m	V_2O_3	1.088
1.008	vw	Fe	1.009					1.052	m	V_2O_3	1.055
				1.154	vw	....	.....				
1.001	vw	V_2O_3	1.001	1.122	w	{ V_2O_3 } {FeV_2O_4}	{1.121} {1.131}	1.028	w	....	.....
								1.018	w	{V_2O_3} {V_2O_2}	{1.020} {1.019}
a_o = 2.855 gives values listed as theoretical pattern for Fe				1.091	w	{FeV_2O_4} { V_2O_3 }	{1.102} {1.088}	1.010	m	Fe	1.009
Pattern given as theoretical for V_2O_3 is that of W. H. Zachariasen (8)				1.055	w	{ V_2O_3 } {FeV_2O_4}	{1.055} {1.058}	1.000	vw	V_2O_3	1.001
				1.020	vw	V_2O_3	1.020				
				1.010	vw	Fe	1.009				
				a_o = 8.468 gives values listed as theoretical pattern for FeV_2O_4				a_o = 4.076 gives values listed as theoretical for V_2O_2			
				a_o = 2.855 gives values listed as theoretical pattern for Fe				a_o = 2.855 gives values listed as theoretical for Fe			
				Pattern given as theoretical for V_2O_3 is that of W. H. Zachariasen (8)				Pattern given for V_2O_3 is that of W. H. Zachariasen (8)			
Composition of original briquets: 73.5% V_2O_3 26.5% Fe				Composition of original briquets: 65.7% V_2O_2 34.3% FeO				Composition of original briquets: 78.8% V_2O_2 21.2% FeO			

(b) FeO-V_2O_3. Preliminary evidence from briquetted mixtures, Nos. 11 and 12, made from FeO and V_2O_3, that these oxides unite to form a compound of the spinel type led to the preparation of a group of nine mixtures, Nos. 24, 32, 34, 30, 28, 27, 26, 29 and 35, by melting the mixed oxides in a platinum crucible in the molecular

Table VIII

X-Ray Data on Materials Listed in Table I-B

Specimen 6				Specimen 10				Specimen 16			
Observed Pattern	Observed Intensity	Due to	Theoretical Pattern	Observed Pattern	Observed Intensity	Due to	Theoretical Pattern	Observed Pattern	Observed Intensity	Due to	Theoretical Pattern
3.000	m	FeV_2O_4	2.994	2.995	w	FeV_2O_4	2.994	2.990	w	FeV_2O_4	2.994
2.550	vs	FeV_2O_4	2.552	2.550	s	FeV_2O_4	2.552	2.550	s	FeV_2O_4	2.552
2.115	w	FeV_2O_4	2.118	2.115	vw	FeV_2O_4	2.118	2.110	w	FeV_2O_4	2.118
2.020	vs	Fe	2.018	2.020	vs	Fe	2.018	2.020	vs	Fe	2.018
1.725	w	FeV_2O_4	1.728	1.726	vw	FeV_2O_4	1.728	1.727	w	FeV_2O_4	1.728
1.620	s	.....	.....	1.620	m	.....	.....	1.615	m	.....	.....
1.492	vs	FeV_2O_4	1.496	1.490	s	FeV_2O_4	1.496	1.490	s	FeV_2O_4	1.496
1.431	m	Fe	1.427	1.427	m	Fe	1.427	1.424	m	Fe	1.427
1.330	w	.....	.....	1.330	w	.....	.....	1.330	vw	.....	.....
1.290	w	.....	.....	1.275	w	.....	.....	1.272	w	.....	.....
1.272	vw	.....	.....	1.165	vs	Fe	1.165	1.210	vw	.....	.....
1.168	m	Fe	1.165	1.126	w	FeV_2O_4	1.131	1.162	s	Fe	1.165
1.125	w	FeV_2O_4	1.131	1.095	m	FeV_2O_4	1.102	1.124	w	FeV_2O_4	1.131
1.095	m	FeV_2O_4	1.102	1.055	vw	FeV_2O_4	1.058	1.090	m	FeV_2O_4	1.102
1.052	m	FeV_2O_4	1.058	1.009	m	Fe	1.009	1.055	vw	FeV_2O_4	1.058
1.010	w	Fe	1.009					1.010	w	Fe	1.009
$a_o = 8.468$ gives values listed as theoretical pattern for FeV_2O_4				$a_o = 8.468$ gives values listed as theoretical pattern for FeV_2O_4				$a_o = 8.468$ gives values listed as theoretical pattern for FeV_2O_4			
$a_o = 2.855$ gives values listed as theoretical pattern for Fe				$a_o = 2.855$ gives values listed as theoretical pattern for Fe				$a_o = 2.855$ gives values listed as theoretical pattern for Fe			
Composition of original briquets: 39% V_2O_3 61% FeO				Composition of original briquets: 23.75% V (91.85) 70.75% FeO 5.50% Fe				Composition of original briquets: 21.5% V (91.85) 78.5% FeO			

proportions 1:1, 1.5:1, 2:1, 2.5:1, 3:1, 4:1, 5:1, 8:1 and 18:1, respectively, and cooling at a rate (175 degrees per minute between 1350 and 1000 degrees Cent.; 90 degrees per minute between 1000 and 800 degrees Cent.) sufficiently rapid to prevent the subsequent decomposition of FeO. All except the first of these, corresponding closely to the formula $FeOV_2O_3$ or FeV_2O_4, could be completely melted and solidified in platinum giving rise to specimens quite suitable for metallographic examination. The melting point of this spinel probably exceeds that of platinum and the sintered mixture contains a certain amount of the still more refractory V_2O_3, as shown by the X-ray pattern of No. 31 analyzed in Table VI. Similar results (Table X) were obtained from another preparation, No. 24, sintered in the usual manner. The principal line series of this pattern shows cubic symmetry, resembles that of magnetite[12] and evidently represents an iron-vanadium spinel, FeV_2O_4, whose a_o value is close to

[12] R. W. G. Wyckoff and E. D. Crittenden, "An X-ray Examination of Some Ammonia Catalysts," *Journal*, American Chemical Society, Vol. 47, 1925, p. 2866.

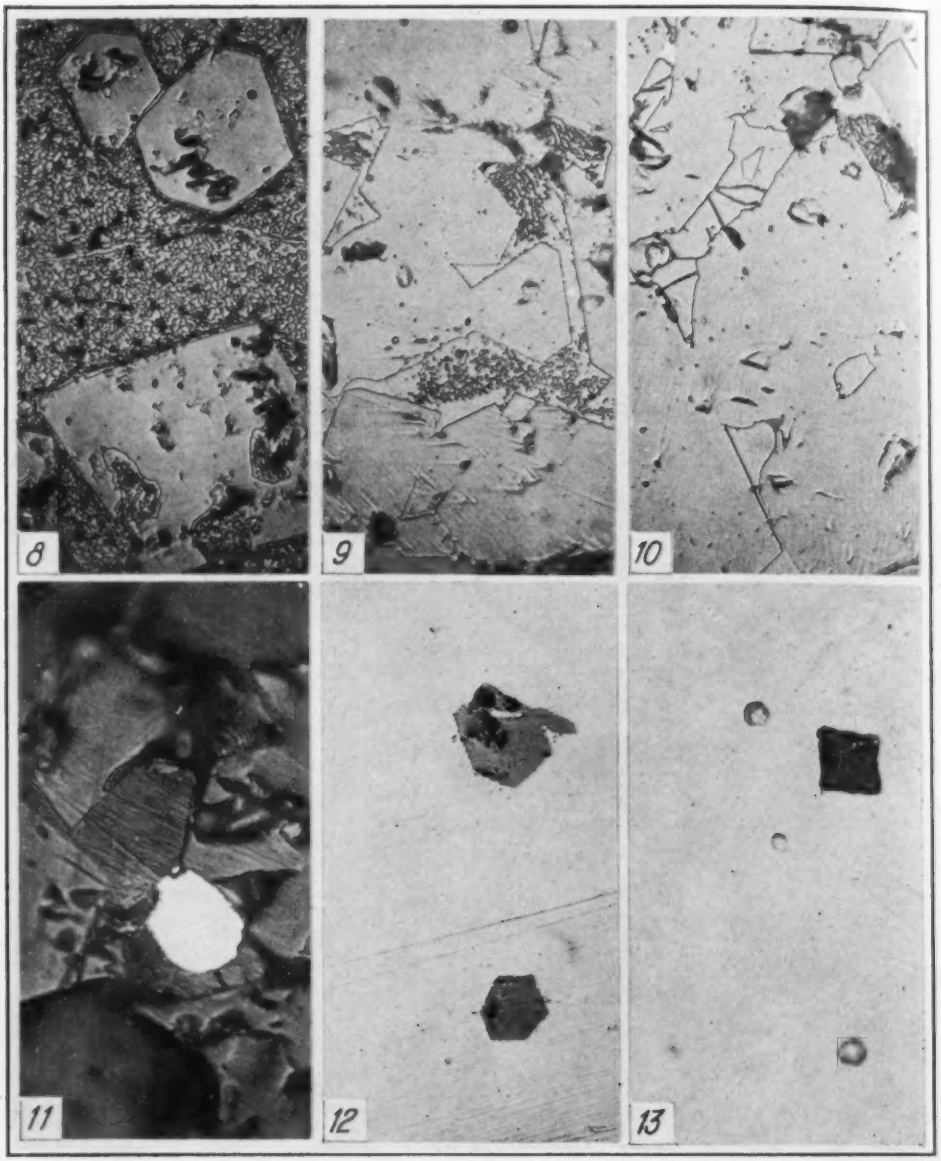


Fig. 8—No. 33 Table I-B. 18 mols. FeO to 1 mol. V_2O_3. Primary FeV_2O_4 in Eutectic Matrix. Etched with HNO_3 + $H.C_2H_3O_2$. × 500.

Fig. 9—No. 28 Table I-B. 3 mols. FeO to 1 mol. V_2O_3 Primary FeV_2O_4 and Eutectic. Etched with HNO_3 + $H.C_2H_3O_2$. × 500.

Fig. 10—No. 12 Table I-B. Primary FeV_2O_4 Containing Patches of FeO Divorced from Eutectic. Etched with HNO_3 + $H.C_2H_3O_2$. × 500.

Fig. 11—No. 16 Table I-B. Shows FeV_2O_4 in Excess, Iron (light) and FeO (dark). Etched with HNO_3 + $H.C_2H_3O_2$. × 750.

Fig. 12—Inclusions of FeV_2O_4 in Electrolytic Iron Melted with V_2O_3 in Magnesia Crucible in Air. Unetched, × 500.

Fig. 13—Electrolytic Iron Melted in Vacuo in V_2O_3 Crucible. Rounded Inclusions (FeO) Etched Out with Saturated Solution Picric Acid in Alcohol. Inclusion of FeV_2O_4 Remains. × 1000.

Table IX

X-Ray Data on Materials Listed in Table I-B

Specimen 26 ($5FeO.V_2O_3$)				Specimen 29 ($8\ FeO.V_2O_3$)				Specimen 7			
Observed Pattern	Observed Intensity	Due to	Theoretical Pattern	Observed Pattern	Observed Intensity	Due to	Theoretical Pattern	Observed Pattern	Observed Intensity	Due to	Theoretical Pattern
2.995	w	FeV_2O_4	2.994	2.995	w	FeV_2O_4	2.994	3.650	w	V_2O_3	3.642
2.550	vs	FeV_2O_4	2.552	2.550	vs	FeV_2O_4	2.552	2.990	m	FeV_2O_4	2.994
2.475	vw	FeO	2.479	2.480	m	FeO	2.479	2.700	m	V_2O_3	2.698
2.150	w	FeO	2.146	2.150	s	FeO	2.146	2.550	s	FeV_2O_4	2.552
2.110	w	FeV_2O_4	2.118	2.115	m	FeV_2O_4	2.118	2.465	w	V_2O_3	2.466
1.722	w	FeV_2O_4	1.728	1.722	w	FeV_2O_4	1.729	2.180	w	V_2O_3	2.179
1.615	s	.....	.....	1.620	s	.....	.....	2.110	m	FeV_2O_4	2.118
1.520	w	FeO	1.517	1.520	m	FeO	1.517	2.020	m	Fe	2.018
1.490	s	FeV_2O_4	1.496	1.490	s	FeV_2O_4	1.496	1.820	w	V_2O_3	1.821
1.325	vw	.....	.....	1.330	w	.....	.....	1.725	w	FeV_2O_4	1.728
1.290	w	FeO	1.294	1.290	m	FeO	1.294	1.688	w	V_2O_3	1.689
1.240	vw	FeO	1.239	1.239	w	FeO	1.239	1.615	s	.....	.....
1.209	vw	.....	.....	1.220	vw	.....	.....	1.490	s	FeV_2O_4	1.496
1.175	vw	.....	.....	1.123	w	FeV_2O_4	1.131	1.420	m	Fe / V_2O_3	1.427 / 1.423
1.121	w	FeV_2O_4	1.131	1.096	m	FeV_2O_4	1.102	1.328	w	V_2O_3	1.324
1.090	m	FeV_2O_4	1.102	1.072	w	FeO	1.072	1.281	m	.....	.....
1.072	vw	FeO	1.072	1.055	w	FeV_2O_4	1.058	1.262	vw	.....	.....
1.049	w	FeV_2O_4	1.058	1.009	vw	.....	.....	1.217	w	V_2O_3	1.214
								1.164	m	Fe / V_2O_3	1.165 / 1.167
								1.120	m	FeV_2O_4 / V_2O_3	1.131 / 1.121
								1.092	s	FeV_2O_4 / V_2O_3	1.102 / 1.088
								1.054	w	V_2O_3 / FeO	1.058 / 1.055
								1.014	vw	Fe	1.009

$a_o = 8.468$ gives values listed as the theoretical pattern for FeV_2O_4
$a_o = 4.291$ gives values listed as theoretical pattern for FeO

Composition of original briquets:
70.5% FeO
29.5% V_2O_3

$a_o = 8.468$ gives values listed as theoretical pattern for FeV_2O_4
$a_o = 4.291$ gives values listed as theoretical pattern for FeO

Composition of original briquets:
79.3% FeO
20.7% V_2O_3

$a_o = 8.468$ gives values listed as theoretical pattern for FeV_2O_4
$a_o = 2.855$ gives values listed as theoretical pattern for Fe
Pattern given as theoretical for V_2O_3 is that of W. H. Zachariasen (8)

Composition of original briquets:
55.5% V_2O_2
44.5% FeO

8.468 Å. The metallographic examination of these mixtures disclosed the presence of an eutectic composed of approximately 18 mols. of FeO to 1 mol. of FeV_2O_4 (No. 33), as shown in Fig. 8 together with some primary FeV_2O_4. The structure of No. 26 reveals primary FeV_2O_4 and eutectic in approximately equal amounts. As the proportion of iron-vanadium spinel increases, the eutectic tends strongly to divorce its constituents and the structural effect is that of an iron-vanadium spinel matrix with enclosed particles of the ferrous oxide constituent. Figs. 9 and 10 show final stages of this process. Beyond the molecular ratio $2FeO.V_2O_3$, this constituent can no

Table X

X-Ray Data on Materials Listed in Table I-B

Specimen 35, ($\frac{1}{2}FeO.V_2O_3$)

Observed Pattern	Observed Intensity	Due to	Theoretical Pattern
3.650	m	V_2O_3	3.642
2.990	m	FeV_2O_4	2.994
2.700	m	V_2O_3	2.698
2.550	s	FeV_2O_4	2.552
2.465	m	V_2O_3	2.466
2.310	vw	.....	.....
2.180	w	V_2O_3	2.179
2.110	m	FeV_2O_4	2.118
1.980	vw	.....	.....
1.880	vw	.....	.....
1.822	m	V_2O_3	1.821
1.722	m	FeV_2O_4	1.728
1.690	w	V_2O_3	1.689
1.614	m	.....	.....
1.489	s	FeV_2O_4	1.496
1.465	vw	V_2O_3	1.465
1.422	m	V_2O_3	1.423
1.324	w	V_2O_3	1.324
1.280	m	.....	.....
1.234	w	V_2O_3	1.233
1.214	w	V_2O_3	1.214
1.192	vw	V_2O_3	1.191
1.169	w	V_2O_3	{1.171} {1.167}
1.122	m	{FeV_2O_4} {V_2O_3}	{1.131} {1.121}
1.092	m	FeV_2O_4	1.102
1.088	m	V_2O_3	1.088
1.053	m	{FeV_2O_4} {V_2O_3}	{1.058} {1.055}
1.021	vw	V_2O_3	1.020
1.001	vw	V_2O_3	1.001

$a_0 = 8.468$ gives values listed as theoretical pattern for FeV_2O_4
Pattern given as theoretical for V_2O_3 is that of W. H. Zachariasen (8)

Composition of original briquets:
19.3% FeO
80.7% V_2O_3

Specimen 24, ($FeO.V_2O_3$)

Observed Pattern	Observed Intensity	Due to	Theoretical Pattern
3.630	w	V_2O_3	3.642
2.995	m	FeV_2O_4	2.994
2.705	w	V_2O_3	2.698
2.550	s	FeV_2O_4	2.552
2.465	w	V_2O_3	2.466
2.110	m	FeV_2O_4	2.118
2.030	vw	.....	.....
1.822	w	V_2O_3	1.821
1.725	w	FeV_2O_4	1.728
1.690	m	V_2O_3	1.689
1.615	s	.....	.....
1.493	vs	FeV_2O_4	1.496
1.465	vw	V_2O_3	1.465
1.425	w	V_2O_3	1.423
1.325	vw	V_2O_3	1.324
1.265	w	.....	.....
1.212	vw	V_2O_3	1.214
1.169	vw	V_2O_3	{1.171} {1.167}
1.127	m	FeV_2O_4	1.131
1.095	s	FeV_2O_4	1.102
1.056	m	FeV_2O_4	1.058

$a_0 = 8.468$ gives values listed as theoretical pattern for FeV_2O_4
Pattern given as theoretical for V_2O_3 is that of W. H. Zachariasen (8)

Composition of original briquets:
32.3% FeO
67.7% V_2O_3

Specimen 28, ($3FeO.V_2O_3$)

Observed Pattern	Observed Intensity	Due to	Theoretical Pattern
2.995	w	FeV_2O_4	2.994
2.860	w	.....	.....
2.550	vs	FeV_2O_4	2.552
2.110	m	FeV_2O_4	2.118
1.826	vw	.....	.....
1.728	w	FeV_2O_4	1.728
1.672	vw	.....	.....
1.618	s	.....	.....
1.492	s	FeV_2O_4	1.496
1.330	vw	.....	.....
1.280	m	.....	.....
1.126	w	FeV_2O_4	1.131
1.093	s	FeV_2O_4	1.102
1.053	w	FeV_2O_4	1.058

$a_0 = 8.468$ gives values listed as theoretical pattern for FeV_2O_4

Composition of original briquets:
59% FeO
41% V_2O_3

longer be recognized and there is therefore the probability of a homogeneity range corresponding to solid solution of FeO in FeV_2O_4.

All of these mixtures were quite brittle and often revealed well crystallized octahedrons of the iron-vanadium spinel on the roughly fractured surfaces. The idiomorphic character of this constituent is also evident from the well shaped polyhedral forms visible in the primary constituent of Fig. 8.

Mixtures 26, 28, 29, and 35 were submitted to X-ray examination. The line series of FeO and FeV_2O_4 were recognized in Nos.

26 and 29 (see Table IX), those of FeV_2O_4 and V_2O_3 in No. 35 (Table X) and only that of FeV_2O_4 in No. 28 (Table X), notwithstanding the occurrence of ferrous oxide in liberal amount in the microstructure of this sample (Fig. 9).

The Binary Systems: Fe-V_2O_2, Fe-V_2O_3, and Fe-FeV_2O_4

(a) Fe-V_2O_2. The diagram, Fig. 7, shows four mixtures, viz., 8, 15, 19, and 25 located on the line joining Fe and V_2O_2. The binary character of No. 19 was clearly indicated in the X-ray pattern (Table XIII). On the other hand, Nos. 8 and 25 deviated sufficiently from the calculated compositions to show lines belonging to the V_2O_3 series (Table XI). The parameter value of iron calculated from the line series observed in three of the four mixtures, $a_o = 2.855$ Å, is identical with the value reported in the International Critical Tables.* The other mixture, No. 15 (Table XIII) which was prepared from our impure vanadium and ferrous oxide showed a few vanadium lines indicating incomplete reaction and gave an abnormally low parameter value for iron, viz., $a_o = 2.786$ Å; the parameter value obtained from a sample of the electrolytic iron used in this investigation after thorough annealing in hydrogen was 2.846 Å. Iron melted in a crucible made of sintered V_2O_2 gave the normal value, $a_o = 2.855$. The weight of evidence is therefore in favor of the conclusion that the iron cell is unaffected by close association with V_2O_2.

(b) Fe-V_2O_3. The system, Fe-V_2O_3, is also represented in Fig. 6 by four mixtures, viz., 5, 14, 17, and 18. The X-ray data, given in Tables VII and XII, show that the mixtures are composed of Fe and V_2O_3, possessing the normal parameter values. Mixture No. 5 was reproduced as 5a, Table IB, by sintering calculated quantities of V_2O_2 and FeO in the usual manner. As expected, this mixture gave the patterns of Fe and V_2O_3, but also a weak pattern of iron-vanadium spinel. It is concluded that this particular mixture deviated appreciably from the intended binary composition and entered the neighboring ternary region, Fe-FeV_2O_4-V_2O_3.

(c) Fe-FeV_2O_4. The system Fe-FeV_2O_4, was not directly represented in our original plan of surveying the entire ternary region bounded by Fe, FeO, V_2O_3, and V, owing to the hitherto unsuspected existence of the iron-vanadium spinel, FeV_2O_4. It was not considered

*Vol. 1, p. 340.

necessary to prepare mixtures along this line which in any event would have to be introduced as a boundary between the observed ternary groups, Fe-FeV_2O_4-FeO, and Fe-V_2O_3-FeV_2O_4.

Ternary Systems: Fe-V-V_2O_2, Fe-V_2O_2-V_2O_3, Fe-V_2O_3-FeV_2O_4 and Fe-FeV_2O_4-FeO

(a) Fe-V-V_2O_2. Only one mixture, No. 9, was allocated to the ternary region, Fe-V-V_2O_2. This gave an X-ray pattern (Table XI) fully in harmony with the conditions represented in Fig. 7, viz., a V_2O_2 line series in combination with a series from the solid solution (containing approximately 74 per cent of vanadium) lying at the end of a line passing through the compositions corresponding to pure V_2O_2 and mixture No. 9. Appropriate literature citations are contained in Table XI.

(b) Fe-V_2O_2-V_2O_3. The ternary system, Fe-V_2O_2-V_2O_3, is represented by three mixtures, only one of them, No. 13 (Table VII), originally allocated to this region. The others, Nos. 8 and 25 (Table XI), have already been described as mixtures deviating somewhat from the originally intended binary compositions.

(c) Fe-V_2O_3-FeV_2O_4. The mixture, No. 7, shown in Fig. 7, which lies inside of the ternary region Fe-V_2O_3-FeV_2O_4, properly indicated the presence of all three of these components in its X-ray pattern (Table IX). In addition to this, mixture No. 5a, as already pointed out, deviated sufficiently from its intended composition to show these three components in its X-ray pattern.

(d) Fe-FeV_2O_4-FeO. The last constituent ternary region, Fe-FeV_2O_4-FeO, is directly represented by three mixtures, 6, 10, and 16, all of them apparently composed entirely of iron and iron-vanadium spinel on the basis of the X-ray evidence secured (Table VIII). Microscopic examination of these specimens, however, proved that ferrous oxide was invariably present, either in eutectic form associated with the iron-vanadium spinel, or divorced from the latter compound as previously shown in Fig. 10. Patches of ferrous oxide in mixture No. 29 are shown in Fig. 11 adjoining the white patch of iron near the center. Reference has already been made to the difficulty of obtaining an X-ray pattern of ferrous oxide in such mixtures.

Finally, it may be pointed out that the binary mixtures along the line FeO-FeV_2O_4, as prepared under present conditions, exhibited a

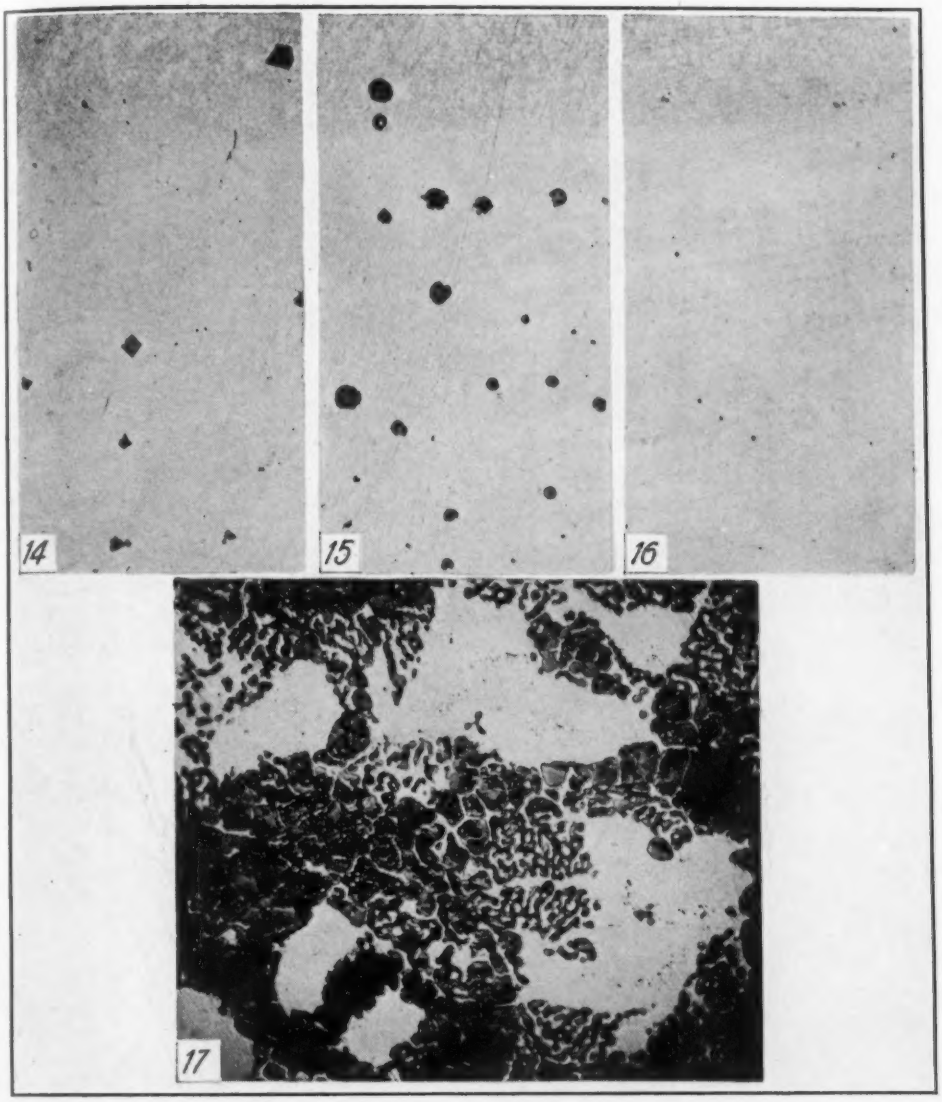


Fig. 14—Electrolytic Iron Annealed in Hydrogen and Melted in Vacuo in Magnesia Crucible Lined with Mixture 75 Per Cent V_2O_3 + 25 Per Cent FeV_2O_4. Inclusions of FeV_2O_4. Unetched. × 250.

Fig. 15—Electrolytic Iron Melted in Magnesia Crucible in Air. Round Inclusions of FeO. Unetched. × 250.

Fig. 16—Electrolytic Iron Annealed in Hydrogen and Melted in Vacuo in Crucible of V_2O_2. Unetched. × 250.

Fig. 17—Structure of Crucible of Composition (20 Per Cent O) Intermediate Between V_2O and V_2O_2 After Use in Melting Electrolytic Iron. Unetched. × 250.

tendency to shift downwards into the ternary field now under discussion. Thus, a few white patches of iron may be seen in Fig. 10, which represents mixture No. 12, intended to contain only ferrous oxide and iron-vanadium spinel.

Table XI

X-Ray Data on Materials Listed in Table I-B

Specimen 8

Observed Pattern	Observed Intensity	Due to	Theoretical Pattern
2.700	vw	V_2O_3	2.698
2.465	vw	V_2O_3	2.466
2.355	vw	V_2O_2	2.351
2.180	vw	V_2O_3	2.179
2.040	w	V_2O_2	2.038
2.020	vs	Fe	2.018
1.694	w	V_2O_3	1.689
1.438	vw	V_2O_2	1.440
1.428	m	Fe	1.427
1.190	vw	V_2O_3	1.191
1.177	vw	V_2O_2	1.176
1.167	s	$\{V_2O_3\}$ $\{Fe\}$	1.165
1.120	vw	V_2O_3	1.121
1.089	vw	V_2O_3	1.089
1.020	vw	$\{V_2O_3\}$ $\{V_2O_2\}$	1.019
1.010	m	Fe	1.009
1.000	vw	V_2O_3	1.001

$a_o = 2.855$ gives values listed as theoretical for Fe

$a_o = 4.076$ gives values listed as theoretical for V_2O_2

Pattern given as theoretical for V_2O_3 is that of W. H. Zachariasen (8)

Composition of original briquets:
70.2% Fe
29.8% V_2O_2

Specimen 25

Observed Pattern	Observed Intensity	Due to	Theoretical Pattern
2.700	w	V_2O_3	2.698
2.465	w	V_2O_3	2.466
2.355	vw	V_2O_2	2.351
2.180	vw	V_2O_3	2.179
2.040	m	V_2O_2	2.038
2.020	vs	Fe	2.018
1.820	w	V_2O_3	1.821
1.690	m	V_2O_3	1.689
1.612	vw	.....	.....
1.465	w	V_2O_3	1.465
1.440	w	V_2O_2	1.440
1.428	m	Fe	1.427
1.390	w	.....	.....
1.320	w	V_2O_3	1.324
1.283	vw	.....	.....
1.233	vw	V_2O_3	1.233
1.228	vw	V_2O_2	1.228
1.191	vw	V_2O_3	1.191
1.176	w	V_2O_2	1.176
1.167	s	$\{V_2O_3\}$ $\{Fe\}$	1.165
1.122	w	V_2O_2	1.121
1.084	w	V_2O_3	1.088
1.052	w	V_2O_3	1.055
1.020	w	$\{V_2O_3\}$ $\{V_2O_2\}$	1.020
1.011	m	Fe	1.009
1.000	vw	V_2O_3	1.001

$a_o = 2.855$ gives values listed as theoretical for Fe.
$a_o = 4.076$ gives values listed as theoretical for V_2O_2
Pattern given as theoretical for V_2O_3 is that of W. H. Zachariasen (8)

Composition of original briquets:
55.5% V_2O_2
44.5% Fe

Specimen 9

Observed Pattern	Observed Intensity	Due to	Theoretical Pattern
2.350	w	V_2O_2	2.351
2.240	vw	.....	.....
2.080	vs	Fe-Vss	2.080
2.040	w	V_2O_2	2.038
1.468	s	Fe-Vss	1.470
1.440	vw	V_2O_2	1.440
1.226	vw	V_2O_2	1.228
1.198	vs	Fe-Vss	1.200
1.174	vw	V_2O_2	1.176
1.048	vw	.....	.....
1.035	m	Fe-Vss	1.040
1.020	w	V_2O_2	1.019

NOTE: The lattice parameter, a_o, for the Fe-V solid solution (74% V-26% Fe) is found to be approximately 2.940. F. Wever and W. Jellinghaus (4) give the value, 2.95, approximately, for this composition. Osawa and Oya (3) give for this percentage composition $a_o = 2.97$ approximately.

$a_o = 4.076$ gives values listed as theoretical for V_2O_2

Composition of original briquets:
80.1% V (91.85)
19.9% Fe

IRON MELTED IN CONTACT WITH OXIDES OF VANADIUM

When pure iron containing the familiar oxide globules is melted in vacuo in contact with V_2O_3, well crystallized idiomorphic (triangular, quadrilateral, hexagonal) inclusions of iron-vanadium spinel can be found in moderate quantity. These were first observed in a sample of electrolytic iron melted together with V_2O_3 powder in a crucible of pure magnesia (Fig. 12). The same constituent (Fig. 13) was identified in a preparation made from electrolytic iron melted in a

Table XII

X-Ray Data on Materials Listed in Table I-B

Specimen 18				Specimen 14				Specimen 17			
Observed Pattern	Observed Intensity	Due to	Theoretical Pattern	Observed Pattern	Observed Intensity	Due to	Theoretical Pattern	Observed Pattern	Observed Intensity	Due to	Theoretical Pattern
3.640	w	V_2O_3	3.642	3.640	s	V_2O_3	3.642	3.640	w	V_2O_3	3.642
2.700	m	V_2O_3	2.698	2.700	vs	V_2O_3	2.698	2.700	s	V_2O_3	2.698
2.465	w	V_2O_3	2.466	2.465	vs	V_2O_3	2.466	2.470	s	V_2O_3	2.466
2.180	w	V_2O_3	2.179	2.300	w	.....	.....	2.270	vw	.....	.....
2.020	vs	Fe	2.018	2.180	s	V_2O_3	2.179	2.180	m	V_2O_3	2.179
1.812	m	V_2O_3	1.821	2.020	m	Fe	2.018	2.020	vs	Fe	2.018
1.683	m	V_2O_3	1.689	1.814	s	V_2O_3	1.821	1.814	m	V_2O_3	1.821
1.612	vw	.....	.....	1.688	vs	V_2O_3	1.689	1.687	s	V_2O_3	1.689
1.463	w	V_2O_3	1.465	1.612	vw	.....	.....	1.610	vw	.....	.....
1.425	s	Fe V_2O_3	1.427 1.423	1.575	vw	.....	.....	1.572	vw	.....	.....
1.326	w	V_2O_3	1.324	1.463	m	V_2O_3	1.465	1.461	w	V_2O_3	1.465
1.259	vw	.....	.....	1.423	s	Fe V_2O_3	1.427 1.423	1.419	s	Fe V_2O_3	1.427 1.423
1.230	vw	V_2O_3	1.233	1.321	m	V_2O_3	1.324	1.320	m	V_2O_3	1.324
1.210	vw	V_2O_3	1.214	1.272	vw	.....	.....	1.275	vw	.....	.....
1.190	vw	V_2O_3	1.191	1.232	w	V_2O_3	1.233	1.231	vw	V_2O_3	1.233
1.170	vw	V_2O_3	1.171	1.211	w	V_2O_3	1.214	1.208	vw	V_2O_3	1.214
1.165	vs	V_2O_3 Fe	1.167 1.165	1.192	vw	V_2O_3	1.191	1.190	vw	V_2O_3	1.191
1.121	vw	V_2O_3	1.121	1.172	vw	V_2O_3	1.171	1.169	vw	V_2O_3	1.171 1.167
1.088	w	V_2O_3	1.088	1.164	m	V_2O_3 Fe	1.167 1.165	1.161	vs	Fe	1.165
1.056	w	V_2O_3	1.055	1.120	m	V_2O_3	1.121	1.118	m	V_2O_3	1.121
1.019	vw	V_2O_3	1.020	1.087	s	V_2O_3	1.088	1.083	w	V_2O_3	1.088
1.009	m	Fe	1.009	1.054	s	V_2O_3	1.055	1.048	w	V_2O_3	1.055
1.000	vw	V_2O_3	1.001	1.022	w	V_2O_3	1.020	1.009	m	Fe	1.009
				1.009	w	Fe	1.009	1.000	vw	V_2O_3	1.001
				1.001	vw	V_2O_3	1.001				
$a_0 = 2.855$ gives values listed as theoretical for Fe				$a_0 = 2.855$ gives values listed as theoretical for Fe				$a_0 = 2.855$ gives values listed as theoretical for Fe			
Pattern given as theoretical for V_2O_3 is that of W. H. Zachariasen (8)				Pattern given as theoretical for V_2O_3 is that of W. H. Zachariasen (8)				Pattern given as theoretical for V_2O_3 is that of W. H. Zachariasen (8)			
Composition of original briquets: 29.9% V_2O_3 70.1% Fe				Composition of original briquets: 48.1% V_2O_3 51.9% Fe				Composition of original briquets: 38.5% V (91.85) 61.5% FeO			

crucible pressed from pure V_2O_3. Although the amount of compound was not large several lines of the iron-vanadium spinel series could be recognized in the X-ray pattern of this iron.

The electrolytic iron used in these experiments contained oxide and it was quite possible in the final product to distinguish between the simple oxide constituent (solid solution of the ferrous oxide type) and the iron-vanadium spinel. In Fig. 13 the oxide globules have been etched away with a saturated solution of picric acid in alcohol leaving a resistant particle of spinel in the region photographed.

Table XIII

X-Ray Data on Materials Listed in Table I-B

Specimen 15				Specimen 19			
Observed Pattern	Observed Intensity	Due to	Theoretical Pattern	Observed Pattern	Observed Intensity	Due to	Theoretical Pattern
2.355	w	V_2O_2	2.351	2.380	m	V_2O_2	2.377
2.150	m	V	2.150	2.055	vs	V_2O_2	2.058
2.040	s	V_2O_2	2.040	2.020	w	Fe	2.018
1.970	m	Fe	1.970	1.925	w	.....	.....
1.938	w	.....	.....	1.690	vw	.....	.....
1.900	w	.....	.....	1.452	vs	V_2O_2	1.455
1.450	s	V_2O_2	1.440	1.428	w	Fe	1.427
1.390	vw	Fe	1.392	1.240	m	V_2O_2	1.240
1.268	vw	.....	.....	1.187	w	V_2O_2	1.188
1.238	m	V_2O_2	1.228	1.168	m	Fe	1.165
1.205	vw	.....	.....	1.088	w	.....	.....
1.176	m	V_2O_2	1.178	1.030	w	V_2O_2	1.029
1.145	vw	Fe	1.137	1.009	vw	Fe	1.009
1.071	vw	V	1.074				
1.021	w	V_2O_2	1.022				
1.002	vw	.....	.....				

$a_o = 4.076$ gives values listed as theoretical for V_2O_2
$a_o = 2.786$ gives values listed as theoretical for Fe

Composition of original briquets:
51.2% V (91.85)
48.8% FeO

$a_o = 4.112$ gives values listed as theoretical for V_2O_2
$a_o = 2.855$ gives values listed as theoretical for Fe

Composition of original briquets:
80% V_2O_2
20% Fe

Obviously, these mixtures fall within the constitutional triangle, Fe-FeO-FeV_2O_4, and the latter compound, as also the former, is appreciably soluble in liquid iron.

When the electrolytic iron is substantially freed from oxygen by annealing in hydrogen and then melted in a crucible of V_2O_3, an exceptionally clean product, virtually free from inclusions, results. The solubility of V_2O_3 in liquid iron is therefore vanishingly small at temperatures in the vicinity of the melting point of the metal.

Several unsuccessful attempts were made to melt iron in a crucible made of iron-vanadium spinel. The molten iron wets the crucible at all points of contact with rapid penetration and ultimate perforation of the crucible wall. A satisfactory regulus could not be obtained even in a magnesia crucible lined with iron-vanadium spinel. However, by using V_2O_3 containing 25 per cent of the spinel for crucible material a coherent globule of metal was obtained. This iron had dissolved an appreciable quantity of iron-vanadium spinel, for it contained scattered (idiomorphic) inclusions of characteristic appearance (Fig. 14). Thus, mixtures in the constitutional triangle, Fe-FeV_2O_4-V_2O_3, yield iron containing only one kind of inclusion, the iron-vanadium spinel, and a mixed oxide slag.

Electrolytic iron saturated with oxide (Fig. 15), when melted in

a crucible pressed from V_2O_2 powder, shows traces of iron-vanadium spinel in the microstructure. In this case, the V_2O_3 necessary for formation of the compound evidently came from reduction of the dissolved ferrous oxide by V_2O_2. Electrolytic iron containing only the small residue of oxygen left after a thorough hydrogen treatment may be melted in a crucible of pure V_2O_2 without visible contamination (Fig. 16). No more than an occasional nonmetallic speck could be found in this material.

The metal, however, wets and slowly penetrates a crucible of this composition. Iron may even be melted in a crucible of V_2O_2 briquetted with a moderate excess of vanadium. The metal resulting from an experiment of this sort is exceptionally free from inclusions and the crucible itself shows patches and a network of infiltrated metal (iron-vanadium solid solution), as illustrated in Fig. 17. The acicular structure (Cf. Fig. 3) commonly encountered in mixtures of vanadium and the dioxide was not observed in this iron-saturated material. Very clean iron may thus be prepared by annealing electrolytic iron in hydrogen and then melting it in vacuo in a crucible pressed from V_2O_2 or V_2O_3 powder. The former crucible material would tend to reduce traces of residual ferrous oxide, introducing a minute quantity of iron-vanadium spinel into the iron, while the latter would supply V_2O_3 directly for formation of spinel and presumably take none of the residual oxygen out of the iron. This higher oxide is not wetted by the iron and may be considered a useful crucible material for preparing pure iron free from inclusions.

These observations indicate that the constitutional triangle, Fe-V_2O_3-V_2O_2, is characterized by the occurrence of clean iron under an inert oxide slag.

We could not detect a change in the parameter of the iron cell due to melting and solidification in any crucible made from an oxide or mixture of oxides of vanadium. There is therefore no appreciable solid solubility of any of these oxides (V_2O_2, V_2O_3 or FeV_2O_4) in iron.

When iron containing oxide is melted with vanadium (also containing some oxide) the solidified metal, which contains vanadium in solid solution, is free from inclusions.

According to the constitutional conditions exhibited in Fig. 7 a very small amount of vanadium would produce iron with mixed inclusions of the FeO and spinel types. Increasing quantities of

vanadium would produce clean iron successfully in contact with (a) iron-vanadium spinel, (b) this spinel in equilibrium with V_2O_3, (c) the two oxides V_2O_3 and V_2O_2 and finally the oxide V_2O_2 alone.

From the evidence presented in this investigation it would appear that the cause of any eventual metallurgical effect of vanadium in pure iron would have to be evaluated in terms of deoxidation (either V or V_2O_2 reduces FeO to metal), the presence and effect of iron-vanadium spinel inclusions, or an effect of the element vanadium in solid solution in iron*. From the general point of view of physical metallurgy it is probable that the last factor is of the greatest consequence.

*Obviously, the presence of other materials than Fe, V, and O in metal or slag would set up new conditions demanding a reconsideration of these conclusions.

October

th (a)
O_3, (c)
.
appear
in pure
er V or
f iron-
lium in
physical
est con-

or slag would